THE FUNCTIONS OF CUL-2 AND CUL-4 IN C. ELEGANS CELL CYCLE REGULATION

by

WEIWEI ZHONG

(Under the Direction of Edward T. Kipreos)

ABSTRACT

CUL-2 and CUL-4 are members of the cullin family of ubiquitin-ligases that facilitate ubiquitin-mediated proteolysis. Here we demonstrate that in *Caenorhabditis elegans*, CUL-2 and CUL-4 are both essential cell cycle regulators. CUL-2 is required at two distinct points in the cell cycle, the G1-to-S phase transition and mitosis. *cul-2* mutant germ cells undergo a G1 arrest that correlates with accumulation of CKI-1, a member of the CIP/KIP family of cyclin-dependent kinase inhibitors. In *cul-2* mutant embryos, mitotic chromosomes are unable to condense, leading to unequal DNA segregation, chromosome bridging, and the formation of multiple nuclei in cells.

C. elegans CUL-4 functions as a central regulator of DNA replication licensing to prevent DNA re-replication. Inactivation of CUL-4 causes massive re-replication of genomic DNA. To maintain genetic stability, eukaryotic cells must precisely replicate the entire genome only once per cell cycle. The presence of licensing proteins, such as Cdt1 and Cdc6, is required to allow the formation of pre-replicative complexes at replication origins. The removal of licensing proteins from chromatin in S phase is crucial to ensure that origins fire only once per cell cycle. Here we show that the *C. elegans* orthologs of Cdt1 and Cdc6 are both required for DNA replication. Both proteins accumulate in *cul-4* re-replicating cells. In wild-type, CDT-1 protein levels peak in G1 phase and drop rapidly in S phase. In cells lacking CUL-4, CDT-1 levels fail to decrease in S phase. Removal of one genomic copy of the *cdt-1* gene suppresses the *cul-4* re-replication phenotype, indicating that CUL-4 prevents DNA re-replication at least partially by negatively regulating CDT-1 protein levels.

INDEX WORDS: *Caenorhabditis elegans*, CUL-2, CUL-4, CKI, CDC-6, CDT-1, cullin, cell cycle, proteolysis, chromosome condensation, DNA replication

THE FUNCTIONS OF CUL-2 AND CUL-4 IN C.ELEGANS CELL CYCLE REGULATION

by

WEIWEI ZHONG

B.S., University of Science and Technology of China, P.R. China, 1997

A Dissertation Submitted to the Graduate Faculty of The University of Georgia in Partial Fulfillment of the Requirements for the Degree

DOCTOR OF PHILOSOPHY

ATHENS, GEORGIA

2002

THE FUNCTIONS OF CUL-2 AND CUL-4 IN C.ELEGANS CELL CYCLE REGULATION

by

WEIWEI ZHONG

Approved:

Major Professor: Edward T. Kipreos

Committee: Michael Bender
Haini Cai
Jacek Gaertig
Claiborne Glover

Electronic Version Approved:

Gordhan L. Patel
Dean of the Graduate School
The University of Georgia
August 2002

DEDICATION

This dissertation is dedicated to my parents for their unconditional love. Their love made all my achievements possible. It was their support that carried me through all the ups and downs in my life. In this uncertain world, if I am sure about anything, it is that they will always be there for me.

ACKNOWLEDGEMENTS

I thank my major professor Dr. Edward T. Kipreos, whose intelligence is beyond my words and whose advice and assistance have been invaluable for me through this program. During all the years, I have benefited tremendously from your guidance. I thank my committee members Drs. Michael Bender, Haini Cai, Jacek Gaertig, and Claiborne Glover for their patience and mentorship. Special thanks to Dr. Cai, who has been more than an advisor but also a friend.

I am grateful to Dr. John S. Willis for friendly discussion and helpful suggestions. I thank Drs. Haini Cai, Mark Farmer, Jacek Gaertig, Charles Keith, James Lauderdale, and Ping Shen for technical advice and for access to reagents and instruments. I thank everyone in the UGA Cellular Biology Department Office for always being willing to help.

I thank current and former member in the Kipreos lab: Vikas Dhingra, Fernado Santiago, Ryan Santurri, Hui Feng, Ji Liu, Hui Jin, Geri K. Burkheimer, Subin Gu, George Punkosdy, Liang Zhou, Erin K. Seabolt, and Amanda Hobe for excellent collaborations and for being wonderful friends. Thanks to members in the Gaertig lab for being helpful neighbors and good friends. Thanks to all my friends and loved ones for your inspiration and the happiness that you bring to my life.

TABLE OF CONTENTS

Page

CHAPTER 1

GENERAL INTRODUCTION

EUKARYOTIC CELL CYCLE

The eukaryotic cell cycle is composed of a series of ordered events. In G1 phase, cells increase in volume and prepare for DNA replication. During S phase, the DNA synthesis phase, cells replicate their DNA once and only once. Then after a gap G2 phase, cells enter mitosis (M phase) that produces two identical daughter cells. Cells can leave the cell cycle and either enter a quiescent G0 phase or undergo terminal differentiation.

Mitosis itself is composed of a complex set of ordered events and can be divided into five phases: prophase, in which cells condense their chromosomes; prometaphase, in which cells align the condensed chromosomes with a mitotic spindle; metaphase, in which the chromosomes are aligned at the equatorial plate of the spindle; anaphase, in which sister chromatids are separated and moved toward opposite spindle poles; and telophase, in which daughter chromosomes arrive at the poles and begin decondensing. At the end of mitosis, cells undergo cytokinesis to divide into two daughter cells.

The discovery of Cyclin and Cyclin-dependent kinase (CDK)

Understanding the regulation of the cell cycle at a molecular level started about thirty years ago. It was observed that when extracts from mitotic *Xenopus* eggs were

microinjected into immature G2 oocytes, it promoted the oocytes to mature and arrest in metaphase of meiosis II (Masui and Markert, 1971). The active factor in mitotic *Xenopus* egg extract is called maturation promoting factor (MPF); it is also known as mitosis promoting factor based on its ability to regulate mitosis (Newport and Kirshner, 1984).

During the same time period, a number of cell division cycle (*cdc*) mutants were isolated in fission yeast and budding yeast (Hartwell et al., 1970; Hartwell et al., 1974; Nasmyth and Nurse, 1981). Subsequent yeast genetic studies revealed that orthologous serine/threonine kinases, Cdc28p in *Saccharomyces cerevisiae*, and Cdc2 in *Schizosaccharomyces pombe*, were essential for promoting S phase and M phase in the two yeasts (Lorincz and Reed, 1984; Beach et al., 1982; Hindley and Phear, 1984). Studies with sea urchin eggs revealed proteins whose abundance fluctuates during the cell cycle (Evans et al., 1983). The cycling of the synthesis and degradation of these proteins led to these proteins being given the name cyclins (Evans et al., 1983).

Xenopus MPF was eventually purified and identified as a complex of two major proteins: one 34 kilodalton subunit and one 45 kilodalton subunit. The 34 kd protein was identified as a homologue of Cdc2p/Cdc28p (Gautier et al., 1988). The other subunit was believed to be a cyclin (Murray et al., 1989). At the same time, biochemical studies in starfish oocytes confirmed that MPF is a heterodimer of Cdc2 and an M phase cyclin, cyclin B (Labbe et al., 1989).

The Cdc28p/Cdc2p family of protein kinases is named cyclin-dependent kinase (CDK). Further genetic and biochemical studies with various species ranging from yeast to mammalian cells led to the conclusion that the eukaryotic cell cycle is driven by the activities of cyclin-dependent kinases.

CDKs promote cell cycle progression

In the cyclin-CDK complex, the catalytic subunit CDK generally has a constant protein concentration throughout the cell cycle, while the regulatory cyclin subunit has fluctuating protein abundance (Morgan, 1997). The association of a cyclin is required for the CDK kinase activity (Morgan, 1997). Oscillations in specific CDK activities promote cell cycle progression.

CDKs regulate the cell cycle in yeast

Although there are seven CDK family members in *S. cerevisiae* and eight in *S. pombe* (Ji and Kipreos, 2000), only Cdc28p in *S. cerevisiae* and Cdc2p in *S. pombe* are essential for cell cycle regulation.

In budding yeast, the G1 cyclins Cln1p, Cln2p, and Cln3p complex with the CDK Cdc28p to promote transcription of genes in G1 phase that prepares cells for S phase (Koch and Nasmyth, 1994). The G1 cyclin-Cdc28p complexes promote the activation of S phase cyclin (Clb5p and Clb6p)-CDK activity in S phase through three mechanisms: activating the transcription of the S phase cyclin genes *CLB5* and *CLB6* (Schwob and Nasmyth 1993); turning off the proteolysis of S phase cyclins, probably by inhibiting the anaphase promoting complex (APC) which mediates Clb degradation (Dirick et al., 1995; Amon et al., 1994); and by promoting the degradation of the CDK-inhibitor Sic1p to promote the G1-to-S transition (Barral et al., 1995). Cln proteins are autophosphorylated by Cln-Cdc28p, which signals Cln ubiquitin-mediated degradation (King et al., 1996).

The S phase cyclins Clb5p and Clb6p complex with Cdc28p to initiate DNA replication (Bell and Dutta, 2002). The Clb-Cdc28p complex also promotes transcription

of the M phase cyclins Clb3p and 4p during S phase (Fitch et al., 1992; Richardson et al., 1992) and Clb1p and 2p during G2 phase (Surana et al., 1991). The mitotic cyclins Clb1p, Clb2p, Clb3p, and Clb4p bind Cdc28p to trigger the formation of the mitotic spindle and nuclear division (Nasmyth, 1996). Together with the two S phase cyclins Clb5p and Clb6p, all six Clb-Cdc28p kinases remain active until late mitosis (Amon et al., 1994). In anaphase, Clb-Cdc28p contributes to the activation of the APC that in turn leads to Clb destruction (King et al., 1996). All Clb proteins are degraded by APC, and the resulting low CDK activity promotes exit of mitosis (Amon et al., 1994; King et al., 1996). APC remains active in degrading Clbs during the following G1 phase until Cln1p and Cln2p protein levels are elevated (King et al., 1996).

CDKs regulate the cell cycle in mammalian cells

Humans have 21 CDKs (Ji and Kipreos, 2000). Unlike the situation in yeast, where a single CDK regulates all major cell cycle transitions, metazoan cell cycle regulation functions are shared by several CDKs. At least five mammalian CDKs, CDK1 (a homologue of Cdc2), CDK2, CDK3, CDK4, and CDK6, are involved in cell cycle regulation (Morgan, 1997).

Higher eukaryotes have CDK-cyclin complexes homologous to those in yeast, except that the cyclins are complexed with different specific CDKs. The G1 cyclins, cyclin D1, D2, and D3, associate with CDK4 and CDK6 to drive cells through G1 phase and to promote the G1-to-S phase transition (Morgan, 1997). The S phase cyclins, cyclin E and cyclin A, assemble with CDK2 to promote DNA synthesis (Morgan, 1997). The M

phase cyclins, cyclin A, cyclin B1, B2, and B3, complex with CDK1 to promote mitosis (Morgan, 1997).

I will briefly present the role of CDK activity in the G1-to-S phase transition in mammalian cells. In G1 phase, cyclin D is transcribed at a high rate, and this leads to high cyclin D protein levels (Ortega, 2002). Active cyclin D-CDK4/6 complexes phosphorylate the Retinoblastoma (Rb) protein (Sherr, 1996). Rb inhibits the transcription factor E2F in G1 phase both by blocking E2F transcriptional activation of target genes and by actively inhibiting target genes by recruiting histone deacetylatase and chromatin remodeling enzymes to the promoters (Ortega, 2002; Harbour and Dean, 2000). The phosphorylation of Rb by Cyclin D-CDK4/6 inactivates the ability of Rb to bind and suppress E2F, thereby allowing the transcription of E2F-controlled genes such as cyclin E (Ortega, 2002). Active cyclin E-CDK2 complexes further hyperphosphorylate Rb to promote the G1-to-S transition and initiation of DNA replication (Ortega, 2002). Cyclin D-CDK4/6 also facilitates the activation of cyclin E-CDK2 by binding Cip/Kip CKIs and preventing them from inhibiting cyclin E-CDK2 activity (Ortega, 2002; Morgan 1997).

Although cell cycle transitions are driven largely by CDK activity, it should be noted that the cell cycle is not just a CDK activity cycle. An active complex of CDK with a particular cyclin does not specify a cell cycle stage. Activation of the M phase Clb2p–Cdc28p instead of the S phase Clb5p-Cdc28p in G1 cells promotes S phase rather than mitosis in *S. cerevisiae* (Amon et al, 1994). Therefore, the state of different subtypes of cyclin-CDKs cannot solely determine the order of cell cycle stages. The

response of a cell to a particular cyclin-CDK activity also depends on the state of CDK substrates.

Regulation of CDK activity

To promote cell cycle progression, cells must ensure proper oscillations of CDK kinase activities. CDK activity is regulated at multiple levels: by the availability of cyclins; by the inhibitory or activating phosphorylation of particular Thr and Ser residues of the CDK, and by the presence of CDK-inhibitory proteins (CKIs) (Morgan, 1997).

CDKs are only active when complexed with a regulatory subunit cyclin (Morgan, 1997). CDKs complex with a set of distinct cyclins (i.e., G1-phase cyclins, S-phase cyclins, or M-phase cyclins). The abundance of a cyclin is strictly regulated during the cell cycle by both transcriptional control and by ubiquitin-mediated protein degradation (King et al., 1996).

CDK kinase activity is also regulated by both activating and inhibiting phosphorylation (Morgan, 1997). Phosphorylation at a site, corresponding to Thr160 of human CDK2, by a CDK-activating kinase (CAK) promotes CDK kinase activity, while phosphorylation at sites, corresponding to Thr14 and Tyr15 of human CDK2, by other kinases orthologous to Wee1 and Myt1 inhibits CDK kinase activity (Morgan, 1997). Dephosphorylation at the inhibitory and activating sites by phosphatases have opposite effects on CDK activities (Morgan, 1997).

The third major mechanism that regulates the CDK activity is the presence of CDK-inhibitors (CKIs). Two CKIs have been identified in budding yeast *S. cerevisiae:* the CKI Sic1 inhibits S phase cyclin-CDK activity in G1 phase to prevent precocious S

phase activation (Schwob et al., 1994), and the CKI Far1 arrests the cell cycle in response to mating pheromones (Henchoz et al., 1997). In mammalian cells, there are at least two CKI families that coordinate cell division with cell differentiation: the INK4 proteins (inhibitors of CDK4) and the CIP/KIP family of CKIs. There are four known INK4 proteins, $p16^{INK4a}$, $p15^{INK4b}$, $p18^{INK4c}$, and $p19^{INK4d}$, and at least three CIP/KIP CKIs, $p21^{CIP1}$, $p27^{KIP1}$, and $p57^{KIP2}$ (Sherr, 1996). The presence of CKIs are regulated by both transcriptional control and ubiquitin-mediated proteolysis (Morgan, 1997).

In summary, the cell cycle is to a large extent driven by CDK activity. CDKs are activated and inactivated at specific points in the cell cycle by regulatory phosphorylation and by association with positively activating cyclins and inhibitory cyclin-dependent kinase inhibitors (CKIs) (Pines, 1995). Cell cycle phases are effected by the transcription of cyclins and CKIs, so that during a given phase, CDKs can only be activated by binding a subset of cyclins and inactivated by a subset of CKIs. The transition from one cell cycle state to another is made irreversible by the ubiquitin-mediated degradation of cyclins and CKIs. Although there exist many protein degradation pathways, the proteolysis pathway that is critical for cell cycle regulation is ubiquitin-mediated protein degradation (King et al., 1996).

UBIQUITIN-MEDIATED PROTEIN DEGRADATION

Ubiquitin-mediated proteolysis is the most common pathway for cell cycle regulated degradation. Many essential cell cycle regulators, such as cyclins and CDK-inhibitor proteins (CKIs), are targeted for degradation by this pathway (reviewed by Deshaies, 1999; Tyers and Jorgensen, 2000).

Ubiquitin

Ubiquitin is a small protein of only 76 amino acid residues (Hershko and Ciechanover, 1998). Ubiquitin is highly conserved, with only three amino acid differences between human and yeast ubiquitin (Hershko and Ciechanover, 1998). There are also a large number of ubiquitin-like proteins which can be covalently attached to substrates. Although these ubiquitin-like proteins act on different substrates and do not lead to protein degradation, they share a similar enzymatic pathway to become covalently bound to target proteins (Wilkinson, 2000).

Ubiquitin-activating enzyme (E1)

The ubiquitin-mediated proteolysis pathway starts with the activation of ubiquitin at its C-terminal Gly residue (Figure 1.1). This step requires ATP and a ubiquitin-activating enzyme (E1). In this step, an initial intermediate ubiquitin adenylate is formed with the release of PPi. Ubiquitin then forms an intermolecular thioester bond to a Cys residue of E1 with the release of AMP (Hershko and Ciechanover, 1998).

Ubiquitin conjugating enzyme (E2)

Activated ubiquitin is transferred from the E1 to a Cys residue of a ubiquitin conjugating enzyme (E2) (Hershko and Ciechanover, 1998) (Figure 1.1). With the assistance of a ubiquitin ligase (E3) that binds the substrate and the E2, the E2 transfers ubiquitin to the target protein (Hershko and Ciechanover, 1998). Although some in vitro evidence suggests that E2 enzymes can directly mediate substrate ubiquitination without

E3s (Goebl et al., 1988), there is currently no evidence that E2s directly bind to their protein substrates in vivo (Ciechanover et al., 2000).

Depending on the type of E3, ubiquitin can be transferred from an E2 to the substrate by two different mechanisms. For the Hect-domain class of E3s, ubiquitin is first transferred to a Cys residue of the E3 enzyme. The ubiquitin-E3 thioester then becomes the donor for amide bond formation with the protein substrate (Hershko and Ciechanover, 1998). In other classes of E3 enzymes (e.g., Cullin/RING finger complexes), an E3 ubiquitin thioester intermediate does not form; instead the E3 binds to both the E2 and the substrate and serves as a scaffold that brings together the E2 and the substrate, allowing ubiquitin to be directly transferred from the E2 to the substrate protein (Zheng et al., 2002).

Ubiquitin ligase (E3)

The substrate specificity of the ubiquitination pathway is largely regulated at the level of the E3. Different targets are recognized by different E3s. In budding yeast, a single E1 enzyme, Uba1p, activates ubiquitin and transfers it to 11 different ubiquitin conjugating enzymes, Ubc1p-8p, 10p, 11p, and 13p. Each E2 then interacts with one or several E3s (Ciechanover, 2000). As E3s specifically bind substrates, they determine the target selection for ubiquitin-mediated degradation. E3s can be single substrate-specific or can recognize multiple substrates via similar motifs (Ciechanover, 2000).

Ubiquitin is attached to the substrate via an amide isopeptide bond between the C-terminal Gly of ubiquitin and an ε-amino group of a Lys residue of the substrate protein

(Ciechanover et al., 2000). Multiple lysine residues in the substrate can function as ubiquitin acceptor sites (Ciechanover et al., 2000).

After the first ubiquitin is transferred to the substrate, a polyubiquitin chain is synthesized by progressively transferring additional activated ubiquitin proteins to internal Lys residues of the previously conjugated ubiquitin molecule. Lys48 of ubiquitin is the residue most commonly utilized for this type of cross-linking (Ciechanover et al., 2000), but linkages to other lysine residues, for example Lys29, have also been reported (Mastrandrea et al., 1999). A branched polyubiquitin chain can be formed if more than one Lys residue on a ubiquitin are used as receptor sites for subsequent ubiquitin addition (Figure 1.1). It is commonly believed that the same E3 protein that conjugates the first ubiquitin to the substrate also elongates the polyubiquitin chain by progressively adding ubiquitin proteins. Once substrate proteins are attached with polyubiquitin chains, they are recognized and degraded by the 26S proteasome (Hershko and Ciechanover, 1998) (Figure 1.1).

There are two major types of E3 complexes that regulate the cell cycle: cullin/RING finger complexes and the cyclosome or anaphase-promoting complex (APC) (King et al., 1996).

The SCF cullin/RING finger complex has its most visible functions during G1 and S phases (King et al., 1996). The core components for the SCF cullin/RING finger complex are Skp1, Cdc53/Cullin-1, an F-box protein, and Rbx1/Roc1/Hrt1 (Tyers and Jorgensen, 2000). The SCF cullin/RING finger complex is believed to be constitutively active as a ubiquitin ligase. The binding of SCF complexes to substrates is regulated by modification of the substrate by phosphorylation (Tyers and Jorgensen, 2000). For

example, in *S. cerevisiae*, the SCF^{Grr1} ubiquitin ligase recognizes its substrate Cln2p (a G1 cyclin) only after Cln2p is phosphorylated (Lanker et al., 1996).

APC functions in mitosis and in the G1 phase, where it is required for the metaphase-to-anaphase transition, exit from mitosis, and for maintaining low levels of mitotic cyclins in G1 phase (Peters, 2002). Vertebrate APC has eight subunits, APC1-8, while budding yeast APC has 11 subunits (Yu et al., 1998a; Zachariae et al., 1996). The APC2 subunit shares similarity to cullins (Yu et al., 1998a), whereas the APC11 subunit shares homology with Rbx1 (Kamura et al., 1999). APC is only active as a ubiquitin ligase when associated with the proteins Cdc20 or Cdh1, which function as substrate-recognition components (Peters, 2002). No substrate modification is needed for APC recognition. Once active, APC^{Cdc20} degrades proteins with the destruction box (D-box) motif and APC^{Cdh1} degrades proteins with the KEN box motif or D-box motif (Pfleger and Kirshner, 2000).

Unlike SCF cullin/RING finger complexes that are constitutively active as ubiquitin ligases, the activity of APC^{Cdh1} and APC^{Cdc20} is regulated by phosphorylation and other factors. APC^{Cdc20} is active only in mitosis. In budding yeast, the phosphorylation of several APC subunits by the CDK Cdc28p is essential for APC^{Cdc20} activity (Peters, 2002). In addition to this regulation, APC^{Cdc20} is also regulated by the Mad1-3 checkpoint proteins (Gardner and Burke, 2000). Mad2p binds to APC^{Cdc20} and inhibits its activity (Gardner and Burke, 2000). When all chromosomes are attached to the spindle, Mad2p dissociates from APC^{Cdc20}. The latter becomes active and promotes the metaphase-to-anaphase transition (Gardner and Burke, 2000). In contrast to Cdc20, Cdh1 is inhibited by CDK phosphorylation during most of mitosis (Peters, 2002). At the

end of mitosis, Cdh1 is activated by dephosphorylation, and APC^{Cdh1} becomes active (Peters, 2002). The active APC^{Cdh1} ubiquitinates Cdc20, causing its degradation and thereby inactivating APC^{Cdc20} (Pfleger and Kirshner, 2000). APC^{Cdh1} promotes mitotic exit by degrading mitotic cyclins and is active in the subsequent G1 phase to maintain low mitotic cyclin levels (Peters, 2002). At the G1-to-S transition, S phase cyclin-CDK complexes inactivate APC^{Cdh1} by phosphorylating Cdh1 (Amon et al., 1994; Huang et al., 2001).

CULLIN/RING FINGER COMPLEX

Cullin/RING finger complexes in budding yeast

The first cullin/RING finger complex to be identified was the budding yeast SCF complex (for Skp1, Cdc53/cullin, F-box protein) (Schwob et al., 1994; Feldman et al., 1997; Mathias et al., 1996). SCF is also the best-studied class of cullin/RING finger complex. It was originally observed that the gene *CDC34*, which encodes a ubiquitin conjugating enzyme E2, was required for the G1-to-S transition (Goebl et al., 1988). Later observations revealed that $skp1^{ts}$, $cdc53^{ts}$, and $cdc4^{ts}$ mutants have a G1 arrest phenotype similar to that of $cdc34^{ts}$ mutants (Bai et al., 1996; Schwob et al., 1994). Genetic and biochemical studies indicated that these genes function in the same pathway to degrade the CDK-inhibitor Sic1p (Schwob et al., 1994; Mathias et al., 1996; Feldman et al., 1997). Functional studies revealed that Skp1p, Cdc53p, and Cdc4p (an F-box protein) form an E3 complex that binds to both Cdc34p (E2) and the substrate Sic1p (Patton et al., 1998). This E3 complex was consequently named the SCF ubiquitin ligase.

A fourth essential component of this E3 complex, Roc1/Rbx/Hrt1, was identified later (Kamura et al., 1999; Ohta et al., 1999; Seol et al., 1999; Tan et al., 1999). Rbx1 has a zinc-binding RING-H2 domain in its C-terminus (Ohta et al., 1999). The highly conserved mammalian RBX1 can rescue the lethal yeast *rbx1*Δ mutant (Ohta et al., 1999).

In the SCF complex, Cdc53p functions as a scaffold to assemble the E3 components so that they can bind and position the E2 and substrate to facilitate ubiquitination. Cdc53p binds Rbx1p, which binds the E2 Cdc34p; Cdc53p also binds Skp1, which binds the F-box protein that directly interacts with the substrate (Deshaies, 1999). A number of mutagenesis studies indicate that the interaction between Skp1p and the F-box protein is mediated through Skp1p binding the F-box motif of the F-box protein (Deshaies, 1999).

In yeast, there are several SCF complexes, which differ only in their associated F-box proteins. By switching F-box proteins, such as Cdc4p, Grr1p, or Met30p, SCF complexes can target different sets of proteins for degradation (Tyers and Jorgensen, 2000). To indicate a specific F-box protein, the SCF complex is denoted by a superscript of its F-box subunit. For example, an SCF complex that contains Cdc4p is denoted as SCF^{Cdc4}. Different SCF complexes have different functions. SCF^{Cdc4} degrades the CKI Sic1p (Shwob et al., 1994; Feldman et al., 1997; Skowyra et al., 1997), the CKI Far1p (Henchoz et al., 1997), Cdc6p (a protein that is required for DNA replication) (Drury et al., 1997; Elsasser et al., 1999) and Gcn1p (a transcription factor) (Kornitzer et al., 1994). SCF^{Met30} degrades Swe1p (a kinase that inactivates the CDK Cdc28p) (Kaiser at al., 1998) and ubiquitinates Met4p (a transcription activator that regulates the sulfur

metabolism MET genes) when intracellular S-adenosylmethionine (AdoMet) increases (Patton et al., 2000). Interestingly, the ubiquitinated form of Met4p protein is stable, although it is inactive as a transcription factor (Kaiser et al., 2000). SCF^{Grr1} degrades Cln1p and Cln2p (G1 cyclins) (Barral et al., 1995) and Gic2p (a protein required for actin rearrangement at the budding site) (Jaquenoud et al., 1998). With such a broad range of substrates, SCF complexes have been shown to be involved in a number of cell cycle and non-cell cycle pathways.

Cdc53p is a member of the cullin family that is found in eukaryotes from plants to mammals (Kipreos et al., 1996). There are three cullins in budding yeast, Cdc53p, Cullin A, and Cullin B (Kipreos et al., 1996). Cdc53p is covalently modified by a small ubiquitin-like protein, Rub1p (Lammer et al., 1998). Although not essential for yeast viability, the attachment of Rub1 optimizes SCF function. The *rub1*Δ strain appears wild-type, but any double mutants between *rub1*Δ and mutants of SCF components have a stronger phenotype than the single SCF mutants (Lammer et al., 1998; Hochstrasser, 1998). This indicates that Rub1 promotes Cdc53 function.

Cullin/RING finger complexes in humans

Three ancestral cullins, corresponding to the three yeast cullins, evolved into five major classes of cullins in metazoa (CUL1 through CUL5) (Nayak et al., 2002). Both *Caenorhabditis elegans* and humans have members in each class (Nayak et al., 2002). Both species have six cullin genes (Nayak et al., 2002). *C. elegans* has two members in the CUL1 class, *cul-1* and *cul-6*; humans have two members of the CUL4 class, *CUL4A* and *CUL4B* (Nayak et al., 2002).

The ancestral *CDC53* gene is predicted to have evolved by gene duplication into the metazoan *CUL1* and *CUL2* genes with *CUL1* sharing most homology with *CDC53* (Kipreos et al., 1996; Nayak et al., 2002). Although human CUL1 binds SKP1, CUL2, CUL3, CUL4, and CUL5 do not bind to SKP1 (Michel and Xiong, 1998). In contrast, human RBX1 interacts with all human cullins (CUL1-5) in both yeast two-hybrid and co-immunoprecipitation assays (Ohta et al., 1999). As cullins and RBX1 are the only two conserved components in this family of complexes, cullin-containing E3 complexes have been named cullin/RING finger complexes. Currently, only the CUL1 and CUL2/RING finger complexes have been characterized in any detail.

CUL1 recruits SKP1, RBX1, and an F-box protein to form a complex similar to the SCF complex in yeast (Tyers and Jorgensen, 2000). The mammalian version of SCF complexes also have a variety of substrates. $SCF^{\beta\text{-}TrCP}$ degrades β-catenin (which is involved in the Wnt-Wingless pathway) and IκBα (an inhibitor of the transcription factor NF-κB) (Suzuki et al., 1999; Latres et al., 1999; Winston et al., 1999). SCF^{Skp2} is involved in the degradation of the CKI $p27^{kip1}$ (Carrano et al., 1999), E2F (Marti et al., 1999), cyclin D (Yu et al., 1998b), and cyclin E (Nakayama et al., 2000).

The crystal structure of the SCF^{Skp2} complex has been solved (Zheng et al., 2002). CUL1 functions as a long stalk-like scaffold that binds to Skp1-Skp2 at its N-terminal end and binds to Rbx1 at the C-terminal end, with Rbx1 bringing the E2 to the E3 complex (Zheng et al., 2002) (Figure 1.2 a).

CUL2 binds to RBX1, Elongin C (which is related to Skp1), Elongin B (which is a ubiquitin-like protein), and the von Hippel-Lindau tumor suppressor protein (VHL), to form a VCB complex (for VHL, Elongin C, Elongin B) that does not include SKP1 or F-

box protein subunits (Pause et al., 1997, Lonergan et al., 1998). Cul-2 binds elongin C, which associates with elongin B and VHL, with VHL directly interacting with substrates (Deshaies, 1999). The CUL2-VCB complex has ubiquitin ligase activity in vitro, which is lost in tumor-derived VHL mutants (Lisztwan et al., 1999). The CUL2-VCB complex has an E3 activity in vivo that promotes the oxygen-dependent ubiquitination of the hypoxia-inducible factor-1α and -2α (HIF-α) (Maxwell et al., 1999). CUL2-VCB complex is also found to mediate ubiquitination of PKCλ, a member of the atypical protein kinase C (PKC) group (Okuda et al., 2001).

VHL shares a B/C box motif with a number of SOCS (Suppressor Of Cytokine Signaling) proteins that also bind to elongin C (Kamura et al., 1998). The SOCS motif is required for the interaction of VHL and elongin C (Kamura et al., 1998). It has been proposed that elongin C, CUL2, and Roc1/Rbx1 function as the core components in this E3 complex, while B/C-box proteins function as adapters for different substrates just like the F-box proteins do in SCF complexes (Figure 1.2 b). Consistent with this model, the SOCS protein SOCS1/JAB has been found to interact with CUL2 and promote TEL-JAK2 tyrosine kinase ubiquitination (Kamizono et al., 2001).

Little is known about other non-SCF cullin/RING complexes. Although not yet biochemically characterized, CUL3-5 may form additional types of cullin/RING finger complexes as well (Figure 1.2c). Non-SCF cullin/RING finger complexes may share additional structural similarities with the SCF cullin/RING finger complexes. For example, like Cdc53p, all human cullins are covalently modified by the ubiquitin-like protein NEDD8 (a Rub1 ortholog) (Tyers and Jorgensen, 2000). Mouse CUL3 is involved in cyclin E degradation. An interesting observation is that while all SCF

substrates must be phosphorylated before they can be targeted by the ubiquitin ligase, phosphorylation may not be necessary for non-SCF cullin/RING finger complexes. In the CUL2-VCB complex-mediated degradation of HIF-1α, the substrate modification required for E3 recognition is an oxygen-dependent hydroxylation of a conserved proline in HIF-1α (Min et al., 2002). Unphosphorylated cyclin E can be degraded by Cul3 (Singer et al., 1999). Since Cul3 was bound to free cyclin E but not to cyclin E-Cdk2 complexes in mammalian cells, it was suggested that Cul3 may select cyclin E for ubiquitination on the basis of its assembly into CDK complexes (Singer et al., 1999).

Human *CUL4A* was found to be amplified and overexpressed in both breast cancer cell lines and untreated primary breast cancers (Chen et al, 1998). The overexpression was observed even in cases without gene amplification, suggesting that *CUL4A* overexpression plays a role in promoting breast cancer (Chen et al, 1998). CUL4A was found to associate with the UV-damaged DNA-binding protein DDB and to mediate the ubiquitination of DDB (Shiyanov, 1999; Chen et al., 2001; Nag et al., 2001). DBB recognizes UV-induced lesions and is believed to be involved in DNA repair (Shiyanov, 1999). DDB activity is missing in a subset of Xeroderma pigmentosum complementation group E (XP-E) patients. Purified DDB corrects the DNA repair deficit when microinjected in XP-E cell lines lacking DDB activity (Keeney et al., 1994). DDB also has a role in transcription regulation, as it interacts with the transcription factor E2F and stimulates E2F-activated transcription (Hayes et al., 1998).

Cullin/RING finger complexes in *C. elegans*

Among the six *C. elegans* cullins, CUL-1 through CUL-4 are essential for normal development as indicated by dsRNA-mediated interference (RNAi) experiments (Kipreos et al., 1996; Feng et al., 1999; Kurz et al., 2002; E. Kipreos, pers. comm.). In contrast, inactivation of *cul-6* by RNAi produced no phenotype (Nayak et al., 2002). Only the function of CUL-1 had been characterized before the launch of the research presented in this dissertation. CUL-1 is required for cell cycle exit in *C. elegans* (Kipreos et al., 1996). In *cul-1* mutants, cells undergo extra rounds of division before they can exit the cell cycle, which results in hyperplasia in all tissues (Kipreos et al., 1996).

Like yeast and human cullins, *C. elegans* CUL-2 and CUL-4 may complex with RBX-1. *rbx-1* RNAi produced two phenotypes. Some progeny exhibit an embryonic lethal phenotype similar to *cul-2* mutants while others exhibit L2 larval arrest similar to *cul-4* mutants (H. Jin and E. Kipreos, pers. comm.). Yeast 2-hybrid data also indicate that Rbx1 interacts with CUL-1, -2, -4, and -5 (E. Kipreos, pers. comm.).

Despite the preliminary observations in human tissue culture cell studies, the functions of CUL-2 and CUL-4 remain largely unknown. Considering the broad spectrum of CUL1 substrates, it is likely that CUL2 and CUL4 have many other unidentified substrate proteins. Compared to our limited knowledge about CUL2 and CUL4 functions in human cells, even less was known about CUL2 and CUL4 functions in other metazoa. The purpose of the research documented in this dissertation was to initiate an investigation of the cellular and organismal functions of these two ubiquitin ligase proteins. The nematode *C. elegans* was used as a model organism for these

studies. The knowledge gained about CUL-2 and CUL-4 functions in *C. elegans* provides new insights into mechanisms of cell cycle regulation in general as well as the functions of paticular cullin/RING finger complexes in metazoa.

Figure 1.1 Ubiquitin-mediated protein degradation. Ubiquitin is activated by a ubiquitin activating enzyme (E1). The activated ubiquitin is transferred to a ubiquitin conjugating enzyme (E2), which transfers it to a target protein with the help of a ubiquitin ligase (E3). Once the substrate protein is covalently modified by a polyubiquitin chain, it is recognized and degraded by the 26S proteasome. (Diagram provided by E.T. Kipreos)

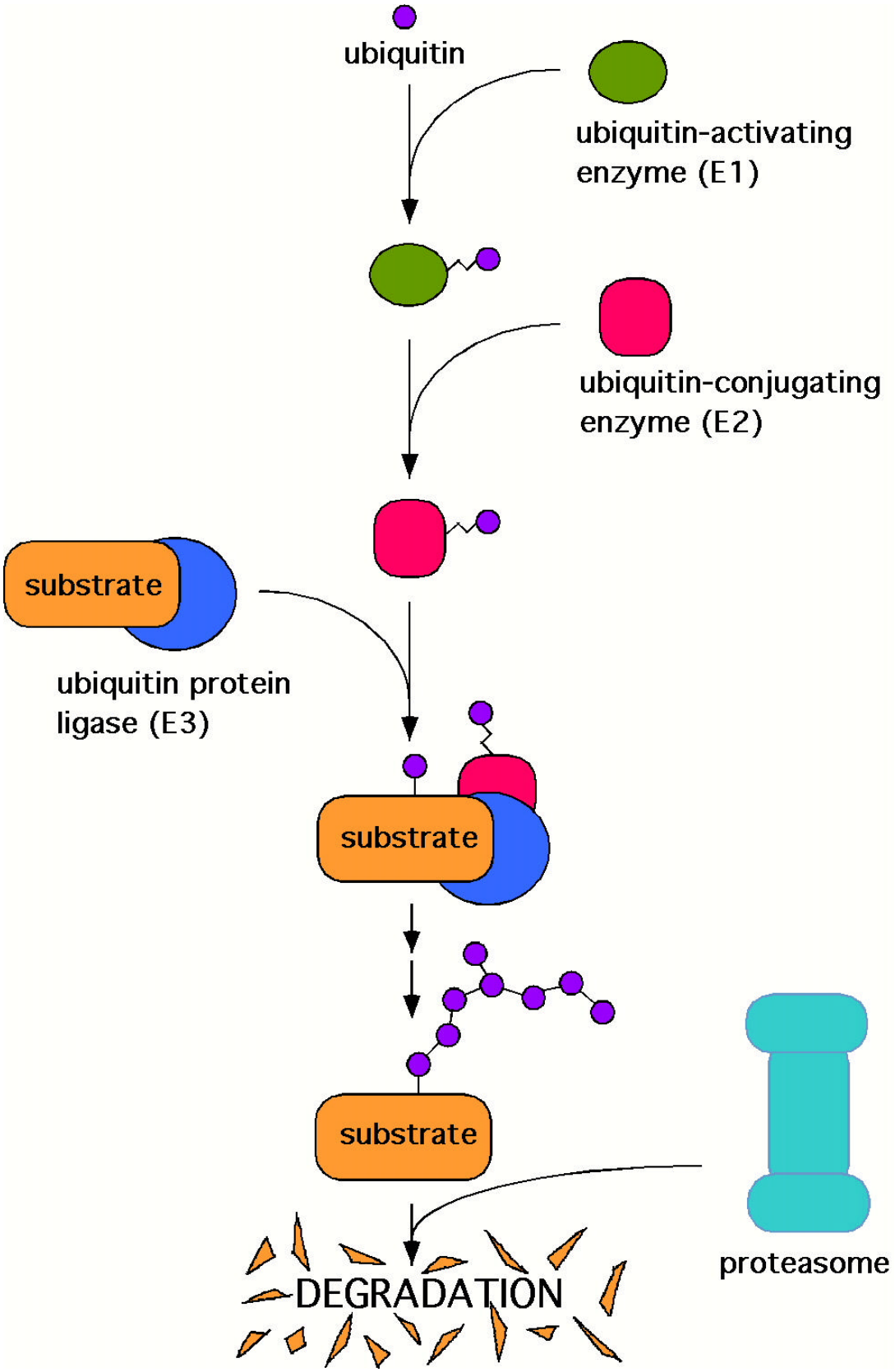
ubiquitin
ubiquitin-activating enzyme (E1)
ubiquitin-conjugating enzyme (E2)
substrate
ubiquitin protein ligase (E3)
substrate
substrate
proteasome
DEGRADATION

Figure 1.2 Cullin/RING finger complexes. (a) The SCF^{Skp2} complex. Top, crystal structure of the Cul1-Rbx1-Skp1-Skp2 complex. Cul1, Rbx1, Skp1, and Skp2 are colored as dark blue, light blue, green, and yellow, respectively. The image is obtained from protein data bank (PDB), using Rasmol software. Below, a cartoon representation of the structure of the SCF^{Skp2} complex. F denotes F-box. (b) An example of non-SCF cullin/RING finger complex in human cells, the CUL2/VBC complex. BC denotes B/C box. (c) Cul4 may also assemble a similar ubiquitin ligase complex with different adaptors recognizing different substrates.

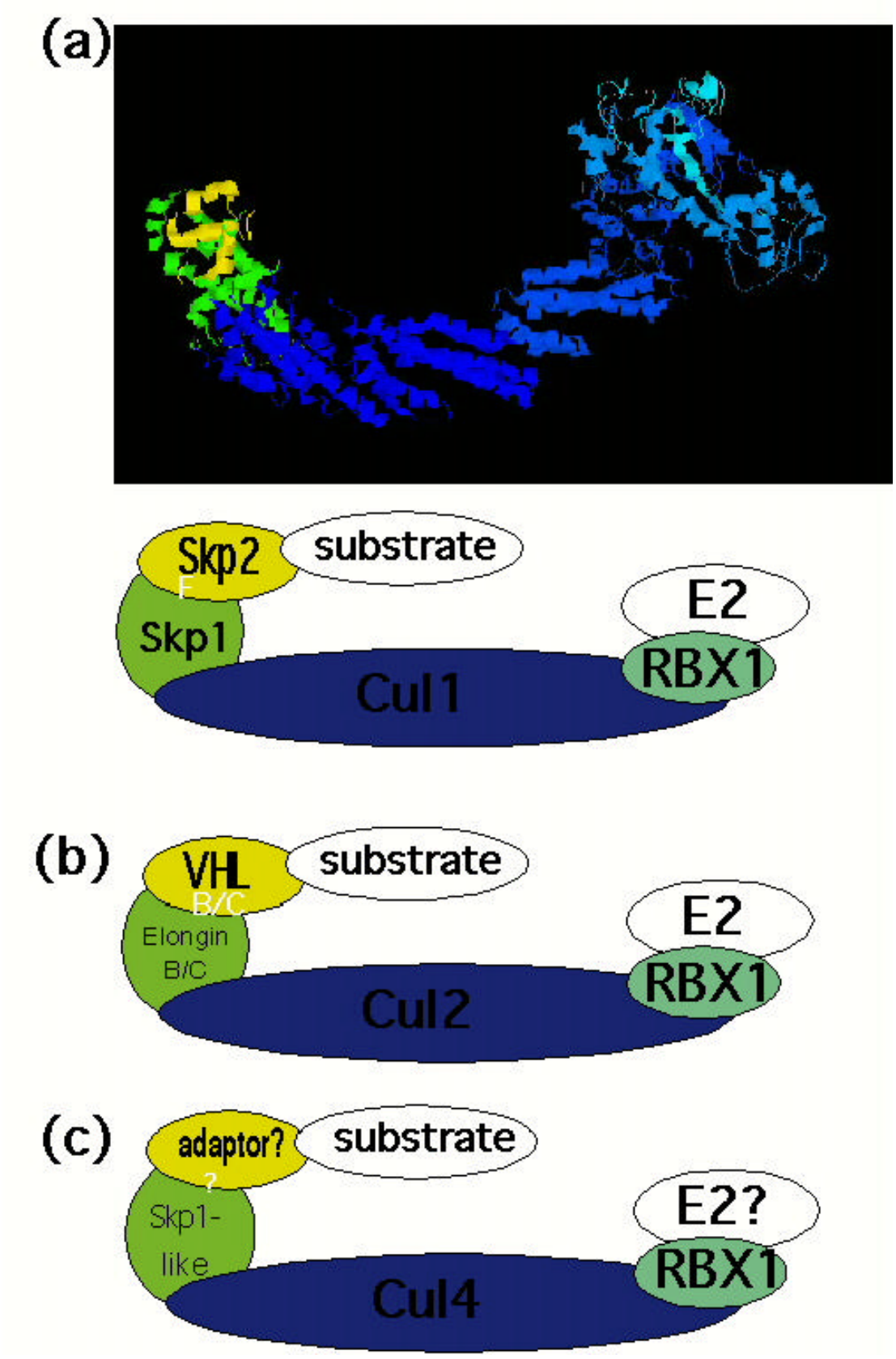
(a)
Skp2
F
substrate
Skp1
E2
RBX1
Cul1
(b)
VHL
B/C
substrate
Elongin
B/C
E2
RBX1
Cul2
(c)
adaptor?
?
substrate
Skp1-
like
E2?
RBX1
Cul4

CHAPTER 2

CUL-2 IS REQUIRED FOR THE G1-TO-S-PHASE TRANSITION AND MITOTIC CHROMOSOME CONDENSATION

Members of the cullin gene family have been shown to function as components of cullin/RING finger ubiquitin ligase (E3) complexes. The human protein CUL-2 functions in an E3 complex with the VHL tumor suppressor protein. Here in this chapter, I will demonstrate that in *Caenorhabditis elegans*, the cullin CUL-2 is required at two distinct points in the cell cycle. First, CUL-2 is required for the G1 to S phase transition, and in the absence of CUL-2, germ cells arrest in G1 phase. This G1 arrest is correlated with accumulation of the cyclin-dependent kinase inhibitor (CKI) homolog CKI-1. Inactivation of *cki-1* suppresses the G1 arrest, suggesting that the arrest results from an inability to regulate CKI-1 levels. Second, CUL-2 is required for normal mitotic progression. In *cul-2* embryos, mitotic chromosomes are unable to condense fully. Missegregation of the uncondensed chromosomal DNA results in chromosome bridging and the formation of multiple nuclei in cells.

BACKGROUND

In this section, I will describe what is known about the molecular process during the normal G1-to-S phase progression and the processes that are required for normal mitotic chromosome condensation, both of which are defective in *cul-2* mutants. Since

CUL-2 is a member of the cullin ubiquitin ligase family, it is necessary to highlight the known functions of ubiquitin-mediated degradation in these processes.

The G1-to-S phase cell cycle transition

The G1-to-S phase transition is best understood in budding yeast. I will use budding yeast as a model to briefly introduce the molecular changes that occur during the G1-to-S phase transition and the known involvement of cullin/RING finger complexes in this process. In *S. cerevisiae*, the G1 cyclins, Cln1p, Cln2p, and Cln3p associate with the CDK Cdc28p to form active G1-cyclin-CDK complexes that allow cells to progress through G1 phase (Nasmyth, 1996). In late G1 phase, the transcription of the S-phase cyclin genes *CLB5* and *CLB6* begins (Nasmyth, 1996). Once the S-phase cyclins are synthesized, they complex with Cdc28p (Nasmyth, 1996). However, these S-phase-cyclin-CDK complexes are inactive during G1 phase because of the presence of the CDK-inhibitor (CKI) Sic1p (Schwob et al., 1994). Sic1p directly associates with the S-phase-cyclin-CDK complexes and inhibits their kinase activity (Schwob et al., 1994). Sic1p is stable during early G1 phase preventing the precocious activation of S-phase -cyclin-CDKs (Schwob et al., 1994). At the G1-to-S phase transition, Sic1p is phosphorylated by Cln1, 2-Cdc28p (Nasmyth, 1996). The phosphorylated form of Sic1p is recognized by the ubiquitin ligase (E3) complex of SCF^{Cdc4} and its associated E2 Cdc34p (King et al, 1996). Sic1p is then targeted for ubiquitin-mediated degradation by the 26S proteasome (King et al, 1996). The active S-phase-cyclin-CDKs then initiate DNA replication presumably by phosphorylating key S phase regulators such as Sld2p (Masumoto et al., 2000). The degradation of the Sic1p protein appears to be the main

regulation of entry to S phase. Inability to degrade Sic1p in *cdc4* mutants results in G1 arrest (Schwob et al., 1994). It is interesting that Cdc53p is involved in the degradation not only of negative cell cycle regulators (e.g., Sic1p) that inhibit CDK activity, but also of the positive cell cycle regulators (e.g., G1 cyclins) that promote CDK activity.

In this chapter, our research demonstrates that CUL-2 negatively regulates CKI-1 and is required for the G1-to-S-phase transition in *C. elegans*. This extends our knowledge about how cullin/RING finger complexes regulate the cell cycle in higher eukaryotes.

Mitotic chromosome condensation

During mitosis, chromatin is bundled into a more condensed state and packs into a compact mitotic chromosome. After mitosis, chromosomes decondense into an extended chromatin form. Why do cells undergo the trouble to enforce such dramatic changes in chromosome structure? The biological importance of the chromosome condensation rises from two potential problems of chromosome segregation.

First, sister chromatids are tangled together after DNA replication (Sundin and Varshavsky, 1981; Weaver et al., 1985). Further, interphase chromosomes (in chromatin form) presumably may tangle with each other because of chromatin diffusion (Koshland and Strunnikov, 1996). In mitosis, sister chromatids are pulled to different poles. The cell separates sister chromatids to divide the chromosomes into two equal sets. Each daughter cell gets one set of chromosomes. If these chromosomes are tangled together, it will be difficult to move the chromosomes. A forced segregation will inevitably cause chromosome fragmentation. This problem will be eliminated if all chromosomes are

condensed with no tangles among them. I will explain how chromosome condensation contributes to detangling in the later topoisomerase II section.

Second, the length of chromatin is much longer than the length of the cell (Koshland and Strunnikov, 1996). If the chromosomes are not condensed in mitosis, the extended stringy chromatin can easily cross the midpoint and be cut by the later cytokinesis. Condensed chromosomes can be concentrated at poles and kept away from the dividing plane.

Current researches have implied that three classes of proteins function in chromosome condensation: histones, topoisomerase II, and the condensin proteins (Koshland and Strunnikov, 1996; Uhlmann, 2001).

Histones

Histones are the major protein component in chromosomes. Histones H2A, H2B, H3, and H4 form an octamer complex called the nucleosome. DNA molecules wrap around nucleosomes to form a 10-nm fiber, which is the base structure in chromatin organization (Koshland and Strunnikov, 1996). The linker histone H1 binds to the nucleosomes and has been implicated in contributing to the more condensed 30-nm fiber (Koshland and Strunnikov, 1996). At the time of chromosome condensation, several modifications of histones have been observed: histones H1 and H2A become hyperphosphorylated, histone H3 becomes phosphorylated, and histones H2A and H2B are de-ubiquitinated (Koshland and Strunnikov, 1996). The importance of many of these correlations is not fully understood.

Histone H1 hyperphosphorylation appears not to be essential for chromosome condensation. In mouse HT210 cells, full chromosome condensation can be induced without histone H1 hyperphosphorylaton (Guo et al., 1995). Normal chromosome condensation is also observed in *Xenopus* mitotic egg extract depleted of histone H1 (Ohsumi et al., 1993). Therefore, histone H1 hyperphosphorylation is not required for the structural reorganization that leads to mitotic chromosome condensation.

Histone H3 phosphorylation, however, appears to have an important role in chromosome condensation. Mitotic chromosome condensation can be induced in interphase cells by treating the cells with the phosphatase inhibitor okadaic acid or fostriecin (Guo et al., 1995). This phosphatase treatment correlates with elevated levels of histone H3 and histone H2A phosphorylation (Guo et al., 1995). In the presence of the protein kinase inhibitor starosporine, the induced chromosome condensation in mouse FT210 cells by adding fostriecin is abolished (Guo et al., 1995). Starosporine blocks histone H3 but not histone H2A phosphorylation (Koshland and Strunnikov, 1996). This suggests that histone H3 phosphorylation may be necessary for mitotic condensation. In contrast, histone H2A hyperphosphorylation may not be essential for this process. Genetic studies in *Tetrahymena* demonstrated that phosphorylation of histone H3 at serine 10 is required for proper chromosome condensation (Wei et al., 1999). It was suggested that in *C. elegans*, the Aurora-like kinase AIR-2 may phosphorylate histone H3 (Speliotes, et al., 2000) .

Histone H2A and H2B are monoubiquitinated during interphase (Koshland and Strunnikov, 1996). This ubiquitin modification disappears in metaphase and re-appears in anaphase (Koshland and Strunnikov, 1996). However, there is no evidence to link

histone de-ubiquitination and chromosome condensation. Ubiquitinated histone H2A and H2B have only one ubiquitin attached, rather than a multi-ubiquitin chain, and this monoubiquitination does not lead to protein degradation.

Topoisomerase II

Topoisomerase II can create a transient double stranded break in DNA, allow a second DNA molecule to pass through the break and then reseal the DNA strands (Hsieh and Brutlag, 1980; Kreuzer and Cozzarelli, 1980). This ability allows one DNA molecule to cross through another and therefore it can resolve intertwining DNA strands in tangled DNA molecules. It can also relax DNA superhelical coils. Topoisomerase II activity is required for a number of cellular processes including transcription, DNA replication, and chromosome condensation (Koshland and Strunnikov, 1996).

Several biochemical and genetic studies have revealed that topoisomerase II activity is required for mitotic chromosome condensation. A temperature-sensitive topoisomerase II mutant in *S. pombe* displays uncondensed, entangled chromosomes after a shift to non-permissive temperature (Uemura et al., 1987). Further, it was observed that chromosome condensation is impaired in topoisomerase II-depleted mitotic extract derived from *Xenopus* eggs (Adachi et al., 1991).

The ability of topoisomerase II to relax DNA superhelical coils cannot account for its essential function in chromosome condensation, as this function can also be achieved by topoisomerase I (Koshland and Strunnikov, 1996). Rather, it is believed that the ability of topoisomerase II to detangle chromatin strands facilitates chromosome condensation (Koshland and Strunnikov, 1996). DNA replication causes sister

chromatids to be catenated (Sundin and Varshavsky, 1981; Weaver et al., 1985). Topoisomerase II allows the passage of one DNA molecule through another, and therefore allows the removal of these tangles between chromosome strands. This enables chromosome condensation and later sister chromatid separation.

Topoisomerase II does not appear to actively initiate condensation of chromosomes. It randomly opens and closes double strands of a DNA molecule to allow the inter-passage of other DNA strands. This is not a deterministic process to remove DNA intertwining between chromatid strands. At a given time, topoisomerase II activity may add or remove DNA intertwining. Active chromosome condensation provides directionality of the tangling-detangling activity of topoisomerase II and prevents chromatin strands from tangling together again. One observation to support this hypothesis is that once chromosome condensation is completed, depletion of topoisomerase II in mitotic *Xenopus* egg extracts has no effect on chromosome morphology (Hirano and Mitchison, 1993). Therefore, other mechanisms are required to maintain chromosomes in their condensed state.

Condensin proteins

Unlike topoisomerase II, the condensin proteins are required for both the establishment and the maintenance of chromosome condensation. The condensin complex was first identified in a biochemical approach to identify proteins that are specific to isolated metaphase condensed chromosomes in *Xenopus* (Hirano and Mitchison, 1994; Hirano et al., 1997). Condensin purified from Xenopus mitotic extracts binds directly to DNA and has ATPase activity (Kimura and Hirano, 1997). It can

introduce positive DNA supercoils in vitro (Kimura and Hirano, 1997). Most condensin subunits are conserved in eukaryotes from yeast to man (Hirano, 2000). Condensin has two subcomplexes, a core complex composed of two subunits XCAP-C and XCAP-E (XCAP stands for *Xenopus* chromosome-associated polypeptides), and a regulatory subcomplex composed of three subunits XCAP-D2, XCAP-H and XCAP-G (Hirano and Mitchison, 1994; Hirano et al., 1997).

XCAP-C and XCAP-E were found to be homologs of *S. cerevisiae* Smc2p and Smc4p proteins, respectively (Hirano, 2000). The SMC (structural maintenance of chromosomes) family of proteins was identified earlier in yeast genetic studies (Larionov et al., 1985; Strunnikov et al., 1993). The *S. pombe* homologs of Smc2p and Smc4p are called Cut14p and Cut3p, respectively (Saka et al., 1994). FISH experiments have shown that *smc2*, *cut14*, and *cut3* mutations perturb chromosome condensation (Saka et al., 1994; Strunnikov et al., 1995). *smc* mutants have phenotypes that are similar to those of topoisomerase II mutants, which is considered a signature phenotype for chromosome condensation defects (Koshland and Strunnikov, 1996). The phenotypes include an inability to properly segregate chromosomes, often resulting in a 'cut' phenotype in which chromosomes are cleaved by cytokinesis; a reduction in the compaction of chromosomes; and reduced chromosome integrity resulting in long chromosome threads as chromosomes are pulled by the mitotic spindle (Koshland and Strunnikov, 1996).

Xenopus immunodepletion and add-back experiments showed that the non-SMC regulatory subcomplex of condensin is required for mitotic chromosome condensation in vitro (Hirano et al., 1997). The *S. pombe* homologs for XCAP-D2, XCAP-H, and XCAP-

G are called Cnd1-Cnd3, respectively. Yeast genetic studies demonstrated that these genes are required for chromosome condensation and segregation (Sutani et al., 1999).

Some experiments indicated that there are other unknown regulators of chromosome condensation. In *Drosophila*, chromosomes of *gluon* (SMC4 homologue) mutant cells are not condensed. However, the length of their axis is shortened equivalent to that observed in wild-type cells (Steffensen et al., 2001). This suggests that condensins may function to condense loops of chromatin extended from the axis, while other mechanisms are required to shorten the chromosome axis.

Currently there is no known requirement for protein degradation in mitotic chromosome condensation. In this chapter, I will demonstrate that CUL-2, a member of the cullin ubiquitin ligase family, is required for mitotic chromosome condensation. This is the first finding that suggests that ubiquitin-mediated proteolysis may be required for mitotic chromosome condensation.

RESULTS

cul-2 mutant and *cul-2* depletion by RNA–mediated interference (RNAi)

One approach to study the function of a gene is to inactivate the gene and study the resulting cellular and organismal defects cause by the loss of gene function. In *C. elegans*, there are two methods commonly used to inactivate gene functions. One is through genomic mutation in which the specific gene has been mutated by point or missense mutations. The other method is RNA-mediated interference (RNAi) in which

double stranded RNA of a specific gene is microinjected into wild-type hermaphrodites to inactivate gene function in their progeny (Fire et al., 1998).

To study *cul-2* function, a *cul-2* deletion mutant, *ek1,* was isolated during a PCR-based mutant screen. The *ek1* mutation was mapped and found to be a 1.2 kb deletion that completely removes exons 2, 3, and 4, as well as the first four base pairs of exon 5, thereby removing the 5' splice site of exon 5 (Figure 2.1). The mutant allele is completely recessive and *cul-2* heterozygotes are indistinguishable from wild-type. From a heterozygous parent, *cul-2* homozygous progeny have normal embryonic development and all postembryonic somatic cell divisions are also normal (Figure 2.2, data not shown). In contrast to somatic cell divisions, there are fewer, larger germ cells in *cul-2* homozygous mutants (Figure 2.2). These *cul-2* homozygous adult hermaphrodites lay a few arrested embryos (17±13 progeny / hermaphrodite n=22; compared to wild-type 288±36 progeny / hermaphrodite n=10) (Figure 2.2).

When we performed RNAi to inactivate *cul-2* function, we observed 100% embryonic arrest approximately 16 hours post-injection. The phenotype of the *cul-2* deficient embryos produced by RNAi was indistinguishable from that of embryos produced by homozygous *cul-2*(*ek1*) (Figure 2.2).

The observation that *cul-2* homozygotes from heterozygous parents show normal somatic development, whereas *cul-2* RNAi produces arrested embryos in the immediate progeny suggested that the *cul-2* maternal product from heterozygous parents is sufficient to allow normal embryonic development.

cul-2 mutant germ cell phenotypes

As mentioned in the previous section, *cul-2* homozygous adult hermaphrodites derived from heterozygous parents have fewer larger germ cells than wild-type animals (Figure 2.3 a, b). This phenotype of fewer germ cells in *cul-2* homozygous animals becomes apparent at the L3 larval stage (36 hours post hatch) (Figure 2.3 c). When *cul-2* homozygotes become young adults (48 hours post hatch), there is no further increase in germ cell number; in contrast, the germ cell number in control group young adults will continue to increase over 60% more (Figure 2.3 c). At 61 hours post hatch, *cul-2* adult homozygotes have on average 270 germ cells while control animals have 1040 germ cells (Figure 2.3 c). *cul-2* germ cell nuclei are two-fold larger than wild-type at the L4 stage ($54 \pm 16\ \mu m^3$ versus $27 \pm 6.1\ \mu m^3$, n=30, respectively; Figure 2.3 a, b).

In *C. elegans*, germ cells are the only cells that divide continuously rather than according to a programmed division plan (Kimble and Hirsh, 1979). Every time a cell divides into two cells, the maternal product is diluted by half assuming equal partitioning. Since germ cells divide continuously, CUL-2 maternal product will be continuously diluted. Eventually, the CUL-2 maternal product will be too diluted to maintain normal function. The germ blast cells Z2 and Z3 divide considerably more than other blast cells in the larvae, producing over 1000 progeny, which is more than the entire somatic cell number. Therefore, CUL-2 maternal product will be lost most effectively in the most extensively divided germ cells. In fact, there is no difference in germ cell number between *cul-2* homozygous animals and control animals until 24 hours post hatch (Figure

2.3 c). The difference becomes greater as the animals develop (Figure 2.3 c). This pattern suggests the dilution of CUL-2 maternal product as germ cells divide.

The observation that there are fewer germ cells in *cul-2* mutants and that they are larger than normal suggested two possible cell cycle defects: 1) an arrest in G1, the growth phase, which would allow the cells to accumulate mass; or 2) entry into a special endoreplication cycle, in which cells bypass mitosis and enter the next cell cycle with doubled DNA content (Hedgecock and White, 1985). Endoreplication also increases cell and nuclear size (Hedgecock and White, 1985). These two possible defects can be distinguished by DNA content. Cells arrested in G1 phase have 2n DNA content, while endoreplicating cells have greater than 2n DNA as a result of multiple rounds of DNA replication. To determine which mechanism applies to the *cul-2* germ cell phenotype, we measured the genomic DNA content of germ cells in *cul-2*(*ek1*) homozygotes and wild-type. Wild-type germ cells have a bimodal distribution with the majority of cells having either 2n or 4n DNA content corresponding to G1 and G2/M phases, respectively (Figure 2.4). In contrast, *cul-2* mutants have a single peak at 2n, indicating an accumulation of cells in G1 phase (Figure 2.4).

To further confirm this result, we reasoned that if *cul-2* germ cells are arrested in G1 phase, there should be fewer *cul-2* germ cells in mitosis. The mitotic index, which indicates the percentage of mitotic cells, was determined by immunofluorescence with the mitotic marker, anti-phosphohistone H3 antibody (Hendzel et al., 1997). We found that the mitotic index decreased from 4.7 ± 2.6% (126 mitotic cells/2680 total) in wild-type young adults to 1.4 ± 2.2% (13 mitotic cells/892 total) in *cul-2*(*ek1*) young adults, a 3.4-fold decrease. The decrease in mitotic division, coupled with the larger germ cell

size and accumulation of cells with 2n DNA content, indicates that *cul-2* germ cells undergo a G1 phase arrest with cells either severely delayed or blocked in entry into S phase. Therefore, CUL-2 is required for normal G1-to-S-phase cell cycle transition.

Accumulation of CKI-1 in *cul-2* germ cells causes G1 arrest

The finding that *cul-2* mutant germ cells undergo G1 arrest, coupled with the insight that the *cul-2* homolog Cdc53p functions as part of an E3 complex to degrade cyclin-dependent kinase inhibitors (CKIs) (Skowyra et al., 1997; Feldman et al., 1997; Henchoz et al., 1997), suggested a model in which CUL-2 also functions to degrade CKIs. An inability to degrade CKIs would be expected to lead to cell cycle arrest. We searched the *C. elegans* genome database for homologues to human CKIs $p21^{CIP1}$ and $P27^{KIP1}$. We discovered two *C. elegans* CKI homologs, *cki-1* and *cki-2*. Like its yeast and mammalian homologues, CKI-1 may function as a G1 phase CDK inhibitor, but the function of CKI-2 is unclear. Overexpression of CKI-1 inhibits cell division (Hong et al., 1998). Only *cki-1* RNAi but not *cki-2* RNAi results in hyperplasia (extra number of cells) (Hong et al., 1998; and data not shown), indicating that *cki-1* functions non-redundantly as a negative cell cycle regulator.

To determine whether the level of CKI-1 was increased in *cul-2* mutant germ cells, we generated polyclonal anti-CKI-1 antibodies. Antibodies were raised in two different rabbits, and the sera were affinity-purified. Purified antibodies from both rabbits gave a similar pattern of staining (data not shown). The specificity of the antibodies was determined by observing the level of staining in embryos homozygous for

mnDf100, a deletion that removes *cki-1*. We observed no specific staining of *mnDf100* embryos indicating that the antibodies were specific for CKI-1 (Figure 2.5 a-d).

We determined the level of CKI-1 in gonad arms of wild-type and *cul-2*(*ek1*). In wild-type animals, CKI-1 is barely detectable above background levels in distal germ cells. This is the mitotic zone of worm gonad in which germ cells undergo active cell cycles. As germ cells enter meiosis, the level of CKI-1 increases and attains the highest intensity in the nuclei of oocytes (Figure 2.5 e). In *cul-2*(*ek1*) gonad arms the level of CKI-1 is higher than in wild-type, particularly in the distal region (Figure 2.5 f). We measured the relative intensity of the anti-CKI-1 immunofluorescence signal in *cul-2*(*ek1*) and wild-type adult gonad arms with a confocal microscope. The amount of CKI-1 signal per distal nucleus in *cul-2*(*ek1*) is 13-fold higher than in wild-type (13 ± 10, n=50, versus 1.0 ± 0.9 arbitrary units, n=36). The intensity of CKI-1 staining level, irrespective of nuclear volume, is 2.5-fold higher in *cul-2* than in wild-type.

This increase of CKI-1 protein in *cul-2* mutants is not due to increased transcription. *cki-1* mRNA levels were determined by RNA *in situ* hybridization. The *cki-1* mRNA *in situ* signal in *cul-2* distal gonads is lower than wild-type (1.0 ± 0.5, n=8, versus 2.1 ± 0.7 arbitrary units, n=10) (Figure 2.5 i-k). Therefore, the accumulation of CKI-1 protein in *cul-2* is post-transcriptional. It is likely due to a failure of protein degradation, considering the ubiquitin ligase function of the cullin family. The decrease of *cki-1* mRNA in *cul-2* mutants may be due to a feedback regulation in response to the increased CKI-1 protein level.

In contrast to *cul-2* mutants, CKI-1 level does not increase relative to wild-type in germ cells of *cul-1* null mutants; *cul-1* is the cullin most closely related to *cul-2* (Nayak et

al., 2002). We also produced affinity-purified antibodies to the CKI-2 protein. We did not observe an increase in CKI-2 protein in *cul-2* gonads.

If the increased level of CKI-1 protein in *cul-2* germ cells was contributing to the G1 arrest, then reducing the level of CKI-1 in *cul-2* mutants should suppress the phenotype. One possible method of reducing the level of CKI-1 is to remove one genomic copy of the *cki-1* gene. Suppression of the G1 arrest phenotype should result in the production of more eggs. To test this prediction, we created the strain *cul-2*(*ek1*) / *unc-64*(e246); *mnDf100 unc-4*(*e120*) / *mnC1*. *mnDf100* is a deficiency that removes both *cki-1* and *cki-2*. This strain segregates *cul-2*(*ek1*); *mnDf100*/*mnC1* animals that are homozygous for *cul-2*(ek1) and heterozygous for *mnDf100*. In these *cul-2* homozygotes, one chromosomal copy of *cki-1/-2* was deleted by the deficiency *mnDf100*. We determined that the germ cell number increased 30% in these animals relative to *cul-2*(*ek1*) alone (353 ± 25 cells versus 278 ± 59 cells, n=11, respectively) and that this correlated with a 3.3-fold higher egg number (57 versus 17), indicating a partial suppression of the *cul-2* germ cell arrest phenotype by the heterozygous *mnDf100* (Table 2.1). Since the *mnDf100* deficiency deletes a large region in the chromosome, in order to clarify whether the *cki-1*/*cki-2* region was the region critical for the suppression, the cosmid T05A6, which contains genomic *cki-1* and *cki-2*, was introduced into the strain. An extrachromosomal array of this cosmid did not affect egg number in a phenotypically wild-type strain (Table 2.1). However, the array abolished the suppression of *cul-2* by heterozygous *mnDf100* (producing on average 15.5 eggs rather than 57 eggs), indicating that the small region including the *cki-1* and *cki-2* genes was responsible for the heterozygous suppression of *cul-2* (Table 2.1).

To determine whether decreasing the level of CKI-1 or CKI-2 was responsible for the suppression of *cul-2*, we injected dsRNA for either *cki-1* or *cki-2* into L4 stage *cul-2* animals and then determined the number of eggs produced as adults. Injection of *cki-1* dsRNA was capable of partially suppressing the *cul-2* arrest, producing 58 ± 21 eggs, which is a 3.4-fold higher egg number than for *cul-2* (Table 2.1). In contrast, injection of *cki-2* dsRNA did not alleviate the *cul-2* germ cell arrest (Table 2.1). Injection of either *cki-1* or *cki-2* dsRNA into wild-type animals did not increase cell number. These results indicate that the *cul-2* G1 phase arrest is dependent on CKI-1 protein level, as reducing the level of CKI-1 suppresses the arrest phenotype.

cul-2 mutant embryonic phenotypes

As mentioned above, *cul-2* homozygous adult hermaphrodites lay a few arrested embryos (Figure 2.2). On average, *cul-2* homozygotes lay only 17 fertilized eggs, compared to almost 300 eggs in wild-type (Table 2.1). These *cul-2* eggs are indistinguishable from arrested embryos produced by *cul-2* RNAi (Figure 2.2). *cul-2* embryos arrest development at an extremely early stage with only 24 ± 4.6 cells (n=20). This arrest does not appear to be due to CKI-1 accumulation, as the level of CKI-1 in *cul-2* embryos is the same as that in wild-type embryos (data not shown). CKI-1 protein is maternally provided and does not appear to inhibit the rapid cell divisions of the early embryo (data not shown). Because substrates of the SCF cullin/RING finger complexes are known to be targeted for ubiquitination by phosphorylation (Deshaies, 1999), it is possible that maternal CKI-1 is not marked (by phosphorylation) for degradation.

To trace back the starting time of the embryonic defects, we examined the process of *cul-2* meiosis and the first mitosis after fertilization in *cul-2* zygotes. Meiosis in *C. elegans* is similar to meiosis in other organisms, where homologous pairs of chromosomes are separated in meiosis I and sister chromatids are separated in meiosis II. In meiosis I, prophase can be differentiated into five different stages: leptotene, when the chromosomes first become visible as fine threads and have not yet associated in pairs; zygotene, when the homologous chromosomes are associating side by side; pachytene, when homologous chromosomes are associated throughout their length; diplotene, when the two chromosomes making up each homologous pair have separated from one another except at nodes (chiasmata) distributed along their length; and diakinesis, when the chromosomes are well separated from one another and the homologous pair of chromosomes are held together by chiasmata.

In *C. elegans*, mature oocytes are arrested at diakinesis. At the time of fertilization, the oocyte nucleus moves toward the distal end of the cell and resumes meiosis I. After meiosis I, the egg segregates one polar body of 2n content DNA. The oocyte nucleus then completes meiosis II and forms an oocyte pronucleus. After meiosis II, a second polar body of 1n DNA is segregated. During the time when the oocyte nucleus is undergoing meiosis, the sperm forms the sperm pronucleus. Once the oocyte and sperm pronuclei are formed, cytoplasmic movements called pseudocleavage occur, which culminate in a deep furrow that appears and regresses near the equator. Concurrently with the deep pseudocleavage furrow, the oocyte pronucleus migrates toward the sperm pronucleus. Once the two pronuclei meet, they move to their final position in the center of the egg. The pronuclear envelopes then break down, and the two

pronuclei fuse into one mitotic zone, commencing prometaphase of the first mitosis. This whole process of meiosis leading to the first mitosis is reviewed by Wood et al., 1988.

Early meiotic events appear normal in *cul-2* mutants. Entry of *cul-2* germ cells into the pachytene stage of meiosis is normal; and oocytes, which are arrested in diakinesis of meiosis I, have the normal 2n DNA content with six chromatid pairs visible upon staining with DAPI, while sperm have normal 1n DNA content (data not shown). In very old *cul-2*(*ek1*) adults (≥4 days post larvae), we observe separation of sister chromatid bivalents in diakinesis. The significance of the phenotype is currently not clear. This separation defect is only observed in old adults that have ceased laying eggs and is therefore unlikely to affect the embryonic defects described later which were analyzed in younger animals. We have observed four fixed *cul-2*(*ek1*) embryos in anaphase of meiosis I and found that in all cases equal segregation of genomic DNA occurred.

Some but not all *cul-2* mutants are defective in later meiotic stages before fertilization. In the case of meiosis II, in contrast to meiosis I, only one third of *cul-2* zygotes show normal DNA distribution pattern (6 out of 18). We observed that approximately half of *cul-2* zygotes fail to extrude a second polar body and that the second polar body was larger than normal in approximately 7% of the cases. In those zygotes with two polar bodies, we observed normal DNA segregation for meiosis II in approximately two thirds of the cases (6/9).

All *cul-2* eggs show the following phenotypes once meiosis is over, namely, cytoskeletal movement defects, multiple nuclei in cells, and increased length of mitosis. I will describe these below.

Cytoskeletal Movement Defects

A basic defect in the cytoskeletal organization of *cul-2* embryos is apparent from three phenotypes. First, migration of pronuclei is defective. In wild-type, the events from formation of pronuclei to zygote fusion take 14 ± 2 minutes (n=10). In contrast, the same process takes almost eight times as long in *cul-2* zygotes, 110 ± 15 min (n=10). The principle defect we observed during this time is a failure of the oocyte pronuclei to travel toward the sperm pronuclei. While sporadic motion occurs, it is not directed. Further, when random movements bring pronuclei together, a secondary migration to the center of the zygote fails to occur. The resulting division plane and subsequent cleavage are not usually oriented in the same location or direction as in wild-type.

Second, mitotic spindles are generally mispositioned and misoriented. The seemingly random placement of the mitotic spindle is observed in the first mitosis as well as in subsequent mitotic divisions.

Third, there are extensive cytoplasmic projections that occur in all directions, starting after the first mitotic division (Figure 2.6 a, c-e). In wild-type embryos, through the use of time-lapse video tape-recording, we observed a brief period after mitosis is completed when small cytoplasmic extensions arise at points immediately adjacent to neighboring cells (data not shown). Interestingly, these cytoplasmic projections are the forerunner of more extensive cortical membrane movements that extend the area of contact between neighboring cells. In *cul-2* mutants, cytoplasmic extensions also begin immediately after mitosis, but these projections are much more extensive and do not lead to increased cell contact (Figure 2.6 a, c-e). The limited extensions of wild-type are generally observed to occur on only one cell surface (e.g., the posterior of the ABa cell).

In contrast, extensions in *cul-2* embryos occur in all directions and produce long processes, up to a cell diameter in length that can "pinch-off" to produce cytoplasts (Figure 2.6 c-e).

Multiple Nuclei in Cells

During mitotic embryonic cycles, multiple nuclei are present in *cul-2* cells (Figure 2.6 a, b, h). Multinuclei can theoretically form by two different mechanisms: 1) a defect in cytokinesis, in which the cell fails to divide into two daughter cells but chromosomes are separated to two poles, so that segregated daughter chromatids form two nuclei in the same cell, or 2) a failure of chromosome condensation and segregation, in which cytokinesis occurs normally, but chromosome fragments resulting from defective chromosome segregation cause the formation of multiple nuclei. In *cul-2* mutants, the second mechanism is clearly observed. *cul-2* cells were observed by DIC microscopy to progress through mitosis with a single mitotic zone, complete cytokinesis, and then immediately form multiple nuclei in the daughter cells (Figure 2.6 f-h). The multinuclei are often of radically different sizes (Figure 2.6 a, b, h). The extra nuclei have nuclear pores, as revealed by immunostaining with an anti-nuclear pore antibody (Figure 2.6 k), suggesting that nuclear membrane formation around chromosomes occurs normally in *cul-2* mutants.

Increased Length of Mitosis

The cell cycle timing of *cul-2* mutants is dramatically lengthened in relation to wild-type. This is observed both for cells with multiple nuclei and cells with a single

nucleus, suggesting that the presence of multiple nuclei is not responsible for the delay in cell cycle progression (Figure 2.7). The increase in cell cycle length is largely due to an increase in the length of mitosis. *cul-2*(*ek1*) mutants have a six-fold longer mitotic period on average than wild-type, 33 ± 19 min and 5.8 ± 1.5 min, n=33, respectively. In contrast, the length of interphase in *cul-2*(*ek1*), while variable, is on average comparable to the first four divisions of wild-type (11 ± 10 min, n=19, versus 12 ± 3.2 min, n=30, respectively).

Occasionally, *cul-2* embryonic cells have "failed mitoses" in which mitosis ends without cytokinesis or internal segregation of chromosomal DNA (Figure 2.7). These failed mitoses result in a doubling of centrosome number. Once a failed mitosis occurs, the presence of multiple centrosomes compounds the difficulty in progressing through mitosis to a normal cytokinesis due to the creation of multi-valent mitotic spindles and therefore the probability of further failures of mitosis increase for that cell. All cells have lengthened mitosis, not just those with extra centrosomes.

To determine which mitotic phase is extended in *cul-2* mitosis, we determined the percentage of cells in each phase of mitosis for those cells with only two centrosomes. Early wild-type and *cul-2*(*ek1*) embryos were fixed and co-stained with anti-phosphohistone H3 antibody (a mitotic marker), anti-AIR-1 (a centrosome marker, Schumacher et al., 1998), and DAPI (to observe the distribution of chromosomal DNA). We observed that the percentage of cells in prometaphase increased from 35% to 65% (n=100) in *cul-2* cells relative to wild-type, with coincident decreases in other stages of mitosis. Therefore, *cul-2* cells have prolonged prometaphase.

Defect in mitotic chromosome condensation in *cul-2* embryos

During prometaphase, the nuclear envelope is no longer intact, and sister chromatids are in the process of being aligned at the metaphase plate by the mitotic spindle. We first examined the structure of the mitotic spindle using anti-tubulin antibody and anti-AIR-1 antibody. At a gross morphological level, the mitotic spindle appears normal (Figure 2.8 a, c). However, the chromosomes in *cul-2* embryos appear strikingly uncondensed (Figure 2.8 b, d). During anaphase, *cul-2* chromosomes do not segregate efficiently to mitotic poles and sheared strands of chromosomal DNA are observed (Figure 2.8 b, d). The formation of nuclei around missegregated chromosomes and chromosome fragments apparently contributes to the observed multiple nuclei, some of which have very little DNA (Figure 2.6 i-k).

The following *cul-2* defects are attributable to chromosome condensation defect in later cell divisions: unequal DNA segregation (Figure 2.6 i-k), DNA bridges between dividing cells (Figure 2.6 l, m), and failed mitoses (Figure 2.7), which produce cells with multiple centrosomes.

To look at the initial state of mitotic DNA condensation, we observed chromosome condensation in the first mitosis immediately after fusion of pronuclei in the zygote. We froze zygotes at the time of fusion of the oocyte and sperm pronuclei, which corresponds to the beginning of prometaphase. Condensed wild-type chromosomes are shown in Figure 2.8e, while non-condensed *cul-2*(*ek1*) chromosomal DNA is shown in Figure 2.8g. We observed uncondensed chromosomes in all *cul-2* zygotes including those that had normal meiosis and entered mitosis with the normal 4n content of genomic DNA (data not shown). In *cul-2* RNAi embryos, all mitoses after the first one have

chromosomes that are as non-condensed as those observed in *cul-2*(*ek1*) embryos. However, we found that at the first mitosis, upon fusion of the pronuclei, the chromosomes enter a prolonged state of partial condensation. This partial condensation perdured for at least five minutes. Figure 2.8f shows elongated chromosomal DNA from a *cul-2* RNAi embryo that was fixed five minutes after fusion of the pronuclei. Note that five minutes after pronuclei fusion, wild-type cells would have progressed through mitosis and be in cytokinesis, indicating that the *cul-2* RNAi embryos were arrested in prometaphase with only partially condensed chromosomes. The elongated character of the chromosomes was similar to that observed in wild-type during prophase, suggesting that partial condensation occurred in the *cul-2* RNAi zygotes, presumably because of the effect of residual CUL-2 protein remaining after RNAi. Antibody staining revealed that, on average, 2% of CUL-2 protein remains after RNAi, visible upon longer exposure as faint nuclear staining (2.0±2.3 a.u., n=10, versus wild-type, 100±57 a.u., n=10). *cul-2* mutants show no nuclear staining.

The *cul-2* embryonic phenotype is superficially similar to that of meiosis defective mutants, such as *mei-1* mutants (Mains et al., 1990). In both cases, there are defects in meiosis with a percentage of embryos failing to extrude one or more polar bodies and the generation of large polar bodies. There are also multiple nuclei observed in cells. However, there are a number of significant differences. Unlike *cul-2*, *mei-1* loss-of-function mutants have normal timing of mitotic divisions and they arrest with hundreds of cells. The percentage of cells with multiple nuclei is very low in *mei-1* embryos, and these nuclei are generally the same size, unlike the high percentage of multiple nuclei in *cul-2* embryos, which have vastly different sizes.

To address whether a failure of meiosis can lead to an inability to condense chromosomes in mitosis, we analyzed chromosome condensation in progeny from homozygous *mei-1*(*b284*) hermaphrodites. We observed that regardless of whether there were more or less chromosomes than wild-type present at pronuclear fusion there was always normal chromosome condensation (Figure 2.8h). By analyzing embryonic cells that had multiple nuclei, we determined that multiple nuclei occur in *mei-1*(*b284*) mutants when there are excess chromosomes (generally 30 or more). However, the chromosomes underwent normal condensation during mitosis (Figure 2.8h). Therefore, the multinuclei phenotype in *mei-1* appears to result from an inability to align excess numbers of chromosomes that derive from defective meiosis, rather than from an inability to condense chromosomes as in *cul-2* mutants, which have uncondensed chromosomes and multiple nuclei even when meiosis occurs normally.

It seems likely that the inability to fully condense chromosomes in *cul-2* embryos is responsible for the other mitotic defects. In later mitosis, attempts to separate uncondensed chromosomes results in DNA bridging and unequal DNA segregation among daughter cells. Subsequently, multiple nuclei form around missegregated chromosomes and chromosomal fragments. This apparently contributes to the observation that the multiple nuclei in *cul-2* embryonic cells often have very little DNA.

DISCUSSION

We have demonstrated that CUL-2 is required in germ cells for cell cycle progression from G1 to S phase. In *cul-2* mutants, germ cells are larger than wild-type and arrest with 2n DNA content. The G1 arrest in *cul-2* mutant germ cells is correlated

with increased levels of CKI-1. Decreasing the level of CKI-1 suppresses the G1 phase arrest, indicating that the *cul-2* G1 arrest is dependent on the presence of CKI-1.

In early *C. elegans* embryos, cells undergo rapid cell divisions without the checkpoint machinery (Edgar and McGhee 1988) and therefore would not undergo a cell cycle arrest in *cul-2* mutants. The few embryos that are created by *cul-2* mutants arrest with only 24 cells on average. Their development is characterized by severe cytoskeletal and mitotic defects. A basic defect in the cytoskeleton organization is apparent from three phenotypes: defective migration of pronuclei, misaligned mitotic spindles, and extensive cytoplasmic projections. A major mitotic defect is a failure in chromosome condensation. This defect is observed from the first mitotic division and produces a number of secondary defects that arise from an inability of the mitotic spindle to align and segregate chromosomes: unequal DNA segregation, DNA bridges formed between segregated DNA, and the formation of multiple nuclei around DNA that had not coalesced.

In early *cul-2*(*ek1*) adults, the predominant germ cell phenotype is a G1 arrest, characterized by few, large nuclei. We do not see any evidence of multinuclei in L4 stage larvae or young adults, i.e., different sized germ cell nuclei or DNA content. However, in old *cul-2*(*ek1*) adults (4-5 days post-larvae), we observe a proportion of germ cells that are irregularly shaped and observe uncondensed mitotic DNA with DNA bridging (data not shown). This suggests, first, that the mitotic defect can manifest in a small percentage of older *cul-2* germ cells that are able to bypass the G1 arrest; and second, that *cul-2* maternal product is apparently still present even in the germ cells of

young adults. In the early embryonic divisions there is no G1 phase (Edgar and McGhee, 1988), and so the mitotic defects are readily apparent.

In *cul-2* embryos, chromosomes fail to condense properly, implicating *cul-2* as either a direct or indirect regulator of mitotic chromosome condensation. The observation that mitotic chromosome condensation requires CUL-2, a ubiquitin-ligase component, indicates that ubiquitin-mediated proteolysis may be required for this process *in vivo*. It is not known at present how CUL-2 facilitates chromosome condensation. In *cul-2* mutant embryos phosphorylation of histone H3 is still observed, indicating that *cul-2* is not required for this process (data not shown). Intriguingly, lack of topoisomerase II or one of the condensin complex components produces phenotypes in yeast and *Xenopus* that are very similar to that observed in *cul-2* embryos (see references in Koshland and Strunnikov, 1996). *C. elegans* has homologs for the major condensin complex components XCAP-C, XCAP-E, and XCAP-D2 (data not shown). Based on the similarity of phenotypes, it is possible that *cul-2* functions directly or indirectly to positively regulate either Topo II or the condensin complex.

SCF complexes function in both G1 and G2/M phases. *cdc34* or *cdc53* mutants in the absence of the CKI Sic1p undergo a G2 or mitotic arrest (Schwob et al., 1994). In contrast, *cul-2* mutant cells complete mitosis, often producing the 'cut' phenotype, similar to that observed in yeast condensin mutants defective in chromosome condensation (Figure 2.5l) (Koshland and Strunnikov, 1996). Cdc34p and Cdc53p are required for the degradation of the Swe1/Wee1 CDK-inhibitory kinase, which negatively regulates entry into mitosis (Michael and Newport, 1998; Kaiser et al., 1998). However, it is unlikely that *cul-2* is required for the degradation of Wee1, as a failure to degrade Wee1 would

lead to a failure to active the mitotic CDK, CDK1. CDK1 activation appears to be unaffected in *cul-2* mutants, because nuclear envelope breakdown and the assemble of the mitotic spindle, both of which require CDK1 activity (Boxem et al., 1999), occur normally.

Could an increase in CKI-1 contribute to the embryonic phenotypes? Theoretically, an inhibition of CDK activity could lead to the mitotic defects, as CDK1/Cdc2 is required for mitotic chromosome condensation (Kimura et al., 1998). Presently, we do not have any evidence to support such a model. We have not observed an increased level of CKI-1 in early *cul-2* embryos relative to wild-type and *cki-1* RNAi does not affect the *cul-2* embryonic phenotype (although we believe that *cki-1* RNAi is not complete as we never see a high percentage of arrested embryos) (data not shown). It is more likely that the *cul-2* embryonic defects occur via other cellular targets.

In *cul-2* mutant germ cells, there is a post-transcriptional increase in the level of CKI-1. Thus, CUL-2 may function as an E3 to target CKI-1 for degradation. Parsimony analysis suggests that the ancestor of yeast *CDC53* also gave rise to the higher eukaryotic cullins *cul-1* and *cul-2* (Kipreos et al., 1996). *C. elegans cul-1* functions as a negative cell cycle regulator. In the absence of CUL-1, blast cells undergo excessive cell divisions due to an inability to exit the cell cycle (Kipreos et al., 1996). CUL-1 is therefore likely to act through the degradation of positive cell cycle regulators, such as G1 phase cyclins, but is unlikely to degrade negative cell cycle regulators whose accumulation would inhibit cell cycle progression. The level of CKI-1 does not increase in *cul-1* mutants. In contrast to *cul-1*, *cul-2* functions as a positive cell cycle regulator and is therefore likely to act through the degradation of negative cell cycle regulators, such as CKIs. In

corroboration of this hypothesis, the level of CKI-1 does increase in *cul-2* mutants. Full confirmation of this model will have to await *in vitro* ubiquitination experiments. Nevertheless, it seems likely that functions of the ancestral *CDC53* gene (degrading positive and negative cell cycle regulators) may have been split among *cul-1* and *cul-2*. Additionally, *cul-2* appears to have acquired cellular functions not observed for *CDC53*. The observation that *cul-2* mutants have defects not only in G1-to-S phase progression but also in cytoskeletal movement and chromatin condensation may be seen as a harbinger of the myriad functions of the SCF correlates in higher eukaryotes. The SCF paradigm in yeast presents a single ubiquitin-conjugating enzyme, Cdc34p, bound by the cullin Cdc53p, which is bound to Skp1p, which is then bound to one of several F-box proteins each capable of targeting multiple proteins for degradation (see Patton et al., 1998). In higher eukaryotes the complexity of targets may radiate outward from the E2 at an expanded rate due to a greater number of E3 components: there are two cullins that are directly descendent from the ancestral *CDC53*, 21 *SKP1* homologs, and at least 366 F-box proteins in *C. elegans* (Nayak et al., 2002; Kipreos and Pagano, 1999). It is likely that the closer the component is to the E2 the more processes will be affected by its absence. A number of points need to be addressed to confirm this hypothesis, including the determination of which E2 (if any) CUL-2 interacts with.

VHL associates with CUL2 in the human VBC complex. Loss of VHL predisposes individuals to tumors of the kidney, retina, and brain (see Kaelin and Maher, 1998). VHL has been suggested to function by sequestering Elongin B and C from Elongin A, a transcription elongation factor for RNA polymerase II (Duan et al., 1995; Kibel et al., 1995). However, VHL has never been shown to affect transcription

elongation rates *in vivo* (Kaelin and Maher, 1998). Further, the level of Elongin B and C have been reported to be 100 to 1000 times higher than the level of VHL, making it unlikely that VHL functions to sequester either protein (Conaway et al., 1998). *C. elegans cul-2* and human VHL produce opposite mutant phenotypes, namely G1 arrest and tumor formation, respectively. In light of our findings that *cul-2* functions as a positive cell cycle regulator, an obvious model is that VHL functions to limit cell division by inhibiting CUL-2, thereby leading to an increase in the level of CKIs. CUL-2 may have cellular functions that are independent of VHL. It has been proposed that different substrate-binding adaptor proteins (besides VHL) bind the CUL-2/Elongin-C/Elongin-B/RBX1 complex (Stebbins et al., 1999; Kamura et al., 1998; and Zhang et al., 1999). One can envision a model in which VHL competes with other adaptors for CUL-2 binding, thereby sequestering CUL-2 from an E3 complex(es) that is required for CKI degradation. In the absence of VHL, CUL-2 would form more of the E3 complex(es) that functions to reduce the levels of CKIs, thereby potentiating hyperplasia. In support of this model, it has been observed that mammalian cells lacking VHL are unable to exit the cell cycle upon serum withdrawal, and this has been correlated with an inability to accumulate the CKI $p27^{KIP1}$ (Pause et al., 1998). Conversely, overexpression of VHL produces a G1 arrest with an increased level of $p27^{KIP1}$(Kim et al., 1998). Human SKP2 in combination with CUL-1 has been found to target $p27^{KIP1}$ for degradation *in vitro* and upon over-expression *in vivo*. However, there appear to be SKP2- and CUL-1-independent pathways for $p27^{KIP1}$ degradation, as inactivation of SKP2 or CUL-1 in certain cell lines has no effect on $p27^{KIP1}$ levels (Yu, Gervais and Zhang, 1998). As *C. elegans* has a VHL homolog (Conaway et al., 1998), the opportunity to determine the

genetic interaction between these genes may prove to be very informative for understanding the function of VHL in tumor progression. Further studies will be required to determine whether CUL-2 is required to negatively regulate CKI levels in humans, and whether the presence or absence of VHL alters human CUL-2 activity.

MATERIALS AND METHODS

C. elegans genetics and observation

General *C. elegans* culture and genetic methods were done as described (Sulston and Hodgkin, 1988). Embryonic lineages were followed with a Zeiss Axioskop microscope, using a strain-free 100X neoplan objective. Images were recorded for later review with an Optronics ZVS-3C75DE CCD camera feeding images into a Panasonic AG-6740 time-lapse VCR. Replaying the tape was required to ensure correct interpretation of cell identity, as cytoplasmic extensions in *cul-2* embryos would continually form and retract, move the cell location, or pinch-off to form cytoplasts.

Egg numbers reported in Table 2.1 were determined by transferring hermaphrodites grown at 20°C to new plates once a day and counting the eggs on the recently vacated plates by removing them with a pick as they were counted.

Germ cell numbers were determined from the progeny of *cul-2*(*ek1*)/*unc-64*(*e246*) hermaphrodites that had been collected as pretzel-stage embryos and upon hatching were transferred to individual plates, grown at 20°C, and counted at a set time post hatch. Germ cell counts were taken in triplicate using a CCD monitor to magnify the cells in animals anesthetized with 20 mM sodium azide. After counting, young larvae were

transferred back to plates to allow later identification of genotype based on germ cell and egg phenotype.

Cell cycle events in the fertilized oocyte were observed in the adult hermaphrodite's body by immobilizing the adult animal with 0.1% tricaine and 0.01% tetramisole (Sigma) as described (Kirby et al., 1990) and viewing with a 64X planapo objective.

Cell number in embryos was determined by fixing embryos in methanol and acetone (10 min each), staining DNA with propidium iodide, and observing nuclei in serial sections from a confocal microscope.

RNA interference

Single-stranded RNAs of *cul-2*, *cki-1* and *cki-2* were created by cutting the pBluescript plasmid containing the full-length clones with XhoI or NotI to linearize next to the coding region. RNA was synthesized from the plasmid template with either the T3 or T7 MegaScript Kit (Ambion) to produce sense and antisense RNA transcripts, respectively. Double-stranded RNA was created by incubation of equal parts sense and antisense RNA, heating at 95°C for 5 min, and then incubating at 70°C for 20 min. To observe RNAi phenotype, dsRNA was injected into the distal gonad arms of young wild-type adults at a concentration of 0.5 to 1 mg/ml. For suppression of the *cul-2*(*ek1*) phenotype by injection of cki dsRNA, L4 animals were injected in their intestines with dsRNA at 0.5 to 1.0 mg/ml. The intestine has been found to be a particularly good target organ for effecting RNAi results in the germ line (Tabara et al., 1998).

Isolation of *cul-2* deletion mutant

The deletion screen used to identify *cul-2* mutants is based on an experimental outline presented by Carl Johnson (NemaPharm, Inc.) at the 1997 International *C. elegans* Meeting. L4 animals, synchronized as described (Kipreos et al., 1996), were mutagenized with 50 mM ethylmethanesulfonate for four hours. Mutagenized animals were allowed to produce progeny for 36 hours. Eggs were collected by treatment with Na-hypochlorite and allowed to hatch overnight in M9 plus 3 µg/ml cholesterol. The F1 progeny were seeded at 20 animals per well in a 96 well plate in NGM medium supplemented with OP50 bacteria. Ninety six 96-well plates were created to produce a library of 370,000 mutagenized genomes. Plates were incubated until wells had cleared of bacteria and all eggs had hatched. Half of the progeny of the F1 were frozen (Sulston and Hodgkin, 1988), and half were used to make DNA (Plasterk, 1995). An aliquot of DNA from every well of a 96-well plate was combined, phenol and chloroform extracted, ethanol precipitated, and resuspended in TE at 3% of the original volume. Two rounds of nested PCR were performed with primer pairs separated by 4.5 kb of genomic sequence (5’ outer primer, TCCACAGGTTATGTACTCACTGAAGCCA;
3’ outer, GCTTGAGGAGGGAGGATAGAACACAAAA;
5’ inner, TGACAAAGTATGGGTGCAGTTGAGACCA;
3’ inner, TAGGCAAATAGCCGTTTGTCGGGAGTAA). Forty cycles of PCR were performed using Taq (Boehringer Mannheim) with an annealing temperature of 70°C and a limiting extension time of 2 min 30 sec. at 72°C. Potential deletion bands were confirmed by determining whether a similar size deletion product was obtained after repeating the PCR with six samples of the original DNA. The well containing the

deletion band was identified after PCR of row and column DNA from the 96-well plate. Animals were recovered from the frozen well and cloned. Single worm PCR was performed on the animals after they had produced progeny to identify animals harboring the *cul-2* mutation. Two deletions were detected in the library; of these, one was recovered after thawing the frozen animals. The mutant isolated, *ek1*, was outcrossed six times and balanced with *unc-64* (e246). The site of deletion was mapped by restriction digestion of PCR products and then sequenced.

Isolation of *cki* cDNAs and analysis of CKI protein

The *cki-1* and *cki-2* genes were identified by homology searches of the *C. elegans* genome database produced by the Genome Sequencing Consortium (Wilson et al., 1994). The 3' sequences of *cki-1* and *cki-2* were obtained by sequencing complementary DNA clones obtained from the *C. elegans* expressed-sequence tag (EST) project, clones yk490e9 and yk374f4, respectively. The 5' ends of both genes were cloned by PCR from a cDNA library (a kind gift of R. J. Barstead) by using internal primers and a 5' primer designed to include the trans-spliced leader SL1. The presence of SL1 indicates that both clones are full length. The cDNAs isolated were sequenced and exactly matched the sequence predicted from the GeneFinder program, with the exception that the *cki-2* cDNA included three extra basepairs on the 5’ splice site of exon 2 to increase the size of the predicted CKI-2 protein by one internal glutamine residue (CAG) at codon 26.

CKI antibody production and immunofluorescence

Antisera to full-length CKI-1, CUL-2, and the amino-terminal 135 amino acids of CKI-2 were produced in rabbits using bacterially-derived histidine-tagged fusion proteins as antigens (vector pET32a+, Novagen). Fusion proteins were isolated under denaturing conditions using Ni-NTA agarose according to manufacturer instructions (Qiagen). Rabbits were immunized and boosted with 0.4 mg of protein per injection. Sera were precleared of antibodies directed against the His-tag by passage over Affigel-10 (BioRad) linked to His-tag, and then affinity purified against the fusion protein antigen linked to Affigel-15 as described (Harlow and Lane, 1988).

Embryos were obtained for immunofluorescence either by hypochlorite treatment or by cutting gravid adults. Embryos were placed on polylysine coated slides and processed using the "freeze-crack" method followed by fixation in -20°C methanol (15-45 min) and -20°C acetone (15 min) and air-dried as described (Miller and Shakes, 1995). Gonad arms were dissected from adult hermaphrodites by placing animals in M9 solution on a polylysine-coated slide and cutting the animals behind the pharynx so that the extruded gonads attached to the slide. Slides were processed using the "freeze-crack" method. Samples were blocked in 3% BSA for 1 hr at room temperature, incubated in primary antibody overnight (1% BSA in PBS), washed 5 times in PBST (PBS, 0.5% Tween-20), incubated in secondary antibody for 2 hr at room temperature (1% BSA in PBS); washed in PBST, incubated 30 min with 1 µg/ml DAPI, and mounted with 90% glycerol, 1 mg/ml p-phenylenediamine.

In addition to those antibodies mentioned above, the following primary antibodies were used: monoclonal anti-nuclear pore antibody MAb414 (BAbCo, Inc.; Aris and

Blobel, 1989), monoclonal anti-α tubulin antibody N356 (Amersham, Inc.), polyclonal anti-phospho-histone H3 antibody (Upstate Biotechnology, Inc.; Hendzel et al., 1997), monoclonal anti-histone antibody MAB052 (Chemicon International, Inc.), and polyclonal anti-AIR-1 antibody, which localizes to centrosomes (Schumacher et al., 1998). The secondary antibodies used were goat anti-mouse conjugated to rhodamine (Cappel) or fluorescein isothiocyanate (FITC), and goat anti-rabbit conjugated to rhodamine or FITC (all from Boehringer Mannheim). Secondary antibodies were precleared with acetone-fixed *C. elegans* powders as described (Miller and Shakes, 1995).

To determine the percentage of cells in the various mitotic stages, we stained wild-type and *cul-2(ek1)* embryos with anti-phosphohistone H3 antibody, anti-AIR-1 antibody and 4,6-diamidino-2-phenylindole (DAPI). Only cells with two centrosomes were analyzed.

Antisense and sense digoxigenin-labeled RNA probes were created from full-length *cul-2* and *cki-1* cDNAs using digoxigenin-11-UTP (Boehringer Mannheim) according to the manufacturer's protocol. Whole animals and dissected gonad arms were frozen immediately beneath a coverslip and processed for *in situ* hybridization as described (Seydoux and Fire, 1995), except that the hybridization and the washes were at 55 °C.

Microscopy and signal quantitation

Germ cell DNA levels were quantitated by lyophilizing animals, fixing with methanol for two minutes, and air drying. Alternatively, dissected gonad arms were fixed

using the “freeze-crack” method described above. Fixed specimens were incubated with 40 µg/ml RNAse A in PBS for 1 hr at 37°C, rinsed in PBS, stained with 50 µg/ml propidium iodide (PI) (Sigma) for 30 min at room temperature, and then rinsed with PBS. Specimens were mounted in 1 mg/ml p-phenylenediamine in 90% glycerol and observed with an MRC600 Biorad confocal microscope. The same confocal microscope image capture settings were used for all specimens of a given experiment and set so that no image saturated (typically, one scan with filter 3, an aperture setting of 5, and gain of 8.0). A 100X objective was used with a scan depth of 0.5 µm. Quantitation was accomplished with Comos software version 7.0 (Biorad). The signal for a nucleus in a given slice was determined by multiplying the average intensity for the nuclei (minus background intensity) by the area. The total signal for a nucleus was obtained by adding the signal from serial sections. DNA content was normalized to haploid genome equivalents by using the DNA content from somatic cells, other than hypodermis or intestine, as internal 2N standards; mitotic germ cells were used as internal 4N standards. Germ cells selected for DNA quantitation were within five nuclear diameters from the distal tip cell. A comparable accumulation of *cul-2*(*ek1*) germ cells with 2n DNA content was observed when the experiment was performed with either young adult animals (Figure 2.3) or L4 stage animals (data not shown).

Quantitation of volume for individual germ cells was accomplished by adding the areas staining with propidium iodide in each serial confocal section and then multiplying by the scan depth of 0.5 µm.

Quantitation of CKI protein level in gonad arms was accomplished by dissection of *cul-2* and wild-type gonad arms on the same slide and processing for

immunofluorescence with anti-CKI and anti-nuclear pore antibody. Confocal scans were taken with the same settings for all gonads (both *cul-2* and wild-type), and quantitation was as above.

Determination of the percentage of mitotic germ cells in *cul-2*(*ek1*) and wild-type was performed by counting the number of nuclei (stained with DAPI) that were within a distance of ten cell-diameters from the distal tip and then counting the number of those mitotic germ cells that were co-stained with anti-phosphohistone H3 antibody.

Microscope images were captured on TechPan film (Kodak) and digitally scanned with a Nikon LS-2000 scanner. The images were processed with Adobe Photoshop version 4.0. For matched images, e.g., CKI-1 level in *cul-2* and wild-type, the same shutter time (in seconds) was used, and the images were processed identically.

ACKNOWLEDGEMENTS

The research presented in this chapter is a collaborate effort by several members in the Kipreos lab. I thank E. T. Kipreos for making the *cul-2* mutant; H. Feng for contributing the immunofluorescence research presented in Figure 2.5 a-h, Figure 2.6 a, i-m and Figure 2.8 a-d, and for determining the prolonged prometaphase in *cul-2* embryos; and G. Punkosdy for confocal studies of chromosome condensation during first mitosis presented in Figure 2.8 e-h. Part of the research presented in this chapter has been published (Feng et al., 2000). The published figures and texts are used in this chapter with permission of Nature Cell Biology.

Table 2.1: Egg Laying Data for *cul-2*(*ek1*)

Genotype	**n**	**Eggs Laid**
N2 (wild-type)	10	288 ± 36
cul-2(*ek1*)	22	17 ± 13
cul-2(*ek1*), *mnDf100 unc-4*(*e120*)/*mnC1*	22	57 ± 18
mnDf100 unc-4(*e120*)/*mnC1*	10	255 ± 50
cul-2(*ek1*), *mnDf100 unc-4*(*e120*)/*mnC1 + ekEX1* (T05A6)*	22	15 ± 20
cul-2(*ek1*)/*unc-64*(*e264*), *mnDf100 unc-4*(*e120*)/*mnC1 + ekEX1**	15	295 ± 51
cul-2(ek1) injected with *cki-1* dsRNA	12	58 ± 21
cul-2(ek1) injected with *cki-2* dsRNA	13	13 ± 25
cul-2(ek1)/unc-64(e246) injected with *cki-1* dsRNA	10	227 ± 41
cul-2(ek1)/unc-64(e246) injected with *cki-2* dsRNA	10	258 ± 58

* ekEx1 is an integrated DNA array containing T05A6 (a cosmid containing *cki-1* and *cki-2*) and the plasmid PRF4 (containing the dominant *rol-6(su1006)* allele).

Figure 2.1 *cul-2* deletion mutant. Line drawing of *cul-2* genomic region on chromosome III with exons represented as boxes and introns as horizontal lines. Shaded areas represent coding regions. The region deleted in *cul-2*(*ek1*) is represented as the missing region bounded by dashed lines, and is inclusive of base pairs 12,166 to 13,393 of cosmid ZK520. Locations of primers used for the deletion screen are presented below the genomic line drawing as half-arrows. kb, kilobase.

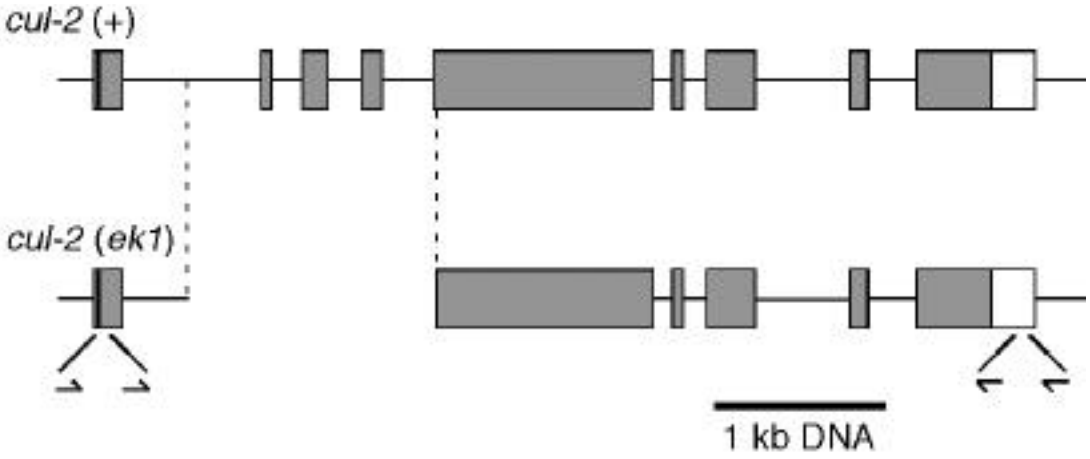
cul-2 (+)
cul-2 (ek1)
1 kb DNA

Figure 2.2 *cul-2* RNAi and *cul-2* mutant phenotype. Left, *cul-2* RNAi produces arrested embryos. Right, *cul-2* homozygous progeny from heterozygous parents can develop to adults. The germ cell phenotypes described in Chapter 2 refer to the phenotypes observed in the germ cells of these *cul-2* homozygous adults. The progeny of these *cul-2* homozygous adults are arrested as embryos. These embryos are indistinguishable from those produced by *cul-2* RNAi. In Chapter 2, the embryonic phenotypes refer to the phenotypes of these arrested embryos.

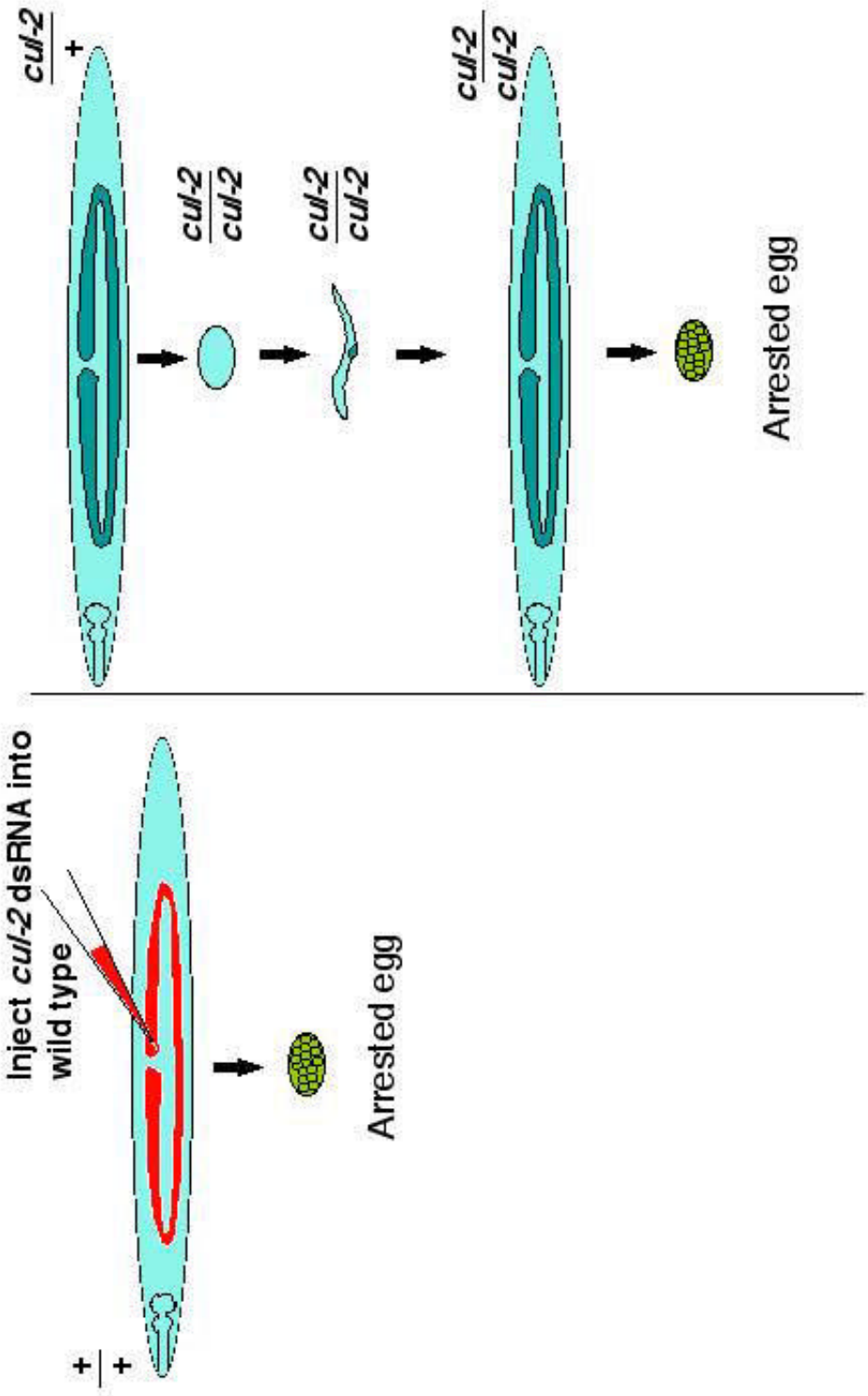
cul-2
+
cul-2
cul-2
cul-2
cul-2
cul-2
cul-2
Arrested egg
Inject cul-2 dsRNA into
wild type
+
+
Arrested egg

Figure 2.3 *cul-2* homozygotes have fewer bigger germ cells.

(a, b) Differential Interference Contrast (DIC) micrographs of the distal gonad arms of wild-type (a) and *cul-2*(*ek1*) (b) L4 stage hermaphrodites. The distal tip cell (DTC) is denoted by an arrow. Scale bars, 10 µm.

(c) Hermaphrodite germ cell number for *cul-2*(*ek1*) homozygotes (diamonds) and *cul-2*(*ek1*)/*unc-64*(*e264*) heterozygotes (squares) grown at 20°C at the following hours post hatching: 13.5 hours (L1 stage); 24 hours (L2); 36 hours (young L4); 48 hours (young adult); and 61 hours (mature adult). *cul-2*(*ek1*)/*unc-64*(*e264*) heterozygotes are indistinguishable from wild-type.

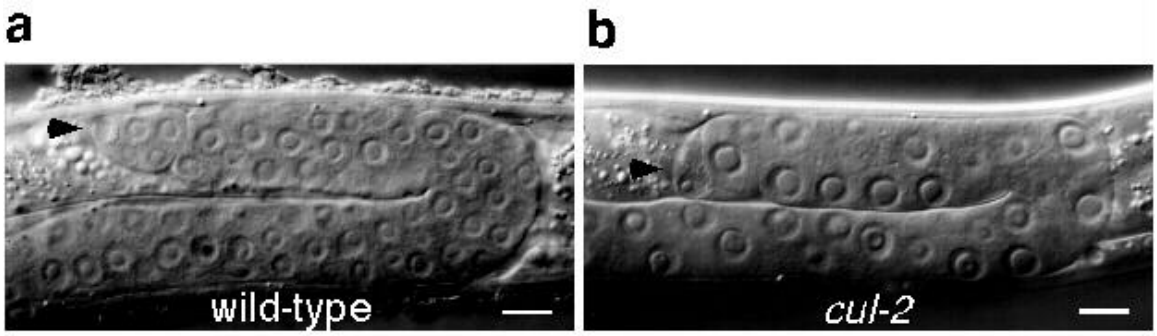
a
b
wild-type
cul-2

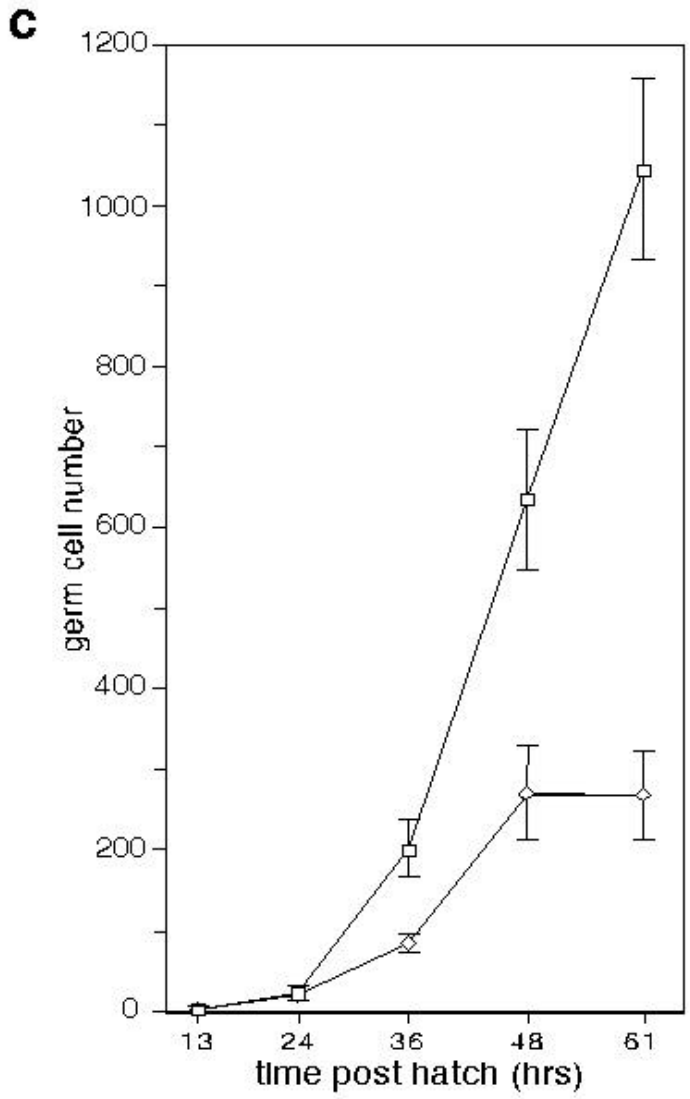
c
1200
1000
800
600
400
200
0
germ cell number
13
24
36
48
61
time post hatch (hrs)

Figure 2.4 Histogram of DNA content of germ cells from young adult *cul-2*(*ek1*) and wild-type hermaphrodites. Dissected gonad arms from young adults were stained with propidium iodide and germ cells within five cell diameters from the DTC were serially scanned with a confocal microscope. The relative amount of DNA was determined by adding the signal from the scanned sections for each nucleus. DNA content was normalized to haploid genome equivalents by using the DNA content from DTCs and mitotic cells within the same animal as 2n and 4n references, respectively.

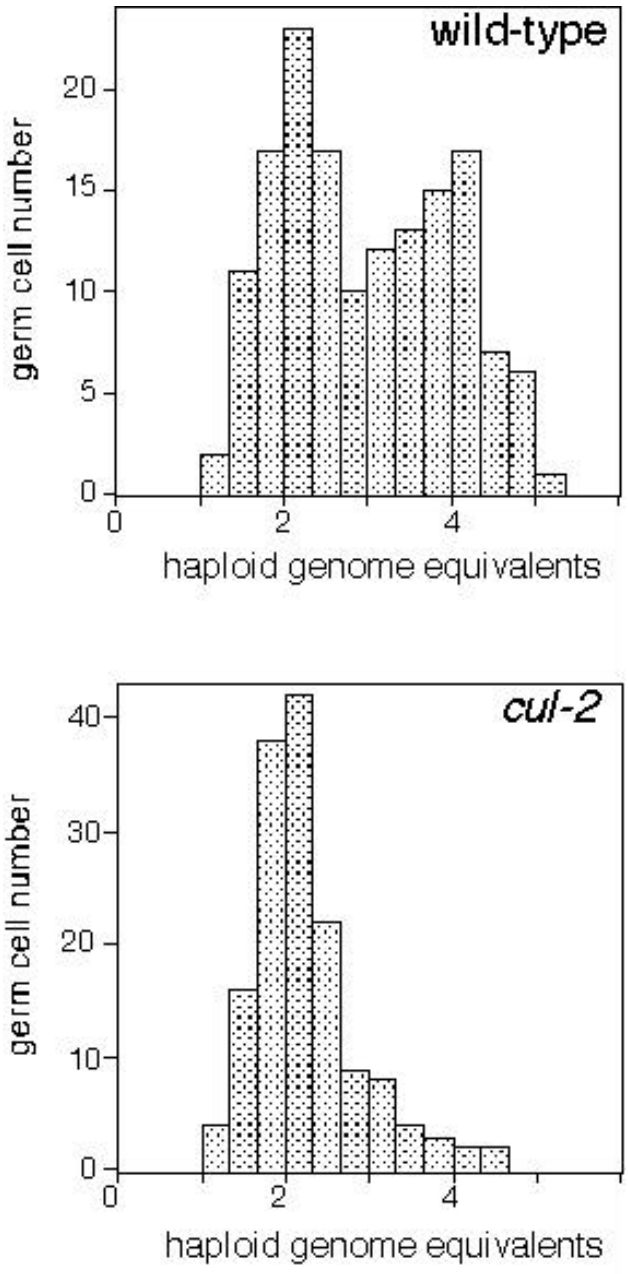
wild-type
germ cell number
0
5
10
15
20
0
2
4
haploid genome equivalents
cul-2
germ cell number
0
10
20
30
40
0
2
4
haploid genome equivalents

Figure 2.5 Level of CKI-1 protein in *cul-2* mutants.

(a-d) Specificity of anti-CKI-1 affinity-purified antibody. 12 hr old wild-type (a and b) and homozygous *mnDf100* (c and d) embryos co-stained with affinity-pure anti-CKI-1 antibody (a and c) and anti-nuclear pore antibody as a control (b and d). *mnDf100* is a deletion that removes *cki-1*.

(e-h) Dissected gonad arms from wild-type (e and g) and *cul-2*(*ek1*) (f and h) adult hermaphrodites were co-stained with affinity-purified anti-CKI-1 antibody (e and f) and DAPI (g and h). For wild-type (e), the mitotic zone at the distal end is bracketed.

(i,j) *in situ* hybridization with digoxygenin labeled *cki-1* antisense probe of wild-type (i) and *cul-2* (j) adult distal gonads. k, Control *in situ* hybridization with *cki-1* sense probe of wild-type adult distal gonad. Scale bars represent 10 µm.

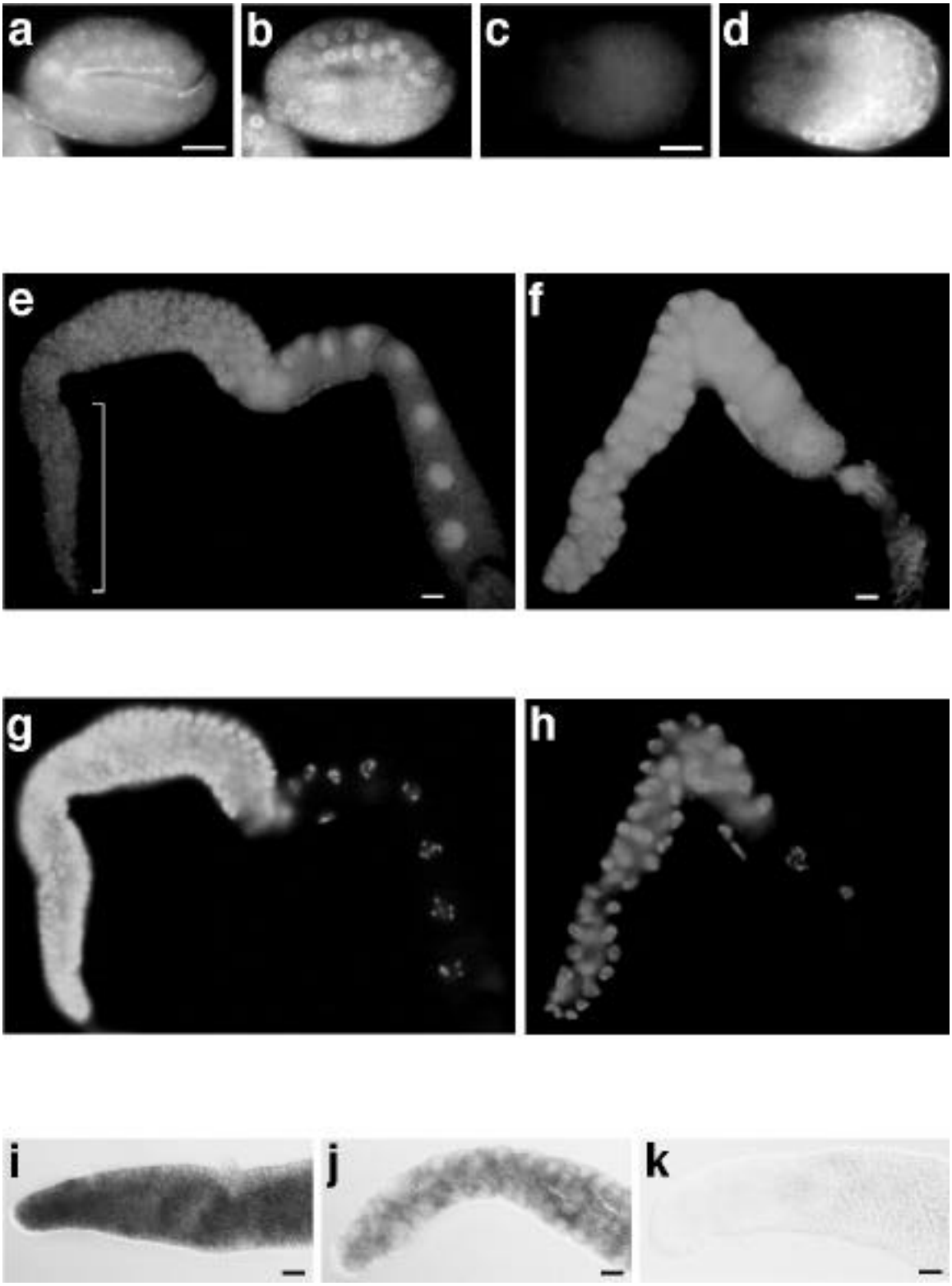
a
b
c
d
e
f
g
h
i
j
k

Figure 2.6 *cul-2* mutant embryonic phenotype.

(a) DIC micrograph of *cul-2*(*ek1*) 2-cell stage embryo. Black and white arrows indicate cytoplasmic extensions of leftward and rightward cells, respectively. Throughout Fig. 6, small arrowheads indicate multinuclei.

(b) DIC micrograph of embryo from wild-type parent injected with *cul-2* dsRNA.

(c-e) Cytoplasmic extension creating a cytoplast. Cytoplasmic extensions can retract or form cytoplasts. Time lapse sequence of DIC micrographs of *cul-2*(*ek1*) embryo (total time, less than eight minutes). In the third panel the cytoplasmic extension has pinched off, creating a cytoplast.

(f-h) Multinuclei in *cul-2* RNAi embryo. Time lapse sequence of DIC micrographs of a *cul-2* RNAi embryo undergoing mitosis and cytokinesis. The three micrographs were taken in the span of 17 minutes.

(i-k) Embryonic arrest phenotype of *cul-2*(*ek1*). *cul-2*(*ek1*) embryo 12 hours after being laid was fixed, observed with DIC (i), and co-stained with 1 µg/ml DAPI to detect DNA (j) and anti-nuclear pore antibody (k). Note the unequal DNA distribution among nuclei.

(l and m) DNA bridge in *cul-2*(*ek1*) mutant. Fixed *cul-2*(*ek1*) mutant embryo stained with DAPI (l) and observed by DIC (m). DNA bridge in (l) is marked by arrowhead.

Scale bars, 10 µm.

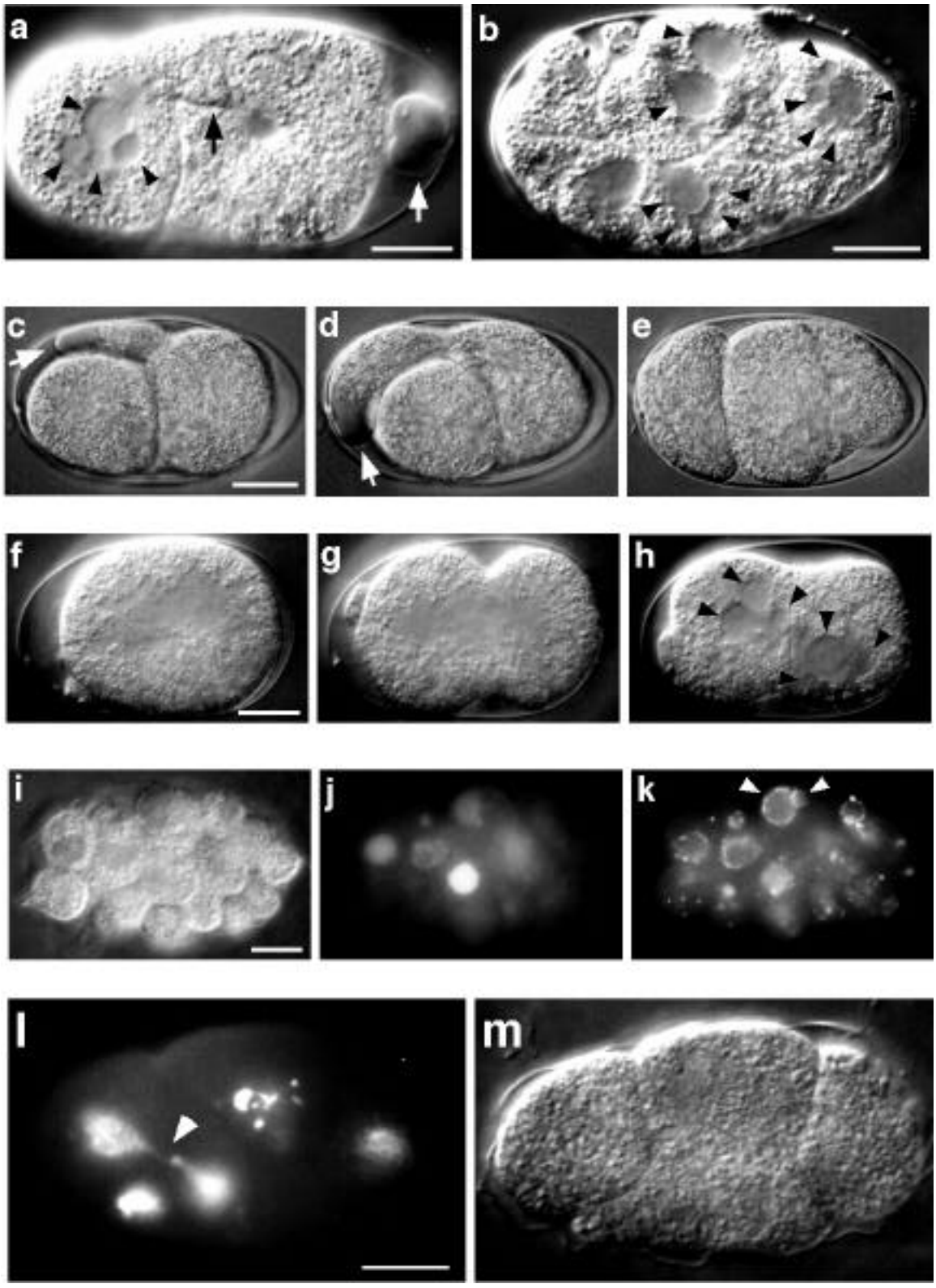
a
b
c
d
e
f
g
h
i
j
k
l
m

Figure 2.7 Cell cycle lineage of wild-type and *cul-2* mutant embryos. Lineage of wild-type embryo from cleavage of zygote to the 24 cell stage (far left). Two representative lineages of *cul-2*(*ek1*) embryos (from four total lineages performed) (middle), as well as a representative lineage from *cul-2* RNAi embryos (from three total lineages performed) (far right). Horizontal lines denote the time of completion of cytokinesis. The zero time point is set at mitosis to create the two-cell embryo. Thicker hollow lines denote mitosis, as determined by the absence of a nuclear envelope. In *cul-2* mutant lineages, numbers on the right side of the lineage denote the numbers of nuclei per cell. Lines leaving at a right angle denote a cytoplast derived from a cytoplasmic extension that had "pinched off" from the main cell.

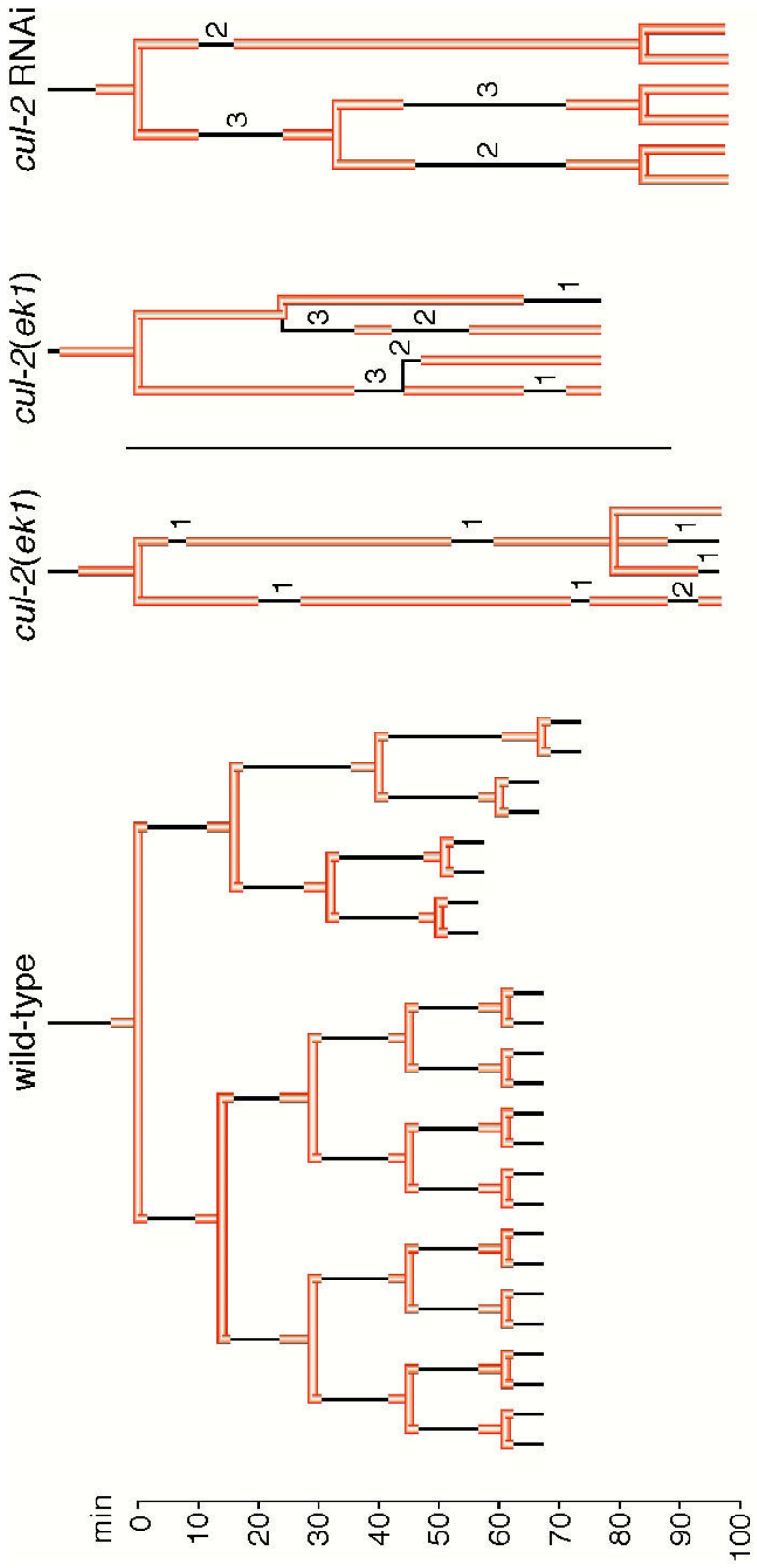
wild-type
cul-2(ek1)
cul-2(ek1)
cul-2 RNAi
min
0
10
20
30
40
50
60
70
80
90
100

Figure 2.8 Chromosome condensation is impaired in *cul-2* mutant embryos.

(a-d) Anaphase in *cul-2* and wild-type two-cell-stage embryos. Wild-type (a, b) and *cul-2(ek1)* (c, d) two-cell-stage embryos were fixed and stained with anti-tubulin antibody (a, c) and DAPI (b, d). a, b, in the wild-type, the left-hand cell, AB cell, is in anaphase while the right-hand cell, P1 cell, is in prophase. c, d, in *cul-2(ek1)* embryos, the left-hand cell is in anaphase, while the right-hand cell is in prometaphase.

(e) Genomic DNA from a wild-type zygote that was fixed immediately upon fusion of maternal and paternal pronuclei and then stained with propidium iodide (PI) to visualize DNA. The PI signal for pronuclear DNA was captured through serial sections with a confocal microscope. A projection of the three-dimensional serial sections collapsed onto two-dimensions was made using NIH Image software version 1.58.

(f) Confocal projection of PI-stained genomic DNA of zygote from wild-type adult injected with *cul-2* dsRNA that was fixed five minutes after fusion of maternal and paternal pronuclei. Note that wild-type embryos progress through mitosis in approximately five minutes, indicating that this zygote was delayed in prometaphase.

(g) Confocal projection of PI-stained genomic DNA of *cul-2*(*ek1*) zygote from a *cul-2* (*ek1*) parent that was fixed immediately after fusion of maternal and paternal pronuclei. (h) Confocal projection of PI-stained genomic DNA of *mei-1*(*b284*) zygote in which neither polar body was extruded.

Note that certain of the 30 chromosomes overlap due to the projection of the 3D sections onto 2-dimensions. The projections in (e), (f), (g), and (h) are representative of 23, 17, 8, and 10 pronuclei fusions examined, respectively. Scale bars, 10 μm.

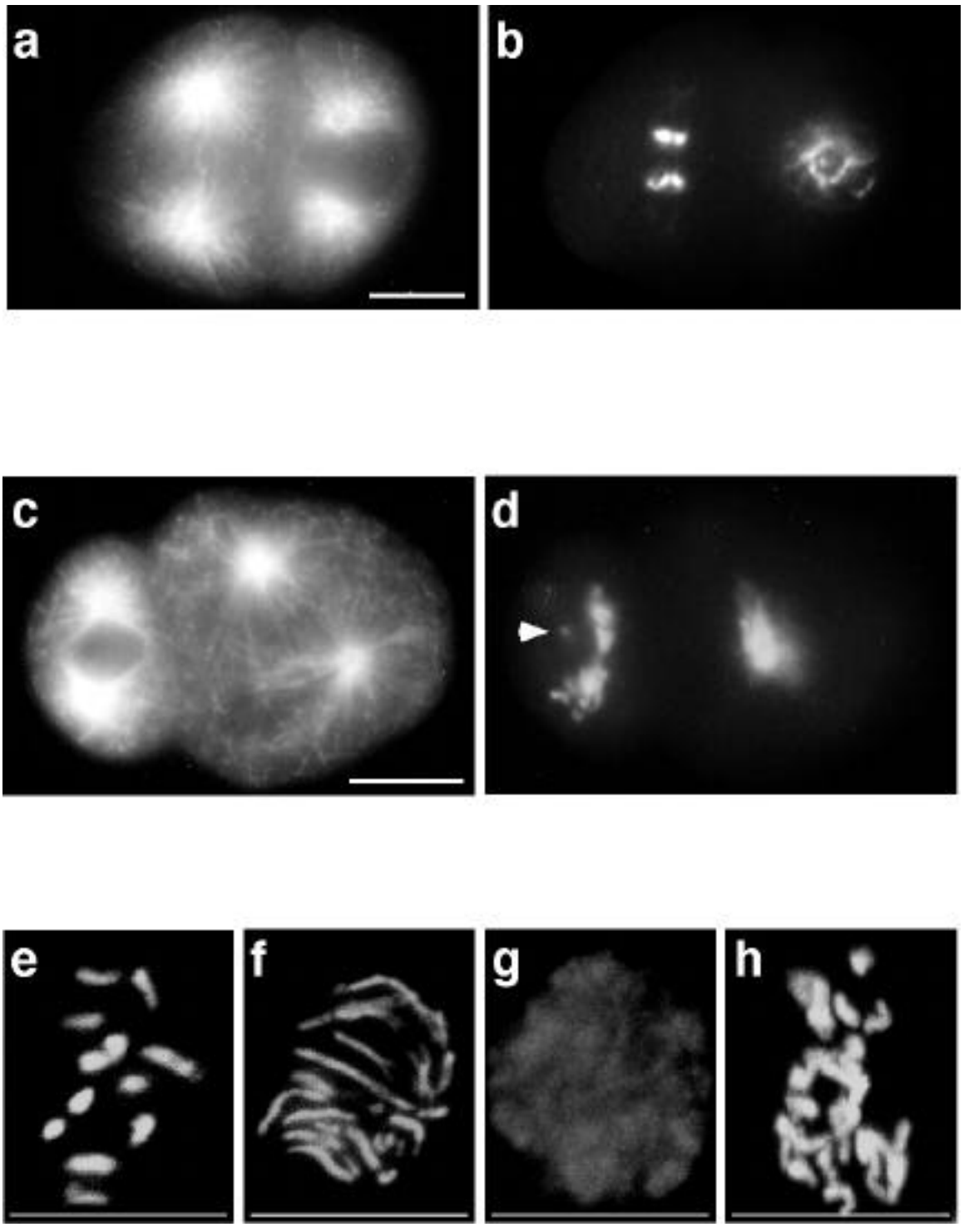
a
b
c
d
e
f
g
h

CHAPTER 3

CUL-4 IS A KEY REGULATOR OF DNA REPLICATION LICENSING

To maintain genome stability, DNA replication is strictly regulated to occur once and only once per cell cycle. In eukaryotes, the presence of licensing proteins such as Cdt1 and Cdc6 enables the association of the replication helicase complex Mcm2-7 with chromatin to form pre-replicative complex (pre-RC) (Blow and Hodgson, 2002; Devault et al., 2002). The removal of licensing proteins from chromatin in S phase after replication is crucial to ensure that origins fire only once per cell cycle (Blow and Hodgson, 2002). Current studies suggest that redundant mechanisms exist in the licensing system to prevent DNA re-replication, as disruption of the regulation of individual licensing proteins failed to induce massive DNA re-replication (Bell and Dutta, 2002).

Here my research shows that inactivation of a single gene *cul-4* in *C. elegans* causes extensive re-replication of genomic DNA, producing cells with up to 100C DNA content. The *C. elegans* Cdt1 ortholog, CDT-1, is required for DNA replication in *C. elegans* and is present in G1 phase nuclei but rapidly disappears as cells enter S phase. In cells lacking CUL-4, CDT-1 does not disappear in S phase nuclei and instead accumulates in re-replicating cells. Elevated level of CDC-6 protein is also observed in these re-repicating cells. Removal of one genomic copy of the *cdt-1* gene suppresses the *cul-4* re-replication phenotype. However, this suppression is not observed by removing

one genomic copy of the *cdc-6* gene. We propose that CUL-4 functions to prevent aberrant re-initiation of DNA replication at least in part by facilitating the degradation of CDT-1.

BACKGROUND

As introduced in Chapter 1, CUL-4 is a member of the cullin family of ubiquitin-ligases. A human homologue of *C. elegans cul-4*, *cul-4A*, was found to be amplified and overexpressed in breast cancer cells (Chen et al., 1998). The CUL-4A protein was found to function in ubiquitination and degradation of the UV-damaged DNA-binding protein DDB (Chen et al., 2001). In this chapter, we demonstrate that in *C. elegans*, CUL-4 functions as a central regulator of DNA replication licensing.

In eukaryotic cells, DNA replication is simultaneously initiated at hundreds of replication origins. Each origin is loaded with a set of proteins called the pre-replicative complex (pre-RC) to initiate DNA replication and the formation of two bi-directional replication forks at each origin. Pre-RC is formed at replication origins during G1 phase, which then awaits activation. S phase CDK activation triggers the initiation of DNA replication. In S phase, it is essential for the cell to distinguish already replicated sections of DNA from un-replicated sections so that the complete genome is replicated only once. This is achieved by the replication licensing control system. Before S phase, unreplicated chromosomes are loaded with licensing proteins that are required for pre-RC formation and subsequent DNA replication. The replication licence is inactivated in the course of DNA replication to prevent replicated DNA from re-replicating.

The pre-RC contains a number of replication factors including the origin recognition complex (ORC), Cdc6, Cdt1, and the mini-chromosome maintenance proteins 2-7 (Mcm2-7) (Bell and Dutta, 2002).

The Mcm2-7 protein complex

One important component of the pre-RC is the mini-chromosome-maintenance 2-7 (Mcm 2-7) proteins (Blow and Hodgson, 2002). The genes encoding Mcm2-7 proteins were initially identified in genetic screens for genes required for maintenance of plasmids in *S. cerevisiae* (Maine et al., 1984). The six Mcm proteins are highly conserved in all eukaryotes (Bell and Dutta, 2002).

Mcm proteins are required for both the initiation and the elongation of DNA replication. In *S. cerevisiae*, when temperature-sensitive *mcm* mutants were shifted to non-permissive temperature prior to S phase, no DNA replication was observed (Labib et al., 2000). Inactivation of ts MCMs in the course of S phase resulted in the arrest of replication fork progression indicating that the MCM proteins are required for DNA elongation (Labib et al., 2000).

Several studies have indicated that the Mcm2-7 complex may function as a DNA helicase. Both biochemical studies in mouse and genetic studies in *S. pombe* demonstrated that Mcm4, 6, 7 may form a complex that has DNA helicase activity (Ishimi, 1997; Lee and Hurwitz, 2001). This helicase activity was inhibited by adding Mcm2, 3, 5 (Ishimi, 1997; Lee and Hurwitz, 2001). These findings suggest a model that Mcm4, 6, 7 may function as a replicative DNA helicase at the replication fork, while Mcm2, 3, 5 may function as inhibitors to this helicase activity. However, this model

appears to be oversimpfied, as it cannot explain the genetic finding that inactivation of any of the six Mcm proteins in S phase causes the arrest of replication fork progression (Labib et al., 2000).

It is suggested that the primary role of the pre-RC is to load Mcm proteins onto chromatin. In *Xenopus* extracts, once the MCM proteins are assembled onto chromatin, removal of the pre-RC components ORC and CDC6 causes no defects in DNA replication (Hua and Newport, 1998; Rowles et al., 1999).

Re-expression of Mcm in S phase failed to rescue the DNA replication arrest caused by Mcm temperature-sensitive mutations (Labib et al., 2000), suggesting that some protein factors that exist prior to S phase are required for Mcm protein loading. At least three proteins are known to be essential for loading Mcm proteins onto origins in budding yeast (Gillespie et al., 2001). They are the origin recognition complex (ORC), Cdc6, and Cdt1. The presence of these proteins allows the Mcm proteins to bind to chromatin, and subsequently licenses the chromatin for replication. The removal or inactivation of these proteins in S phase prevents the re-load of Mcm proteins to origins, and therefore prevents the origin from re-firing (Blow and Hodgson, 2002).

Origin recognition complex

The origin recognition complex (ORC) consists of six subunits Orc1-Orc6. ORC specifically binds DNA replication origins and is conserved in all eukaryotes (Bell and Dutta, 2002). Both immunodepletion of ORC in *Xenopus* egg extracts (Romanowski et al., 1996; Carpenter et al., 1996) and ORC mutant studies in *Drosophila* (Pflumm and

Botchan, 2001; Pinto et al., 1999) suggested that the ORC is required for initiation of DNA replication.

The cell cycle regulation of ORC binding to DNA varies among different species. In the yeast *S. cerevisiae* and *S. pombe*, ORC constitutively binds to chromatin throughout the cell cycle (Tanaka et al., 1997; Ogawa et al., 1999). However, the activity of ORC is regulated during the cell cycle by phosphorylation of the ORC subunit Orc2p by CDK (Nguyen et al., 2001). This phosphorylation appears to negatively regulate ORC activity (Blow and Hodgson, 2002; Vas et al., 2001). Similarly, *Drosophila* ORC remains associated with chromatin throughout the cell cycle (Pak et al., 1997). In contrast, studies of *Xenopus* egg extracts suggested that ORC are removed from chromosomes during M phase (Romanowski et al., 1996; Carpenter et al., 1996), probably due to the phosphorylation of some ORC subunits by CDK (Findeisen et al., 1999). The case in mammalian cells is more complicated. Only a subset of mammalian ORC subunits remain tightly associated with chromatin throughout the cell cycle. ORC1 only associates with the chromatin during G1 phase and dissociates from chromatin in S phase (Natali et al., 2000; Kreitz et al., 2001). There is evidence that the human ORC subunit ORC1 is degraded during S phase to prevent re-replication (Kreitz et al., 2001), but other studies reported that human ORC1 is stable through the cell cycle (Okuno et al., 2001). Hamster Orc1 protein is stable, but its association with chromatin is cell cycle regulated. Hamster Orc1 binds to chromatin in G1 phase, and as cells enter S phase, Orc1 is ubiquitinated into a mono- or diubiquitinated form and released from chromatin (Li and DePamphilis, 2002). This ubiquitination does not lead to proteolysis, as the concentration of Orc1 is constant throughout the cell cycle (Li and DePamphilis, 2002).

Cdc6

Cdc6 is required for pre-RC assembly after the step of ORC loading and before the step of Mcm2-7 loading, although the mechanism by which Cdc6 recruits MCMs to chromatin remains unclear. Studies in budding yeast and *Xenopus* have demonstrated that Cdc6 requires ORC to bind to chromatin (Coleman et al., 1996) and that the loading of Cdc6 onto chromatin is required for Mcm2-7, but not ORC, association with chromatin (Coleman et al., 1996; Aparicio et al., 1997).

In yeast, Cdc6p protein level is cell cycle regulated. CDK activity restricts the transcription of *CDC6* to late mitosis and G1 phase (Blow and Hodgson, 2002). Cdc6p protein is subjected to ubiquitin-mediated protein degradation in S phase. In *S. cerevisiae*, Cdc6p is phosphorylated by S phase CDK and degraded in S phase by SCF^{Cdc4} ubiquitin ligase-mediated proteolysis (Drury et al., 1997; Elsasser et al., 1999). In *S. pombe*, the Cdc6p homolog Cdc18p is degraded through a similar pathway which uses an E3 complex composed of Skp1p, Cullin-1p, and a heterodimer complex composed of two F-box proteins, Pop1p and Pop2p (Kominami and Toda, 1997; Kominami et al., 1998).

Mammalian Cdc6 is regulated by a different mechanism. Human CDC6 is phosphorylated by CDK and exported from the nucleus to the cytoplasm at the entry of S phase (Saha et al., 1998; Petersen et al., 1999). Mammalian Cdc6 has both a KEN-box motif and a D-box motif (Petersen et al., 2000, see Chapter 1). Cdc6 is ubiquitinated and degraded by the ubiquitin ligase APC-CDH1 in mitosis (Petersen et al., 2000).

In fission yeast, it is believed that the cell cycle regulation of Cdc6p protein is important for preventing the reassembling of Pre-RC after the initiation of DNA

replication. Overexpression of *CDC18* (the *S. pombe CDC6*) causes DNA re-replication (Nishitani and Nurse, 1995). However, overexpression of either wild-type or mutant Cdc6 in human cells or *S. cerevisiae* failed to induce re-replication (Bell and Dutta, 2002), suggesting that further redundant mechanisms exist in preventing DNA re-replication. Moreover, it is controversial whether the human CDC6 is cell cycle-regulated to prevent DNA re-replication. Although much of the soluble CDC6 protein is exported out of nucleus during S phase, a significant fraction of chromatin-bound CDC6 is observed through G1, S, and G2 phases (Coverley et al., 2000; Mendez and Stillman, 2000).

Cdt1

Cdt1 is conserved in eukaryotes including *S. pombe*, *Xenopus laevis* (called XCDT1), *Drosophila melanogaster* (called Double parked / Dup), and humans (Bell and Dutta, 2002). *S. cerevisiae* Cdt1 has not yet been identified. In both *S. pombe* and *Xenopus*, Cdt1 is required for MCM loading and is necessary for replication initiation (Nishitani et al., 2000; Maiorano et al., 2000). In *S. pombe*, Cdt1 physically interacts with Cdc18 (the homolog of *S. cerevisiae* Cdc6) and both proteins are required for MCM loading (Nishitani et al., 2000). In *Drosophila*, the Cdt1 homolog Double parked (DUP) protein is required for DNA replication (Whittaker et al., 2000). DUP co-localizes with ORC at DNA replication origins, and this DUP localization is ORC-dependent (Whittaker et al., 2000).

The cell cycle regulation of Cdt1 appears to be more conserved than Cdc6 and ORC. In both human and yeast, Cdt1 protein level fluctuates according to cell cycle

progression. Cdt1 protein level peaks at G1 phase and decays in S phase (Nishitani et al., 2000; Nishitani et al., 2001). However, the protein degradation pathway for Cdt1 remains unclear. In vertebrate cells, Cdt1 is also regulated by the inhibitor geminin. In S and G2 phases, geminin is expressed at high levels and inhibits Cdt1 activity (Blow and Hodgson, 2002). In late mitosis, geminin is degraded by the APC ubiquitin proteolysis pathway and the protein level remains low in G1 phase (Blow and Hodgson, 2002).

These licensing mechanisms are redundant in preventing DNA licensing. In mammalian cells, disruption of the regulation of a single licensing factor has failed to induce DNA re-replication (Bell and Dutta, 2002). In yeast, inactivation of one regulatory mechanism may induce DNA re-replication, but only to a limited extent (Nishitani and Nurse, 1995). Massive re-replication is only observed when regulation of at least two licensing proteins is altered, such as co-overexpression of *CDT1* and *CDC6* in *S. pombe* (Yanow et al., 2001). Here in this chapter, my research shows that inactivation of the single gene *cul-4* causes extensive DNA re-replication, suggesting that CUL-4 is a key regulator in DNA licensing.

RESULTS

cul-4 developmental expression

I determined the developmental expression of *cul-4* by RNA *in situ* hybridization. The *C. elegans cul-4* gene is expressed primarily in the germline of adult hermaphrodites, with a low level of expression in the intestine in young adults (Figure 3.1 a, b). *cul-4* mRNA is provided to embryos as maternal product, and the level of *cul-4* mRNA

decreases during embryogenesis (Figure 3.1 c, d). In larvae, *cul-4* is expressed in proliferating tissues, most notably in the intestine and hypodermis (Figure 3.1 e).

Inactivation of *cul-4* by RNAi

To probe *cul-4* function, we used dsRNA-mediated interference (RNAi) to inactivate the *cul-4* gene (Fire et al., 1998). To evaluate the efficiency of *cul-4* RNAi, we used RNA *in situ* hybridization to detect the residual *cul-4* mRNA level in the gonads of the animals after injection. Quantitation of *in situ* hybridization signals revealed that while the intensity of *cul-4* antisense signal for wild-type animals is 100 ± 23 arbitrary units (n=10) , antisense signal for *cul-4* RNAi animals is reduced to 11 ± 28 a.u. (n=10). The background level, as determined by sense signal for wild-type, is 0 ± 16 a.u. (n=10). Injection of *cul-4* dsRNA into adult hermaphrodites, therefore, reduced *cul-4* mRNA levels to not significantly higher than background levels (Figure 3.1 f-h). We conclude that *cul-4* RNAi is efficient in eliminating *cul-4* mRNA and thus inactivating *cul-4* gene function.

Inactivation of *cul-4* leads to polyploidy

The *cul-4* RNAi phenotype in the progeny of injected hermaphrodites was predominantly a developmental arrest at the L2 larval stage. *cul-4* RNAi produced 10-50% embryonic lethality in the F1 progeny. Animals that hatched were arrested at all larval stages depending on the penetrance of RNAi. The majority (80%) of larvae that hatched were arrested at the L2 larval stage.

In arrested *cul-4* RNAi L2 larvae, we observed a dramatic increase in the size of larval blast cells. To visualize cell size by DIC microscopy, we took advantage of the temperature-sensitive homozygous *clr-1*(*e1745*) mutants (Hedgecock et al., 1990). Cell boundaries become apparent in *clr-1* mutants after shifing to restrictive temperature. Figure 3.2 demonstrates the size differential between a hypodermal seam cell in *clr-1* L2 larvae (Figure 3.2 a) and *cul-4* RNAi *clr-1* L2 larvae (Figure 3.2 b). *cul-4* RNAi seam cells also have increased nuclear volume (more than nine times bigger than normal cells) (Figure 3.2 a, b). It is interesting to note that the size of the adjacent hypodermal cells is not affected by inactivation of *cul-4* (Figure 3.2 a, b). One difference between the seam cells and the hypodermal cells is that hypodermal cells do not proliferate, but seam cells have several post-embryonic divisions in wild-type animals. When we examined other blast cell lineages in *cul-4* RNAi animals, we observed phenotypes similar to those of the seam cells. Larger cells and larger nuclei were found in P cells (Figure 3.2 c, d) and somatic gonad cells (Figure 3.2 e, f).

Cell lineage studies revealed that this increase in nuclear volume and cell size is coupled with reduced division of these cells. During the course of postembryonic development, seam cells divide before each molt, and some of their daughters join the hyp7 hypodermal syncytium by cell fusion (Wood et al., 1988). Hyp7 is a cylindrical multinucleate cell that envelopes most of the *C. elegans* body. The hyp7 syncytium has 23 nuclei upon hatch and 133 nuclei in adult animals (Hedgecock and White, 1985). In wild-type animals, the first seam cell divisions occur in L1 larval stage, contributing 18 extra nuclei to hyp7 (Hedgecock and White, 1985). In *cul-4* RNAi animals, the first divisions of seam cells do not occur, although seam cell nuclear volume increases (data

not shown). Accordingly, hyp7 does not get extra nuclei after the animal is hatched. In wild-type animals, the P cell lineage generates neurons in the L1 larval stage (Wood et al., 1988). In *cul-4* RNAi animals, huge P cells with fewer neurons were observed. The phenotype of reduced division is also observed in *cul-4* intestine cells. Wild-type animals have 20 intestine cells at hatch, some of which undergo one mitosis to produce more intestine cells (Hedgecock and White, 1985). At L2 larval stage, there are 30 ± 3 (n=10) intestine cells in wild-type, but only 25 ± 3 (n=10) intestine cells in *cul-4* RNAi animals.

In the case of the somatic gonad cell lineage, an interesting phenotype observed is that when larger somatic gonad cells are observed in *cul-4* RNAi animals, sperm differentiation is also often observed in these arrested L2 larvae. In wild-type animals, spermatogenesis does not occur until the L4 larval stage. However, germ cells in *cul-2* RNAi animals often enter meiosis prematurely to become sperm although the animals are arrested at the L2 larval stage (Figure 3.2 f). We presume that this premature spermatogenesis is the result of a failure of the somatic gonad cell lineage to produce distal tip cells (DTCs) that are required to keep germ cells from entering meiosis (Seydoux and Schedl, 2001). DTCs arise from two ancestor somatic gonad cells, Z1 and Z4, during L1 larval stage. It is believed that DTCs produce a molecular signal LAG-2, which interacts with the receptor GLP-1 in adjacent germ cells to keep the germ cells mitotic (McCarter et al., 1997; Seydoux and Schedl, 2001). Laser ablation of DTCs at early larval stages such as the L2/L3 molt causes all germ cells to enter meiosis prematurely and differentiate into sperm (McCarter et al., 1997). It is possible that in *cul-4* RNAi animals, reduced divisions of somatic gonad cells causes a failure to produce DTCs, which results in a phenotype that is identical to that of DTC ablation.

The enlarged *cul-4* RNAi blast cells contained a dramatically elevated level of genomic DNA. DNA staining by propidium iodide revealed that most of the *cul-4* RNAi seam cells have DNA contents varying between 8C to 42C, compared to the 2C found in wild-type (Figure 3.2 g, h). DNA content increased with time, and two to three day post-hatch *cul-4* RNAi larvae were observed to have cells with over 100C DNA content.

Polyploidy in *cul-4* seam cells is caused by DNA re-replication

There are three distinct mechanisms that can generate increased ploidy (Figure 3.3). First, a failed mitosis mechanism, in which a failure to separate genomic DNA and perform cytokinesis during mitosis causes cells to enter G1 phase with a doubled DNA content, as occurs in the *C. elegans lin-5* mutant (Lorson et al., 2000). In failed mitosis, entry into mitosis is normal, and cells potentially proceed through early stages of mitosis normally, but mitosis fails before cytokinesis and cells do not separate into daughter cells. The second mechanism is endoreplication, in which cells bypass mitosis and enter the next cell cycle with doubled DNA content (Edgar and Orr-Weaver, 2001). In endoreplication, unlike in failed mitosis, cells do not enter mitosis at all. Certain cells undergo endoreplication under normal conditions, such as the *C. elegans* intestine cells and hypodermal cells (Hedgecock and White, 1995). Finally, there is the re-replication model, in which cells remain in S phase and continuously reinitiate DNA replication (Blow and Hodgson, 2002).

These three mechanisms can be distinguished by three criteria. First, the occurrence of mitotic entry distinguishes a failure of mitosis from endoreplication and re-replication, both of which do not entail mitosis. Second, in both the failed mitosis

mechanism and endoreplication, cells do not arrest in S phase, but instead continue to cycle through G2 and G1 phases. Finally, endoreplication and the failed mitosis mechanism increase ploidy through doublings of genomic DNA, while re-replication is not quantized.

To determine which mechanism causes the increased ploidy in *cul-4* RNAi cells, we tested each of these criteria, focusing on the seam cell lineage. First, using antibody against phosphorylated histone H3, which is one of the earliest mitotic markers (Hendzel et al., 1997), we observed that 3.8% (42/1116) of seam cells in unsynchronized wild-type larvae were mitotic, while only 0.09% (1/1109) of *cul-4* RNAi seam cells were mitotic, a 42-fold decrease (Figure 3.4). Further, mitotic entry (as indicated by nuclear envelope breakdown) was not observed in the seam cell lineage of *cul-4* RNAi L1 larvae when followed by DIC microscopy (0/3 cells), while mitotic entry was readily apparent in wild-type L1 larvae (2/2). Therefore, the lack of mitotic entry in *cul-4* RNAi blast cells precludes the failed mitosis mechanism.

Second, we measured the duration of S phase in seam cells using a reporter construct in which the S phase-specific ribonucleotide reductase (rnr) promoter drives green fluorescence protein (GFP) expression (Hong et al., 1998). I used the seam cell V4 as a representative for all seam cell lineages. In wild-type seam cell V4, GFP expression was turned on at about one hour before cell divisions, indicating S phase (Figure 3.5). The GFP signal perdured until one hour after cytokinesis. The fluorescence then stayed off until the next division. In contrast, we found that *cul-4* RNAi seam cells initiated rnr::GFP expression at the developmentally correct time, but remained in S phase continuously over the ten hours between cell divisions, while wild-type cells had

no GFP expression for eight of those hours (Figure 3.5). This suggests that *cul-4* RNAi seam cells are arrested in S phase. However, due to the perdurance of the GFP protein, I cannot rule out the possibility of *cul-4* RNAi seam cells underwent endoreplication with an extremely short gap of time in between S phases. S phase arrest was further confirmed by labeling newly synthesized DNA with BrdU. Positive BrdU staining indicates cells that are replicating DNA, indicative of S phase replicating DNA. I labeled synchronized populations at 8-12 hr post hatch. 14.3% (73 out of 510) of wild-type seam cells were in S phase, and this number increased to 28.5% (148 out of 520) in the *cul-4* RNAi population. Interestingly, when arrested *cul-4* RNAi L2 larvae were labeled with BrdU, an even higher percentage of seam cells had positive staining (33.8%, 44 out of 130), probably due to a more complete depletion of CUL-4 over the time. Note that wild-type animals are adults at this time, and no seam cells are in S phase. This observed cell cycle arrest in S phase supports the re-replication model and argues against the other two models. The fact that not all *cul-4* RNAi seam cells are BrdU positive is probably due to variations in RNAi penetrance.

Finally, we measured the DNA content of the *cul-4* RNAi cells. We observed that the DNA content of *cul-4* RNAi seam cells increases continuously rather than in doublings of 2C as is found for endoreplication in wild-type intestine cells (Hedgecock and White, 1985) (Figure 3.6). Wild-type intestine cells endoreplicate once at each of the four larval stages (Hedgecock and White, 1985). In the histogram of wild-type intestine cell DNA content, a quantized distribution of five discrete peaks at 2C, 4C, 8C, 16C, and 32C can be clearly identified (Figure 3.6). The first peak comes from cells before endoreplication and the latter four peaks correspond to each of the four endoreplication

cycles in the intestine cells. In contrast, *cul-4* RNAi seam cells show a non-quantized continuous DNA content distribution (Figure 3.6). Taken together, these data indicate that the dramatically increased ploidy in *cul-4* RNAi cells results from re-replication of genomic DNA.

CUL-4 negatively regulates CDT-1

The re-replication phenotype suggested a defect in the control of replication licensing. As introduced in the bacground section, the degradation of licensing proteins Cdc6/18p and Cdt1p in S phase is crucial to prevent DNA re-replication in fission yeast (Figure 3.7). We want to test the hypothsis of CUL-4 regulating these two licensing proteins in *C. elegans*. *C. elegans* has one ortholog of the DNA replication licensing factor Cdt1 (Nishitani et al., 2000; Maiorano et al., 2000). In pairwise alignments, the *C. elegans* CDT-1 protein has 23%, 20%, 19%, and 17% identity with its human, *D. melanogaster*, *S. pombe*, and *S. cerevisiae* orthologs, respectively.

The *C. elegans* CDT-1 is essential for DNA replication. Inactivation of *cdt-1* by RNAi produced embryos defective for DNA replication. *cdt-1* RNAi embryos have defects in genomic DNA segregation during early mitotic divisions with unequal DNA segregation and DNA bridges between dividing cells (Figure 3.8 a), perhaps resulting from partially replicated DNA. *cdt-1* RNAi embryos arrest with approximately 60 cells but contain only trace amounts of DNA, indicating a virtually complete cessation of DNA replication (Figure 3.8 b). The nuclear pore staining in these cells appear relatively normal (Figure 3.8 b). This phenotype is similar to that observed in other species when

cell divisions occur without DNA synthesis (Kimelman et al., 1987; Gerhart et al., 1984; Hara et al., 1980).

We generated affinity-purified antibodies against the full CDT-1 protein and used them to probe the CDT-1 expression pattern. In newly hatched larvae, no cells have high level CDT-1 expression. However, CDT-1 is transiently increased in all blast cells prior to their division. We examined the timing of CDT-1 expression in the first cell divisions of the seam cells V1-V6, which undergo mitosis at 4 hours post hatch (Sulston and Horvitz, 1977) (Figure 3.5). CDT-1 expression started at approximately 20 min, reached a maximum at approximately 1 hour 20 min – 2 hours and then disappeared by 2 hr 20 min post-hatch (Figure 3.9). The disappearance of CDT-1 expression coincides with the onset of S phase at 2 hr post-hatch (Figure 3.5). This observation matches that found in fission yeast and humans in which Cdt1 levels drop precipitously in S phase (Nishitani et al., 2000; Nishitani et al., 2001). CDT-1 expression in the seam cells did not resume until after the mitotic division. In *cul-4* RNAi animals, the expression of CDT-1 also began at approximately 20 min post hatch, but in marked contrast to wild-type, the signal did not disappear at 2 hr but continued through the time corresponding to the wild-type mitotic division (Figure 3.9). In two-day old arrested *cul-4* RNAi larvae, we observe a variation in the level of CDT-1 in enlarged cells: the majority have high levels of nuclear localized CDT-1 expression, a minority have both nuclear and cytoplasmic staining (Figure 3.9), and a subset have no detectable CDT-1 expression, perhaps reflecting transcriptional regulation. In an attempt to address the difference between the *cul-4* RNAi seam cells with CDT-1 staining and those without, we labeled the animals with BrdU and co-stained them with anti-CDT-1 antibody and anti-BrdU antibody. We found that among *cul-4*

RNAi seam cells, those that have CDT-1 staining are also positive for BrdU labelling (data not shown), suggesting that higher level of CDT-1 coincides with active DNA re-replication.

CUL-4 negatively regulates CDC-6

We also investigated CDC-6, the *C. elegans* ortholog of Cdc6, another important replication licensing factor. Similar to CDT-1, the *C. elegans* CDC-6 is also essential for DNA replication. Inactivation of *cdc-6* by RNAi produced embryonic lethality. In early stage embryos, we observed a "shredded DNA" phenotype (Figure 3.10), similar to those observed in cell fusion experiments when S phase cells enter mitosis (Johnson and Mullinger, 1975), indicating a potential defect in DNA replication. However, unlike *cdt-1* RNAi embryos, *cdc-6* RNAi embryos arrest cells at the 60-cell stage with visible amounts of DNA (Figure 3.10), indicating that DNA replication can still occur at a certain level in *cdc-6* RNAi embryos. Extremely unequal DNA distribution is observed in *cdc-6* RNAi cells (Figure 3.10), suggesting that DNA replication defects still exist in *cdc-6* RNAi cells although these are not as severe as those in *cdt-1* RNAi cells.

To detect the CDC-6 protein level in *cul-4* RNAi cells, I developed a peptide antibody against the C-terminus of CDC-6. The antibody specifically recognizes CDC-6. The antiserum recognizes bacterially expressed full-length CDC-6 at a 1:10,000 dilution in a Western blot assay. In immunofluorescence, the antibody stains mitotic chromosomes in wild-type embryos. This staining disappears in *cdc-6* RNAi embryos (Figure 3.11 a).

cul-4 RNAi seam cells accumulate both nuclear and cytoplasmic CDC-6 protein (Figure 3.11 b). In *cul-4* RNAi-arrested L2 larvae, CDC-6 staining is only observed in the large re-replicating seam cells, but not in normal sized cells that do not show the *cul-4* phenotype, suggesting a correlation between CDC-6 accumulation and the *cul-4* re-replication phenotype (Figure 3.11 b). In *cul-4* RNAi arrested larvae, 32% (128 out of 400) seam cells have CDC-6 staining, which coincides with the observation in another independent experiment that 34% of seam cells in *cul-4* RNAi-arrested larvae have positive BrdU labeling, further suggesting a correlation between CDC-6 accumulation and active DNA re-replication. In an unsynchronized wild-type larval population, 8% (25 out of 300) of the seam cells have both nuclear and cytoplasmic CDC-6 staining while others have no staining. Presumably, these 8% of cells are cells that are undergoing active cell cycle progression.

Suppression of the *cul-4* phenotype by *cdt-1* deficiency but not *cdc-6* deficiency

If increased CDT-1 or CDC-6 protein levels were contributing to the *cul-4* re-replication phenotype then removal of one copy of the gene might reduce the protein level sufficiently to suppress the phenotype. To probe for this genetic interaction, we performed *cul-4* RNAi in a strain heterozygous for a deficiency, *qDf4*, that removes the *cdt-1* gene, and in a strain heterozygous for a deficiency, *hDf6*, that removes the *cdc-6* gene. The *cul-4* re-replication phenotype in seam cells was suppressed five-fold in the *qDf4* deficiency strain (5.7±4.3C versus 27±11C, n=15 each) (Figure 3.12). In contrast, there was no significant suppression of the *cul-4* re-replication phenotype in the strain heterozygous for *cdc-6* (19±10C, n=15) (Figure 3.12). This suggests that the increased

CDT-1 levels in *cul-4* RNAi animals contribute to the re-replication phenotype. Interestingly, while the *cul-4* re-replication phenotype was suppressed in the *qDf4* heterozygotes, the L2 larval arrest still occurred, suggesting that these phenotypes arise from two separable CUL-4 functions.

DISCUSSION

We have demonstrated that CUL-4 is a major regulator of DNA replication licensing. Inactivation of *cul-4* by RNAi causes massive DNA re-replication. Polyploidy is observed mostly in the seam cells (Figure 3.2 a, b, g, h). DNA re-replication is also observed in other post-embryonic blast cells (including P cells, somatic gonad cells, and intestine cells) (Figure 3.2 c-f), but to a lesser extent and at a lower frequency. The lower frequency and lesser extent of DNA re-replication in other blast cells is probably due to RNAi penetrance.

Most of the re-replicating cells in *cul-4* RNAi animals are diploid in wild-type animals, including seam cells, P cells, and somatic gonad cells. Intestine cells have the highest ploidy among wild-type cells (Hedgecock and White, 1985). In a normal adult animal, intestine cells achieve 32C DNA content by endoreplication (Hedgecock and White, 1985). In *cul-4* RNAi arrested L2 larvae, intestine cells have relatively modest DNA content, ranging from 4C to 16C, compared to seam cells, which have up to 100C DNA. However, the DNA content of intestine cells in *cul-4* RNAi larvae is higher than that observed in wild-type L2 intestine cells, which have 4C DNA content. These results suggest that the DNA content in *cul-4* RNAi cells is unrelated to whether the cells endoreplicate or not in wild-type animals. This observation fits with our conclusion that

the increased ploidy in *cul-4* RNAi cells is caused by DNA re-replication rather than endoreplication. However, the intestine cells in *cul-4* RNAi animals may be affected by both mechanisms.

Polyploidy and reduced cell division do not cause developmental arrest. The *C. elegans lin-5* mutants have increased ploidy and reduced cell number caused by failed mitoses, but the mutants grow substantially and develop into adults (Lorson et al., 2000). In contrast, *cul-4* RNAi animals are arrested as L2 larvae. The larval arrest phenotype is therefore probably due to other CUL-4 functions. Furthermore, a *cdt-1* deficiency was able to partially suppress the DNA re-replication phenotype, but not the L2 arrest, indicating that CUL-4 may be essential for developmental events other than DNA replication.

CUL-4 negatively regulates CDC-6 and CDT-1. Both proteins accumulate in *cul-4* RNAi re-replicating cells (Figure 3.9 b, Figure 3.11 b). CUL-4 potentially may function as the ubiquitin ligase for the degradation of both CDC-6 and CDT-1 in *C. elegans*. Inactivation of *cul-4* by RNAi leads to re-replication in seam cells of up to 100C. The re-replication scale in *cul-4* seam cells exceeds any known re-replication phenotype observed from disruption of a single licensing protein, and is similar to that observed in *S. pombe* when both *CDT1* and *CDC6* are co-overexpressed (Yanow et al., 2001), suggesting that both CDC-6 and CDT-1 may be CUL-4 substrates. The observation that *cdc-6* deficiency failed to suppress the *cul-4* phenotype does not contradict with this model, as it is unknown whether the protein level of CDC-6 is decreased in the heterozygous deficiency strains. In addition, the heterozygous *cdt-1* deficiency strain has an average of 5.7C rather than 2C DNA content. The inability to

completely suppress the *cul-4* re-replication phenotype by *cdt-1* deficiency suggests additional *cul-4* substrates in this process. However, this may as well reflect the CDT-1 protein level in the deficiency strain.

Cullins have been found to degrade DNA licensing proteins. In *S. cerevisiae*, the cullin Cdc53p is required for ubiquitin-mediated degradation of Cdc6p (Deshaies, 1999). However, the yeast *CDC53* gave is most closely related to *cul-1* and *cul-2* in *C. elegans*, not *cul-4* (Kipreos et al., 1996). A DNA re-replication phenotype is not observed in *cul-1* and *cul-2* mutants. It is possible that some functions of the ancestral Cdc53p are carried out by other cullins in higher eukaryotes.

More studies are needed to determine whether the accumulation of CDC6 in *cul-4* seam cells is due to indirect effects, as it is unknown whether *C. elegans* CDC6 is regulated by proteolysis during the cell cycle. Cdc6 regulation is not conserved between species. In yeast, it is regulated by protein degradation in S phase, while in human cells, it is regulated by nuclear export (Bell and Dutta, 2002). Further research is needed to address whether CDC-6 protein level or subcellular localization is cell cycle-regulated in *C. elegans*.

Cdt1 function and regulation are conserved from yeast to man (Nishitani et al., 2000; Nishitani et al., 2001). CDT-1 is required for DNA replication in *C. elegans*. *cdt-1* RNAi produced a more severe DNA replication defect than that observed for *cdc-6* RNAi (Figure 3.8, 3.10). The *cdt-1* deficiency strain, but not the *cdc-6* deficiency strain, suppresses the *cul-4* RNAi re-replication phenotype (Figure 3.12). Taken together, these data suggest a more important role of CDT-1 in the regulation of DNA replication. *C. elegans* CDT-1 protein level peaks in G1 phase nuclei and disappears in S phase (Figure

3.9 a), suggesting regulation of CDT-1 by proteolysis in *C. elegans*. In cells lacking CUL-4, CDT-1 does not disappear in S phase nuclei and instead accumulates in re-replicating cells (Figure 3.9). It is possible that CUL-4 functions as an E3 to mediate ubiquitination and degradation of CDT-1.

During the rapid early cell divisions of *Xenopus* embryos, Cdt1 is regulated by binding to the inhibitory protein geminin (Wohlschlegel et al., 2000; Tada et al., 2001). Inactivation of geminin in *Drosophila*, however, leads to only limited increases in ploidy in a subset of cells (Quinn et al., 2001). Further, geminin does not appear to be the major source of Cdt1 regulation in mammalian tissue culture cells, where ubiquitin-mediated degradation of Cdt1 is more important (Nishitani et al., 2001). The molecular pathway responsible for targeting the degradation of Cdt1 has not been defined. We propose that in *C. elegans* a CUL-4 complex promotes the ubiquitin-mediated degradation of CDT-1 and that this degradation is important for limiting DNA replication licensing.

MATERIALS AND METHODS

Worm strains

The following strains of *C. elegans* were used: CB3241 [*clr-1*(*e1745*)], VT765 [*unc-36*(*e251*);mais 103; rnr::GFP], KR926 [*hDf6 dpy-5*(*e61*) *unc-13*(*e450*)/*szT1*; *unc-3*(*e151*)/*szT1*], RE249 [*qDf4*/*szT1* I; +/szT1], SP783 [*unc-4*(*e120*) *mnDf99*/*mnC1*].

Microscopy

Live animals were mounted on M9 solution or anesthetized with 1 mM levamisole. Animals were observed by differential contrast interference (DIC) and

immunofluorescence microscopy using a Zeiss Axioskop. Images were either taken with TechPan film (Kodak) and scanned by a Nikon LS-2000 scanner or taken with a Hamamatsu ORCA-ER digital camera with Openlab 3.0.8 software. All images were processed with Adobe Photoshop 6.0. Matched images were taken with the same exposure time and processed identically.

RNA interference

RNAi was performed using double-stranded RNA (dsRNA) derived from cDNA clones for *cul-4* (cDNA clone yk34c8, GenBank acc. no. D36543), *cdt-1*/Y54E10.15 (yk10c5, acc. no. D34651), and *cdc-6*/C43E11.10 (yk428f5, acc. no. C46988), all of which either contain the entire coding region or lack less than 50 bps of the coding region. Sense and antisense RNA were made using the T3 and T7 MegaScript kits (Ambion), respectively. Equal amounts of sense and antisense RNA were mixed and annealed to create double-stranded RNA (dsRNA). dsRNA was annealed and injected at a concentration of 0.5-1 mg/ml into young adults as described (Fire et al., 1998).

cul-4 RNAi was also conducted by the feeding method (Timmons and Fire, 1998), which generated identical phenotypes. Full-length cDNA was cloned into the double T7 promoter vector pPD 129.36 and transformed into the RNase III-deficient strain HT115. The bacteria were induced with IPTG to generate *cul-4* dsRNA. L4 wild-type animals were transferred onto plates seeded with these induced bacteria. Their progeny were scored for phenotype.

Antibody production

Anti-CDT-1 sera were produced in rabbits using purified recombinant His-tagged full-length CDT-1 fusion protein expressed from the pET15b vector (Novagen). Affinity purification was performed with His-CDT-1 fusion protein linked to activated CL4B Fast flow Sepharose (Amersham). Two different affinity-purified anti-CDT-1 antibodies gave the same pattern of immunofluorescence staining. Further, *cdt-1* RNAi eliminates anti-CDT-1 staining in early embryos (not shown).

Antiserum for CDC-6 was produced in rabbits using a peptide containing the C-terminus of the protein as antigen. The peptide sequence is CTAKSAISDNAMLDQIGLLQF. The peptide was conjugated to mcKLH, BSA, and OVA using Imject Maleimide Activated Immunogen Conjugation Kit (Pierce). Antisera from two different rabbits produced the same immunofluorescence staining pattern.

Immunofluorescense

The following control antibodies were used: mouse monoclonal antibody against nuclear pore (Mab414, BabCo), monoclonal anti-histone antibody (MAB052, Chemicon), monoclonal antibody against gap junctions (Francis and Waterston, 1991) (MH27, Developmental Studies Hybridoma Bank), monoclonal antibody agains BrdU (Sigma), and rabbit polyclonal antibody against phosphorylated histone H3 (Upstate Biotechnology). Secondary antibodies were anti-rabbit and anti-mouse Alexa Fluor 488, 546, and 633 (all from Molecular Probes). DNA was stained with either 1 µg/ml DAPI, or with 50 µg/ml propidium iodide after 20 µg/ml RNAse A treatment for 1 hour at 37° C.

For anti-CDT-1 immunofluorescence, animals were fixed on poly-lysine-coated slides using the "freeze-crack" method followed by –20°C methanol and acetone fixation, and incubated with primary and secondary antibodies as described (Miller and Shakes, 1995). For anti-CDC-6 immunofluorescence, samples were prefixed in 80% ethanol for 20 min at -20°C before methanol and acetone fixation. For BrdU labelling, animals were cultured 6 hours in 0.5 mg/ml 5-bromo-2'-deoxyuridine (BrdU, Sigma) in M9 solution with bacteria OP50. Animals were washed three times with M9 before fixed using the freeze-crack method or Bouin's fixative (Lorson et al., 2000). DNA was denatured in 4N HCl for one hour before antibody staining.

In situ hybridization

Antisense and sense digoxigenin-labeled RNA probes were created from full-length *cul-4* cDNA using Ambion MegaScript T7 and T3 kits with digoxigenin-11-UTP (Roche). *In situ* hybridization was performed on whole animals or gonad arms dissected from injected animals two days post injection as described (Feng et al., 1999). Sheep anti-digoxigenin-AP Fab fragments (Roche) was precleared with acetone-fixed *C. elegans* powder (Harlow and Lane, 1988) and used at 1:1500 dilution.

Signal quantification

For DNA quantification, animals were fixed using the "freeze-crack" method and stained with propidium iodide as described above. Cells of interest were serially scanned with an MRC600 Biorad confocal microscope (Feng et al. 1999). Images were analyzed as described by Feng et al. (1999) using NIH image software.

For *in situ* signal quantification, microscope images were captured by an AxioCam Digital camera and Axio Vision 2.0 software. Manual exposure time (7 ms) was used on all specimens so that no image saturated. Images were analyzed in NIH image for average intensity of the signal.

For GFP and antibody staining signal quantification, images were taken by a Hamamatsu ORCA-ER digital camera with Openlab 3.0.8 software. Quantification of immunofluorescence signals was standardized relative to the signal from anti-histone antibody used as a permeabilization control. For GFP expression, generally two to three animals were observed per time point, and the signals were averaged.

ACKNOWLEDGEMENTS

I thank E. T. Kipreos for making the anti-CDT-1 antibody and H. Feng for contributing the immunofluorescence research presented in Figure 3.9.

Figure 3.1 *cul-4* mRNA levels. (a and b) *in situ* hybridization of wild-type adult hermaphrodites with *cul-4* antisense (a) or control sense (b) RNA probes. Note that *cul-4* is not expressed in non-proliferating somatic cells in (a). (c-e) *in situ* hybridization with *cul-4* antisense probe of a two-cell stage embryo (c), two-fold-stage embryo (d), and L2 larvae (e). (f and g) *in situ* hybridization with antisense *cul-4* probe of a dissected gonad from a wild-type adult hermaphrodite (f) and a wild-type adult injected with *cul-4* dsRNA (g). (h) Control *in situ* hybridization of wild-type adult distal gonad using sense *cul-4* probe. Scale bars represent 10 µm.

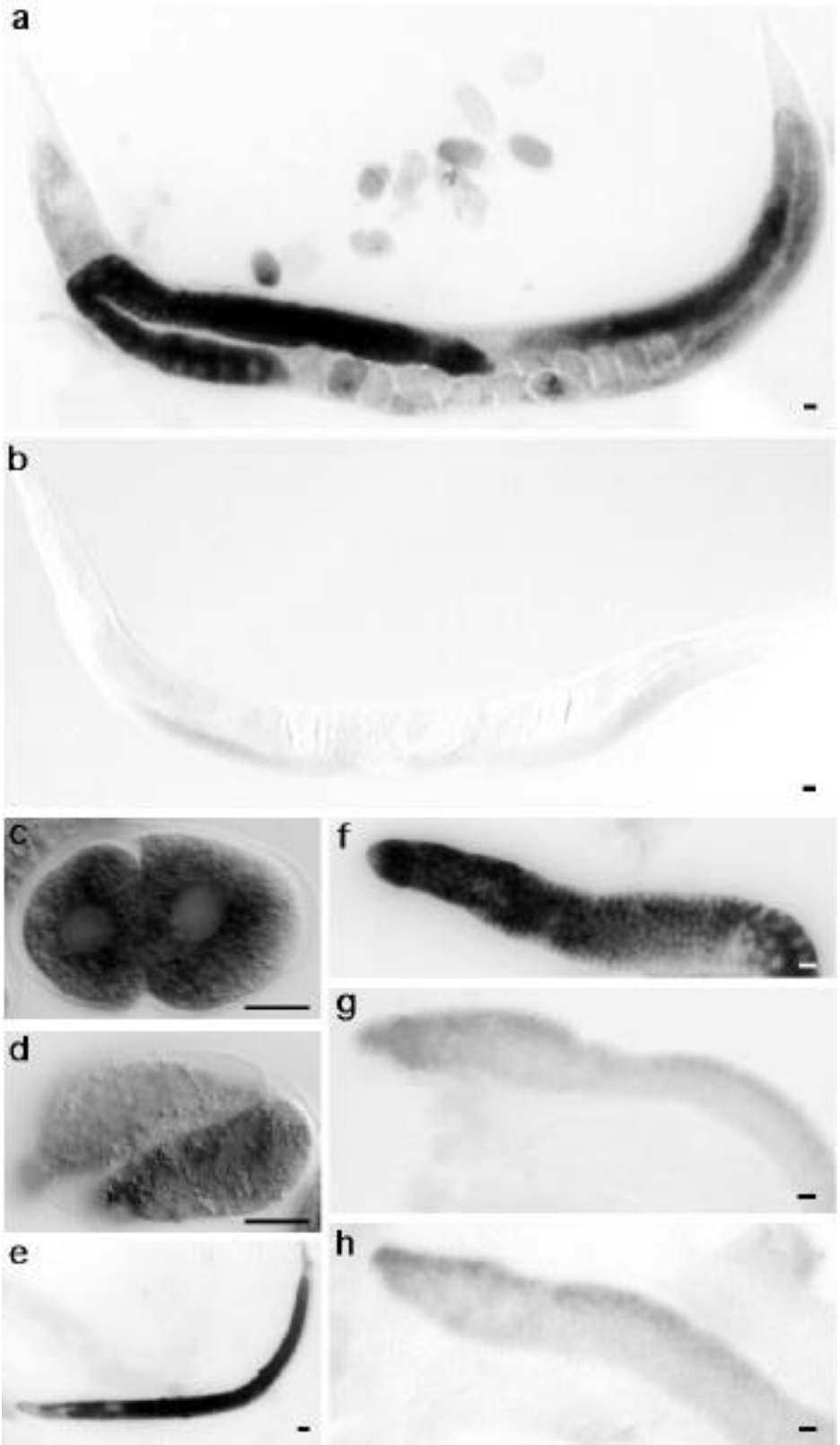
a
b
c
f
g
d
e
h

Figure 3.2 *cul-4* RNAi phenotype.
(a and b) DIC images of a control *clr-1*(*e1745*) L2 larvae (a) and an arrested *cul-4* RNAi *clr-1*(*e1745*) L2 larvae (b) shifted to the *clr-1*(*e1745*) non-permissive temperature. Se, seam cell. H, hypodermal cell.
(c and d) DIC micrograph of the ventral side of a wild-type L2 (c) and a *cul-4* RNAi arrested L2 (d); arrows indicate P cells.
(e and f) Germ line of a wild-type L2 (e) and a *cul-4* RNAi arrested L2 (f), arrow heads indicate DTC in e and ancestor of DTC in f, arrows indicate germ cells in a wild-type and sperm in a *cul-4* RNAi animal. (g and h) DAPI stain of genomic DNA of a wild-type L2 larvae (g) and a *cul-4* RNAi arrested L2 larvae (h). Scale bars represent 10 µm.

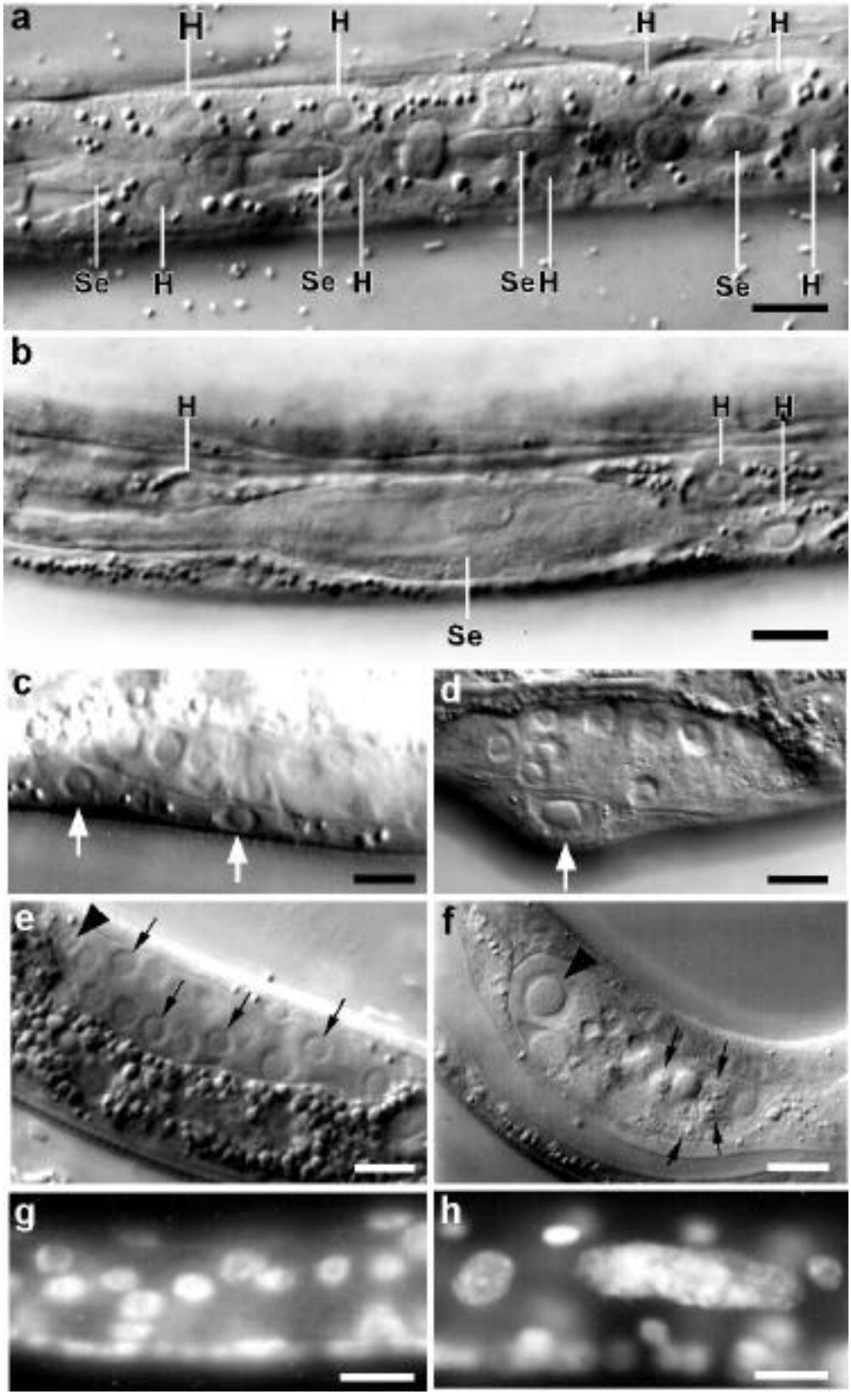
a
H
H
H
H
Se
H
Se
H
SeH
Se
H
b
H
H
H
Se
c
d
e
f
g
h

Figure 3.3 Three mechanisms that generate increased ploidy. Dark lines represent the cell cycle pathway present for each mechanism. Thin lines represent the normal cell cycle process.

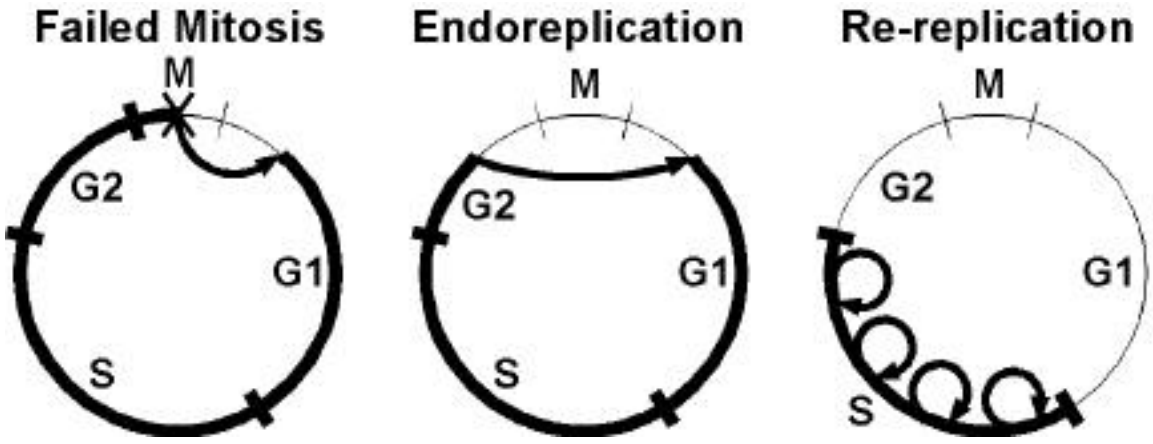
Failed Mitosis
M
G2
G1
S
Endoreplication
M
G2
G1
S
Re-replication
M
G2
G1
S

Figure 3.4 Wild-type (left) and *cul-4* RNAi (right) L2 larvae were fixed and stained with anti-phospho histone H3 antibody to mark mitotic cells (top) and DAPI (bottom). The names of mitotic seam cells in wild-type are listed. Scale bars represent 10 μm.

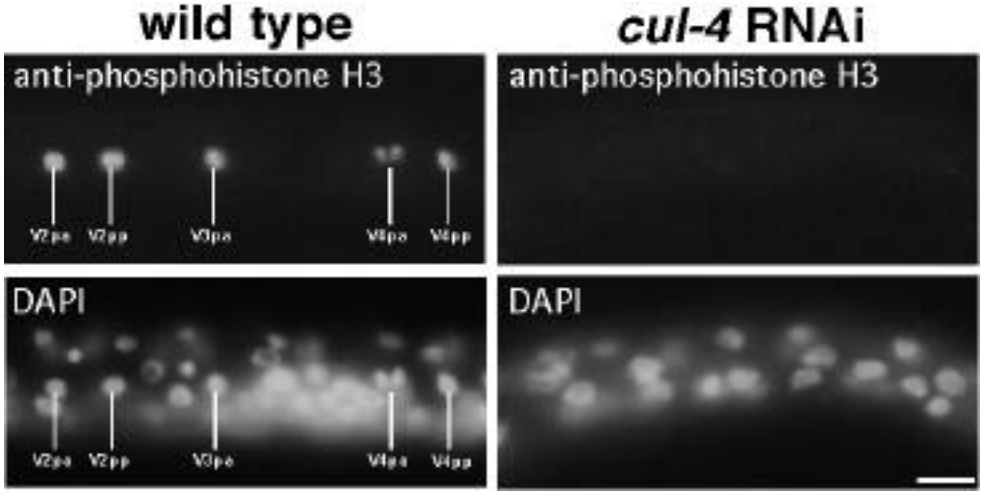
wild type
cul-4 RNAi
anti-phosphohistone H3
anti-phosphohistone H3
DAPI
DAPI

Figure 3.5 L1 lineage and rnr::GFP expression pattern of the seam cell V4 in wild-type (left) and *cul-4* RNAi (right) larvae. The zero time point is set at hatch. Plus symbols (+) denote rnr::GFP expression at each time point; minus symbol denotes lack of expression. The number of plus symbols denotes the relative intensity of GFP fluorescence. In uninjected control animals, the seam cell V4 divides at about 5 hr post hatch, and one of its daughters, V4p, divides at about 15.5 hr post hatch. The other daughter fused into the hyp7 syncytium, as indicated by "syn". rnr::GFP, an S phase marker, is turned on about one hour before the division. The GFP is turned off and green fluorescence disappeared about one hour after the division. GFP stays off between the two divisions. In *cul-4* RNAi animals, V4 does not divide and rnr::GFP stays on for hours.

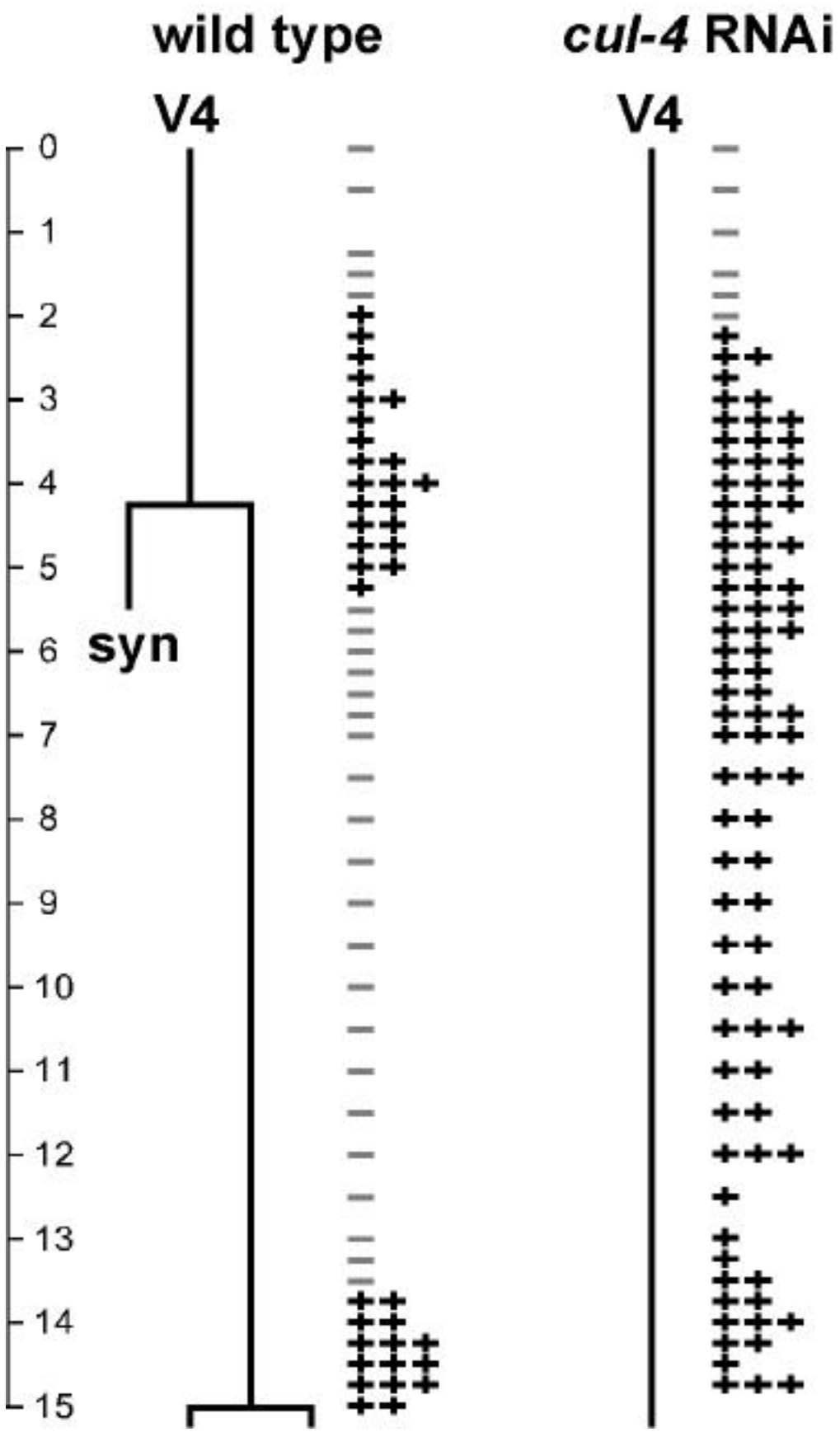
wild type
V4
0
1
2
3
4
5
6
7
8
9
10
11
12
13
14
15
syn
cul-4 RNAi
V4

Figure 3.6 Histogram of DNA content of intestine cells from wild-type animals (left) and of seam cells from *cul-4* RNAi animals (right). One *cul-4* RNAi seam cell with 165C DNA content is not plotted.

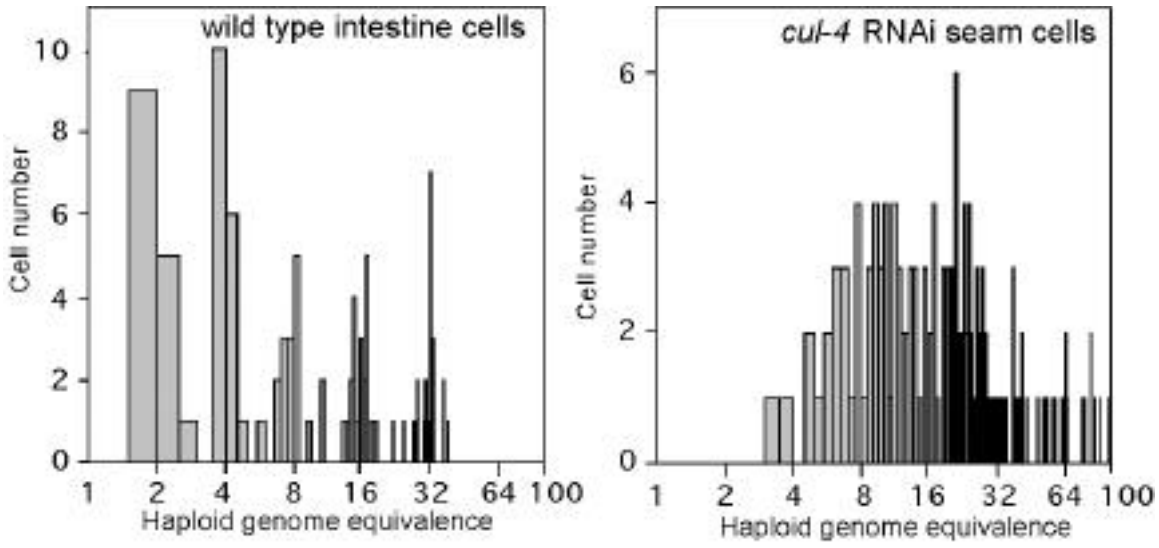
wild type intestine cells
Cell number
Haploid genome equivalence
1
2
4
8
16
32
64
100
0
2
4
6
8
10
cul-4 RNAi seam cells
Cell number
Haploid genome equivalence

Figure 3.7 DNA licensing control in fission yeast. In early G1 phase, ORC is bound to DNA replication origins. In late G1 phase, licensing proteins Cdc6/18 (called Cdc6 in budding yeast and Cdc18 in fission yeast) and Cdt1 are loaded to origins. The presence of Cdc6/18 and Cdt1 enables MCM proteins to be loaded onto chromatin to allow DNA replication. In S phase, Cdc6/18 and Cdt1 are removed from chromatin and degraded by ubiquitin-mediated proteolysis after DNA replication. The removal of Cdc6/18 and Cdt1 ensures that MCM proteins can not be reloaded to the origins, and therefore prevents origins from re-firing.

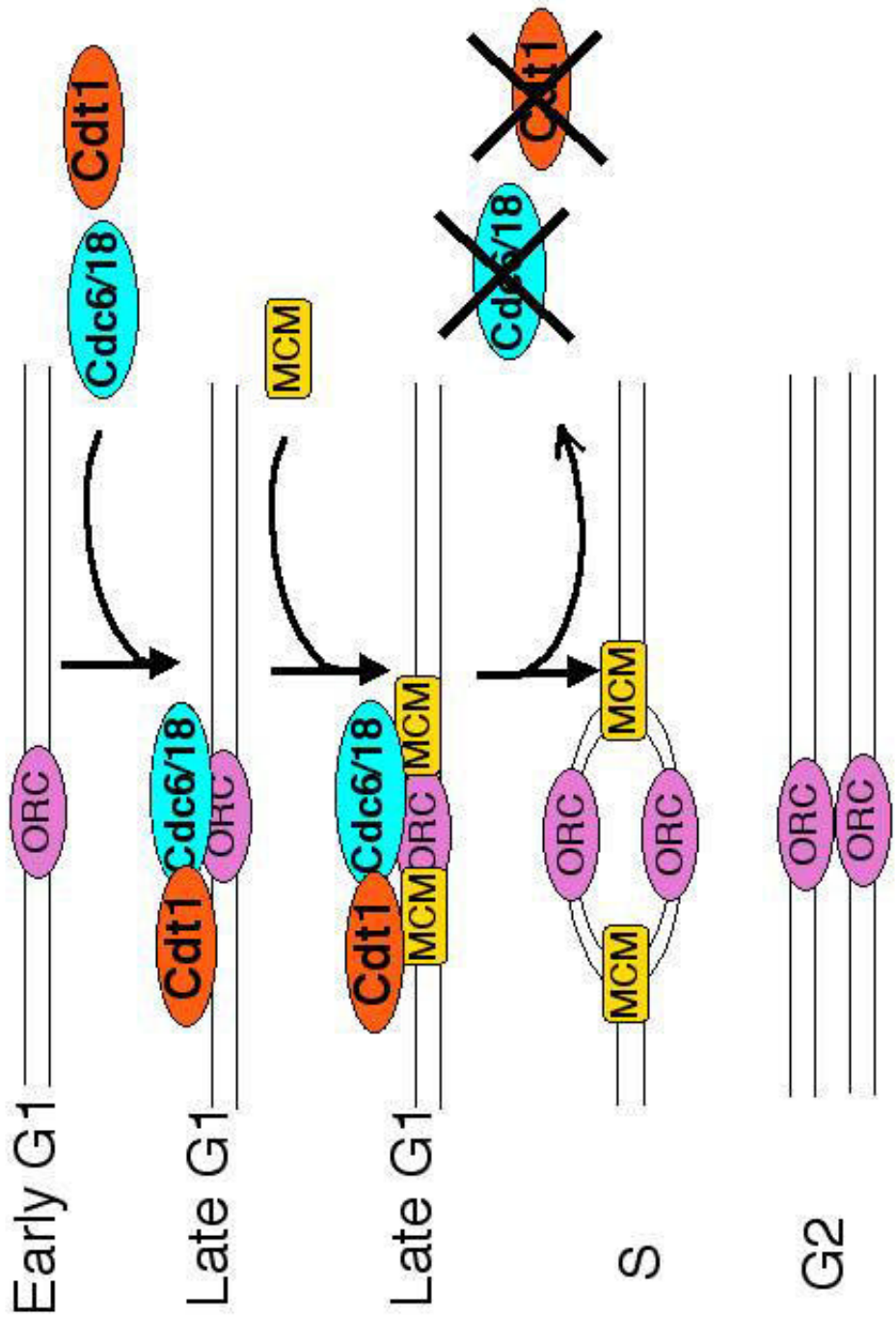
Early G1
Late G1
Late G1
S
G2
ORC
Cdc6/18
Cdt1
MCM

Figure 3.8 CDT-1 RNAi phenotype. (a) DIC and DAPI stain of 2-cell stage wild-type and *cdt-1* RNAi embryos. Arrow heads indicate polar bodies. (b) DIC, DAPI, and anti-nuclear pore stain of wild-type 60 cell stage and arrested *cdt-1* RNAi embryo. Scale bars represent 10 µm.

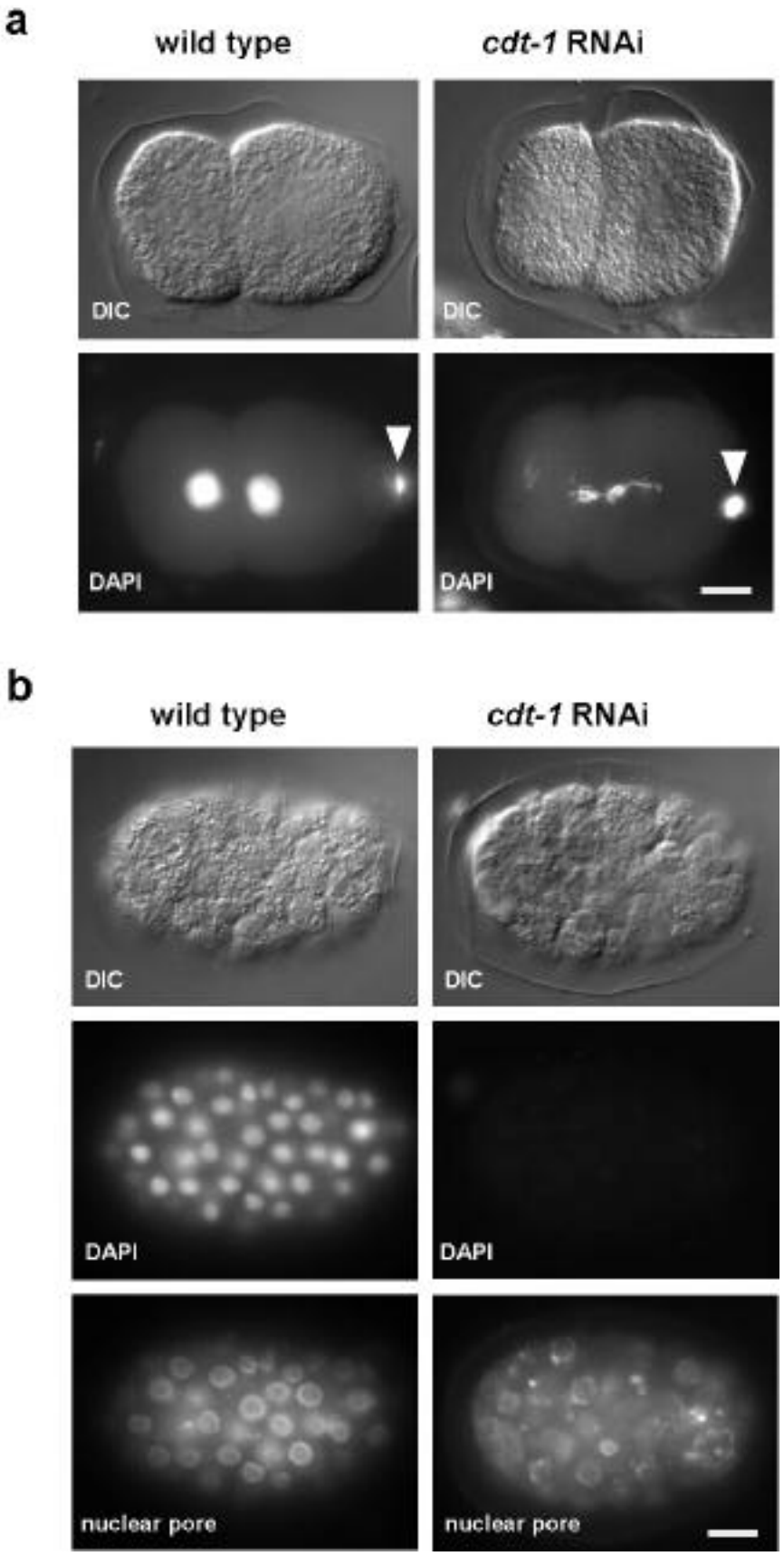
a
wild type
cdt-1 RNAi
DIC
DIC
DAPI
DAPI
b
wild type
cdt-1 RNAi
DIC
DIC
DAPI
DAPI
nuclear pore
nuclear pore

Figure 3.9 CDT-1 protein levels. (a) Upper panel, numbers of seam cells expressing CDT-1 during different cell cycle stages. Wild-type and *cul-4* RNAi L1 larvae were fixed at different time points post hatch, stained with the antibody against CDT-1. The average number of seam cells with nuclear CDT-1 staining (out of a total of 6 seam cells) per animal was plotted at each time point. Black squares denote wild-type and red diamonds denote *cul-4* RNAi seam cells. Lower panel, wild-type and *cul-4* RNAi L1 larvae 2 hr 30 min post-hatch, stained with CDT-1 (green), and DAPI (blue). Anti-gap junction antibody MH27 (Francis and Waterston, 1991) staining (red) is overlaid to highlight V1 and V2 seam cell boundaries. (b) Enlarged seam cell in arrested *cul-4* RNAi L2 larvae stained with anti-CDT-1 antibody (green) and DAPI (blue). Scale bars represent 10 µm.

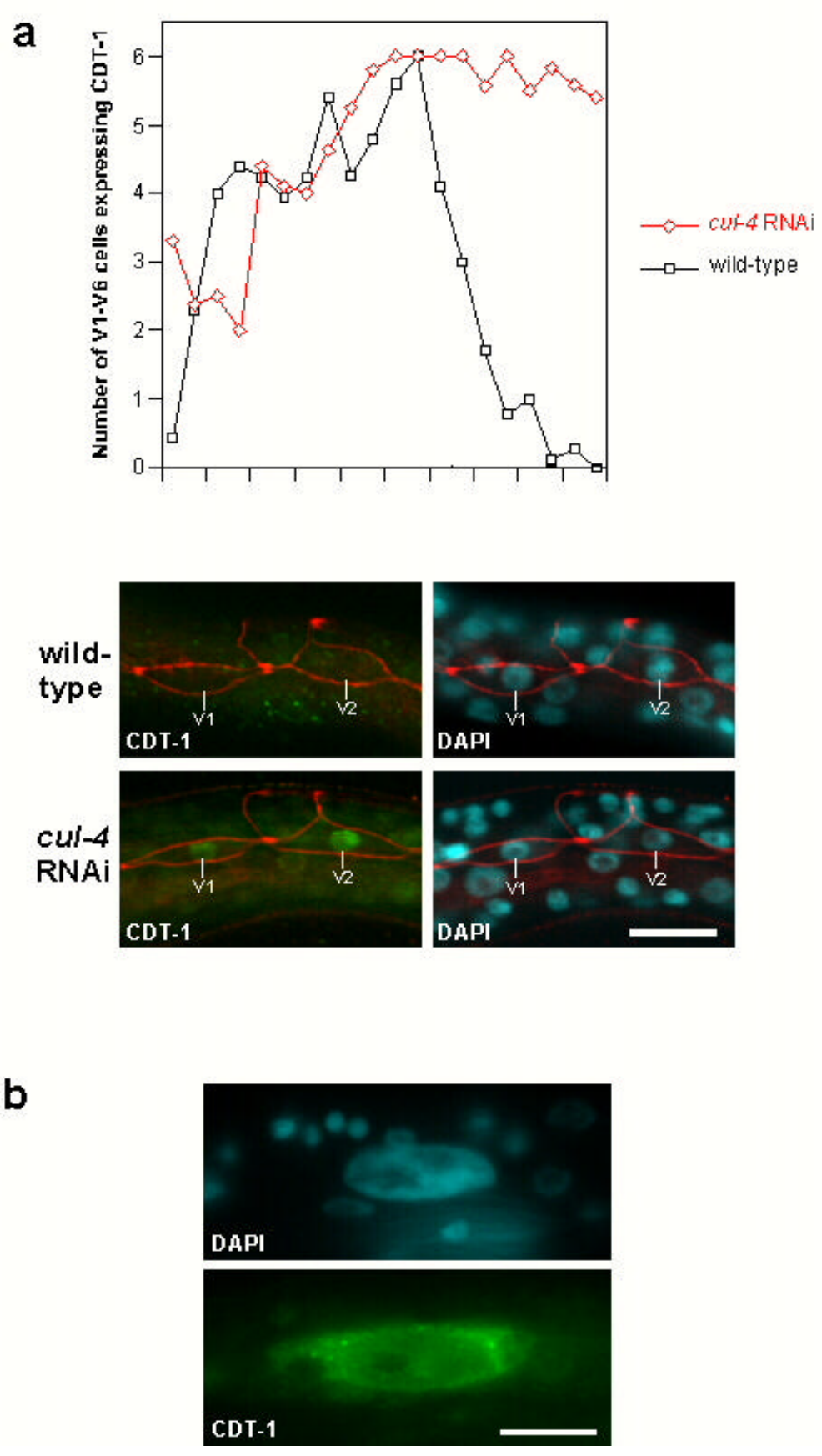
a
Number of V1-V6 cells expressing CDT-1
0
1
2
3
4
5
6
cul-4 RNAi
wild-type
wild-type
cul-4 RNAi
V1
V2
CDT-1
DAPI
b
DAPI
CDT-1

Figure 3.10 *cdc-6* RNAi phenotype. Top, DIC and DAPI of a 2-cell stage *cdc-6* RNAi embryo, note the shredded DNA phenotype. Bottom, DIC, DAPI, and anti-nuclear pore stain of an arrested *cdc-6* RNAi embryo. Note the unequal DNA distribution and the size differences among cells. Scale bars represent 10 μm.

***cdc-6* RNAi: 2-cell stage embryo**

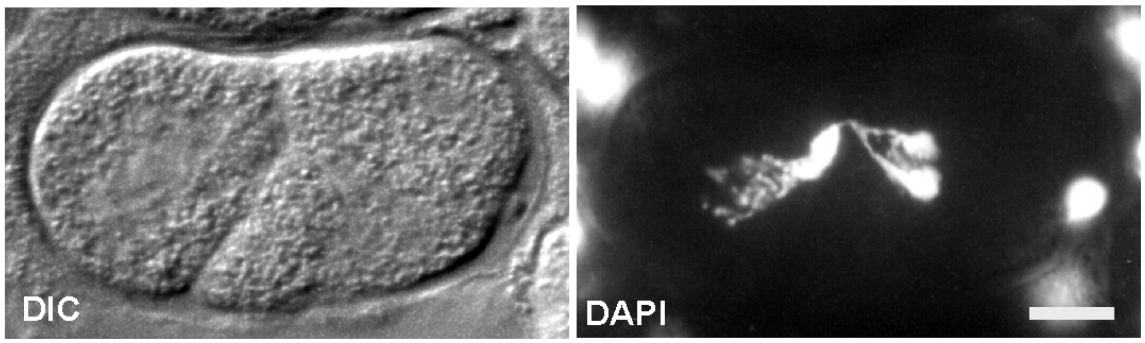

***cdc-6* RNAi: arrested embryo**

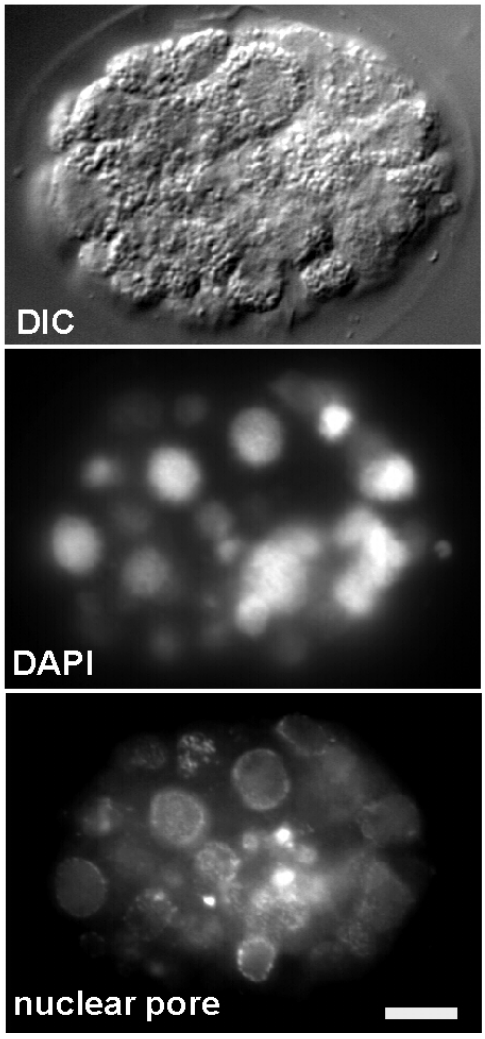

Figure 3.11 CDC-6 protein levels. a) CDC-6 antibody specificity. DIC, DAPI, and anti-CDC-6 stain of a wild-type embryo (left) and a *cdc-6* RNAi embryo (right). Anti-CDC-6 antibody recognizes mitotic chromosomes in wild-type cells. The staining disappears in *cdc-6* RNAi cells. b) Enlarged seam cell in arrested *cul-4* RNAi L2 larvae stained with DAPI (left) and anti-CDC-6 antibody (right). Scale bars represent 10 µm.

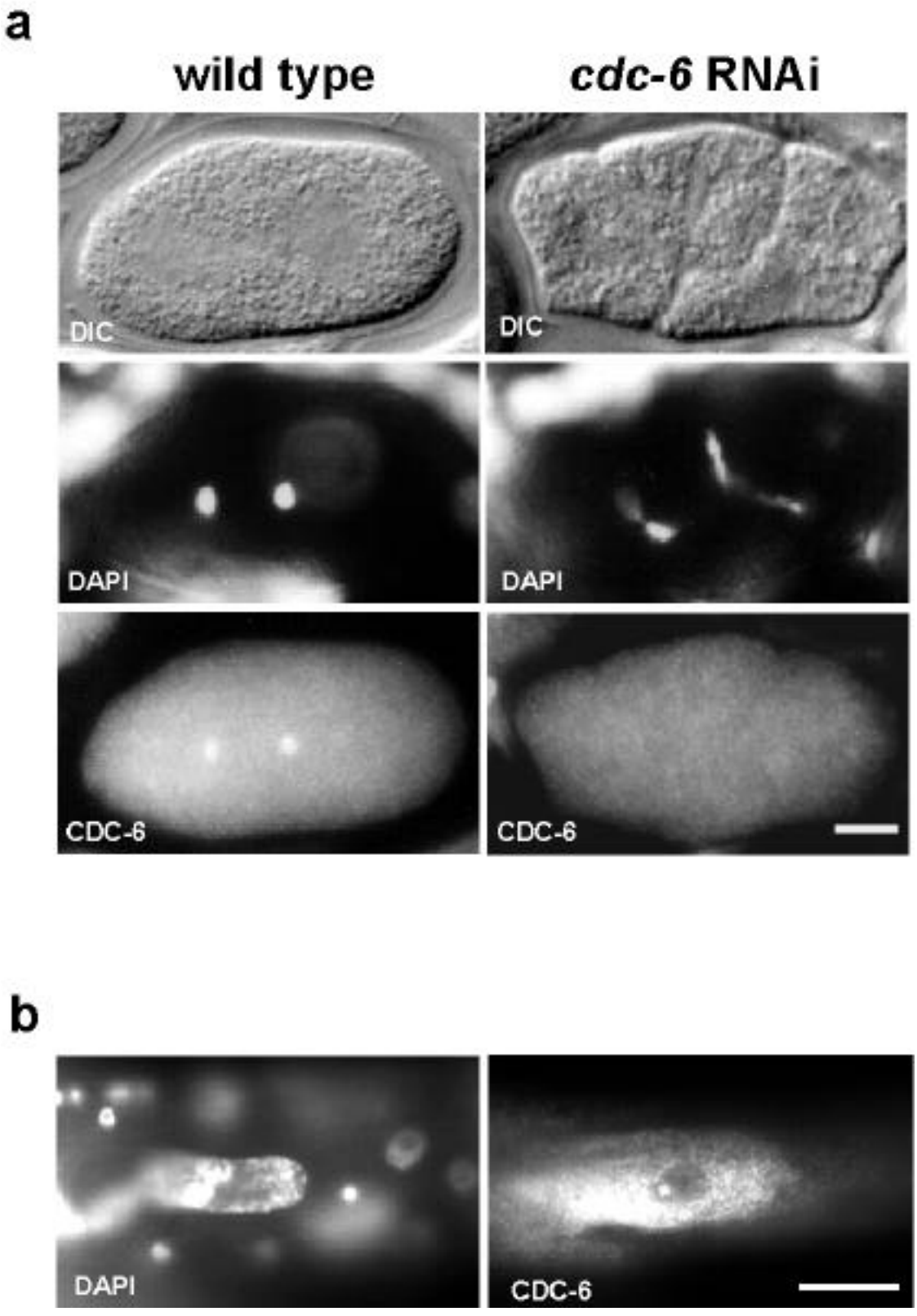
a
wild type
cdc-6 RNAi
DIC
DIC
DAPI
DAPI
CDC-6
CDC-6
b
DAPI
CDC-6

Figure 3.12 DNA content of seam cells in wild-type and strains heterozygous for deficiencies *qDf4*, which deletes *cdt-1*, and *hDf6*, which deletes *cdc-6*. Heterozygous strains of both of these deficiencies are wild-type (not shown).

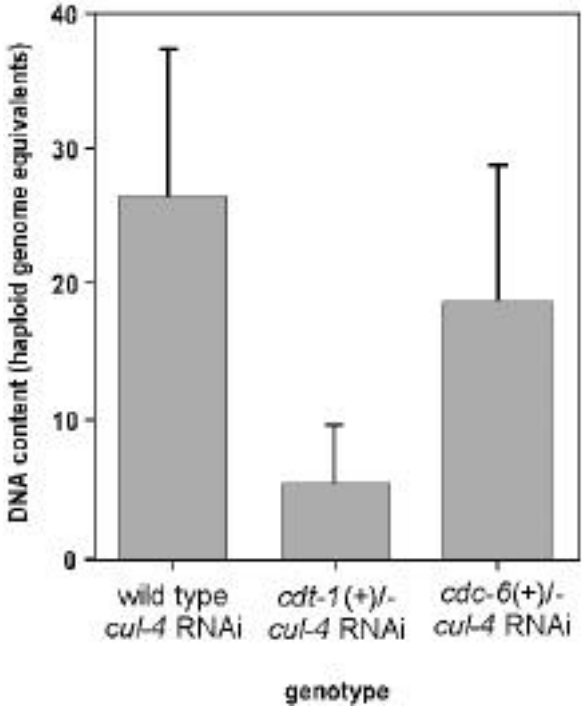
DNA content (haploid genome equivalents)
40
30
20
10
0
wild type
cul-4 RNAi
cdt-1(+)/-
cul-4 RNAi
cdc-6(+)/-
cul-4 RNAi
genotype

CHAPTER 4

GENERAL DISCUSSION

Ubiquitin-mediated proteolysis of cell cycle regulators is a driving force that makes cell cycle transitions irreversible. In the ubiquitin pathway, substrate protein specificity is determined by ubiquitin ligases. The family of cullin/RING finger ubiquitin ligase complexes is one of the two major classes of ubiquitin ligases that regulate the cell cycle.

A great deal of information is known about the SCF class of cullin/RING finger complexes that has the cullin CUL1 or Cdc53p as a component. SCF complexes function to ubiquitinate a variety of cell cycle regulators and metabolism regulators (Tyers and Jorgensen, 2000). In comparison to our knowledge about SCF complexes, information about the functions of the other cullins is rather limited. The research presented in this dissertation was initiated with the goal of characterizing the functions of two major cullins, CUL-2 and CUL-4, in *C. elegans*. I have described the experimental results in Chapter 2 and Chapter 3. Below, I will briefly discuss the major conclusions from the research, their contributions to our understanding of cell cycle regulation, and future research directions.

CUL-2 negatively regulates CKI-1, and is required for the G1-to-S-phase transition

We observed that *cul-2* mutant germ cells were unable to progress from G1 to S phase. This indicates that CUL-2 normally functions to promote entry into S phase. We were able to uncover the molecular pathway for this CUL-2 function by showing that

these *cul-2* mutant cells had a posttranscriptional accumulation of the CKI-1 protein and that decreasing the level of CKI-1 suppressed the G1 phase arrest phenotype. Therefore, our results indicate that CUL-2 promotes the G1-to-S phase transition by negatively regulating the level of a CDK inhibitor.

Our research suggests a model in which *C. elegans* CUL-2 functions as the ubiquitin ligase that mediates the degradation of CKI-1 at the G1-to-S phase transition to promote cell cycle progression. Future in vitro ubiquitination experiments are needed to determine whether CKI-1 is a direct ubiquitination substrate of CUL-2 or is degraded through a pathway downstream of CUL-2.

CUL-2 is required for mitotic chromosome condensation

Starting as early as the first mitosis, *cul-2* mutant embryos have strikingly uncondensed mitotic chromosomes. We observed that *cul-2* mutant embryos have defective DNA segregation, chromosome fragmentation, DNA bridging, and multiple nuclei. These phenotypes are similar to those observed in other known chromosome condensation mutants such as topoII mutants and condensin mutants, and suggest that they are all secondary defects arising from the primary defect in DNA condensation (Koshland and Strunnikov, 1996).

This research is the first to show that a ubiquitin ligase is required for mitotic chromosome condensation, thereby providing the first evidence that ubiquitination regulates this process. This research extends our knowledge about the mechanisms that control mitotic chromosome condensation. Identification of the CUL-2 substrates that must be ubiquitinated to allow chromosome condensation will provide valuable insights

into this novel regulatory pathway. The *cul-2* mutant allele isolated in this research will likely greatly facilitate future experiments to identify the substrates.

Other functions of CUL-2

This research has further expanded the known cellular functions for which CUL-2 is required by showing that *cul-2* mutant embryos have severe cytoskeletal defects and delays in mitotic progression. We provided the first in vivo evidence that a cullin/RING finger ubiquitin ligase is required for cytoskeletal organization in metazoa. We currently have not identified the molecular pathway through which CUL-2 effects cytoskeletal organization.

We also do not know the molecular pathway by which CUL-2 allows timely mitotic progression. As we discussed in Chapter 2, we do not believe that this phenotype is a secondary consequence of a failure of mitotic chromosome condensation, as condensin mutants, which have severe chromosome condensation defects, do not show a delay in mitotic progression. Potential models of how CUL-2 promotes mitotic progression naturally invoke interaction with the APC, which functions as a central regulator of mitotic progression. APC^{Cdc20} must be active to promote anaphase. In vertebrates, the F-box protein Emi1 inhibits APC^{Cdc20} activity (Reimann et al., 2001). Emi1 is degraded in early mitosis by an APC-independent pathway, which is currently unknown (Reimann et al., 2001). Our observation of a prolonged prometaphase in *cul-2* mutant embryos provides the exciting hypothesis that CUL-2 may function to degrade either an ortholog of Emi1 or a protein with a similar function to inhibit the APC.

CUL-4 functions as a central regulator of DNA replication licensing

One central problem in eukaryotic DNA replication is to duplicate the entire genome precisely once per cell cycle. Eukaryotic DNA replication is initiated at hundreds of replication origins, and therefore these origins must be strictly regulated to only fire once per cell cycle. This high degree of regulation is achieved by the DNA replication licensing system. Licensing proteins are required for DNA replication initiation, and the removal of licensing proteins from replicated chromatin in S phase prevents DNA re-replication. To date, disruption of the regulation of any single known licensing protein in any eukaryote has failed to induce massive DNA re-replication. Rather, massive re-replication has only been observed upon disruption of multiple, redundant mechanisms. In budding yeast, disruption of three redundant safeguards produces only marginal levels of re-replication (Nguyen et al., 2001). In fission yeast, disruption of two safeguards by overexpressing both Cdt1 and Cdc6 causes massive re-replication (Yanow et al., 2001). In mammals, no manipulation of the replication licensing control system has induced any level of re-replication. Surprisingly, we found that inactivation of the single *C. elegans cul-4* gene causes extensive re-replication, with cells reaching over 100C DNA content. We conclude that CUL-4 functions as a key regulator of the replication licensing system. *cul-4* is also the first known gene whose inactivation causes significant DNA re-replication, in contrast to other systems in which re-replication has been induced by overexpression of proteins, not by inactivation.

CDT-1 and CDC-6 are required for DNA replication

Current knowledge about metazoan licensing control is still incomplete, although a few licensing proteins including Cdc6 and Cdt1 have been identified. Like its fission yeast homolog, mammalian Cdt1 functions as a DNA licensing factor whose protein level decreases in S phase (Nishitani et al., 2000; Nishitani et al., 2001). In contrast, the function of Cdc6 as a replication licensing factor is not conserved in yeast and humans. In yeast, Cdc6p is degraded by SCF^{Cdc4}-mediated proteolysis in S phase (Drury et al., 1997; Elsasser et al., 1999). In human cells, a fraction of Cdc6 remains chromatin-bound throughout S phase (Coverley et al., 2000; Mendez and Stillman, 2000), while soluble Cdc6 is exported from the nucleus in S phase (Saha et al., 1998; Petersen et al., 1999). There is evidence that human ORC1 is also regulated as a DNA replication licensing protein, as it dissociates from chromatin and may be degraded in S phase (Natali et al., 2000; Kreitz et al., 2001). Studies on these proteins in other species would fill in the gaps in this evolutionary picture. However, before my research, the *C. elegans* replication licensing system was completely unknown.

We characterized the *C. elegans* CDT-1 DNA replication licensing protein. Inactivation of *cdt-1* by RNAi produces arrested embryos with virtually no DNA in the cells, suggesting that the *C. elegans* CDT-1 has a conserved role in DNA replication licensing. We also found that CDT-1 protein level peaks in G1 phase and disappears in S phase, indicating that CDT-1 is regulated by proteolysis, as is true in both yeast and human cells (Nishitani et al., 2000; Nishitani et al., 2001).

The *C. elegans* DNA replication licensing protein CDC-6 has also been partially characterized in this study. We found that the *C. elegans* CDC-6 protein is required for DNA replication, suggesting a conserved role in replication licensing. It is presently unknown whether the *C. elegans* CDC-6 is regulated either by proteolysis as in yeast or by nuclear translocation as in human cells. This question can be solved in future studies by using the CDC-6 antibody that I created for this study.

CUL-4 negatively regulates CDT-1 and CDC-6

Besides the characterization of the *cul-4* DNA re-replication phenotype, we also determined the molecular mechanism by which CUL-4 functions to prevent DNA re-replication. We showed that CUL-4 negatively regulates both CDT-1 and CDC-6 protein levels. Both proteins accumulate in *cul-4* re-replicating cells. In particular, we showed that in *cul-4* RNAi cells, CDT-1 failed to be degraded in S phase nuclei. We also showed that decreasing the level of CDT-1 suppresses the *cul-4* re-replication phenotype.

It is known that in both yeast and humans, Cdt1 protein level decreases in S phase (Blow and Hodgson, 2002). One question that has remained unsolved is how Cdt1 is degraded in S phase. Our research provides the first insight into the pathway responsible for Cdt1 degradation. We propose that CDT-1 is degraded by CUL-4/RING finger ubiquitin ligase-mediated ubiquitination. Future work by other laboratories will undoubtably test whether CUL4 also negatively regulates CDT1 levels in mammals and other metazoa.

In both budding yeast and fission yeast, Cdc6p/Cdc18p is degraded through the action of the SCF ubiquitin ligase complex (Drury et al., 1997; Elsasser et al., 1999;

Kominami and Toda, 1997; Kominami et al., 1998). If *C. elegans* CDC-6 is regulated by proteolysis, our result that CDC-6 accumulates in *cul-4* cells suggests that CUL-4 functions in the ubiquitin ligase complex required for CDC-6 degradation. On the other hand, if CDC-6 is regulated by subcellular localization, future research will be needed to identify additional CUL-4 substrates that regulate CDC-6 nuclear export.

The scale of DNA re-replication observed in *cul-4* cells exceeds that in any known re-replication phenotype resulting from disregulation of a single licensing factor, suggesting that more than one DNA replication licensing factor may be regulated by CUL-4. In the future, it would be rewarding to characterize other *C. elegans* DNA replication licensing factors and their interaction with CUL-4, in particular ORC1, which functions in humans as a replication licensing protein (Natali et al., 2000; Kreitz et al., 2001).

In summary, the research in this dissertation has provided genetic evidence that CUL-2 and CUL-4 function to regulate central aspects of the cell cycle, thereby contributing important pieces to a more complete picture of cell cycle regulation. Significantly, my research has laid the groundwork for future studies on the molecular functions of CUL-2/ and CUL-4/RING finger complexes.

REFERENCES

Adachi, Y., Luke, M., Laemmli, U. K. (1991). Chromosome assembly in vitro: topoisomerase II is required for condensation. Cell. *64*, 137-148.

Amon, A., Irniger, S. and Nasmyth, K. (1994). Closing the cell cycle circle in yeast: G2 cyclin proteolysis initiated at mitosis persists until the activation of G1 cyclins in the next cycle. Cell. *77*, 1037-1050.

Aparicio, O. M., Weinstein, D. M. and Bell, S. P. (1997). Components and dynamics of DNA replication complexes in *S. cerevisiae*: redistribution of MCM proteins and Cdc45p during S phase. Cell. *91*, 59-69.

Aris, J. P. and Blobel, G. (1989). Yeast nuclear envelope proteins cross react with an antibody against mammalian pore complex proteins. J. Cell Biol. *108*, 2059-2067.

Bai, C., Sen, P., Hofmann, K., Ma, L., Goebl, M., Harper, J. W. and Elledge, S. J. (1996). SKP1 connects cell cycle regulators to the ubiquitin proteolysis machinery through a novel motif, the F-box. Cell. *86*, 263-274.

Barral, Y., Jentsch, S. and Mann, C. (1995). G1 cyclin turnover and nutrient uptake are controlled by a common pathway in yeast. Genes Dev. *9*, 399-409.

Beach, D., Durkacz, B. and Nurse, P. (1982). Functionally homologous cell cycle control genes in budding and fission yeast. Nature. *300*, 706-709.

Bell, S. P. and Dutta, A. (2002). DNA replication in eukaryotic cells. Annu. Rev. Biochem. *71*, 333-374.

Blow, J. J. and Hodgson, B. (2002). Replication licensing--defining the proliferative state? Trends Cell Biol *12*, 72-78.

Boxem, M., Srinivasan, D. G. and van den Heuvel, S. (1999). The *Caenorhabditis elegans* gene ncc-1 encodes a cdc2-related kinase required for M phase in meiotic and mitotic cell divisions, but not for S phase. Development *126*, 2227-2239.

Carpenter, P. B., Mueller, P. R. and Dunphy, W. G. (1996). Role for a *Xenopus* Orc2-related protein in controlling DNA replication. Nature. *379*, 357-360.

Carrano, A.C., Eytan, E., Hershko, A. and Pagano, M. (1999). SKP2 is required for ubiquitin-mediated degradation of the CDK inhibitor p27. Nature Cell Biol. *1*, 193-199.

Chen, L.C., Manjeshwar, S., Lu, Y., Moore, D., Ljung, B. M., Kuo, W. L., Dairkee, S. H., Wernick, M., Collins, C. and Smith, H. S. (1998). The human homologue for the Caenorhabditis elegans *cul-4* gene is amplified and overexpressed in primary breast cancers. Cancer Res. ***58***, 3677-3683.

Chen, X., Zhang, Y., Douglas, L. and Zhou, P. (2001). UV-damaged DNA-binding proteins are targets of CUL-4A-mediated ubiquitination and degradation. J Biol Chem. *276*, 48175-48182.

Ciechanover, A., Orian, A., and Schwartz, A. (2000). Ubiquitin-mediated proteolysis: biological regulation via destruction. Bioessays *22*, 442-451.

Coleman, T. R., Carpenter, P. B. and Dunphy, W. G. (1996). The *Xenopus* Cdc6 protein is essential for the initiation of a single round of DNA replication in cell-free extracts. Cell. *87*, 53-63.

Conaway, J. W., Kamura, T., and Conaway, R. C. (1998). The elongin BC complex and the von Hippel-Lindau tumor suppressor protein. Biochim. Biophys. Acta *1377*, M49-M54.

Coverley, D., Pelizon, C., Trewick, S. and Laskey, R.A. (2000) Chromatin-bound Cdc6 persists in S and G2 phases in human cells, while soluble Cdc6 is destroyed in a cyclin A-cdk2 dependent process. J Cell Sci. *113*, 1929-1938.

Deshaies, R.J. SCF and Cullin/Ring H2-based ubiquitin ligases. Annu. Rev. Cell. Dev. Biol. *15*, 435-67 (1999).

Devault, A., Vallen, E. A., Yuan, T., Green, S., Bensimon, A., and Schwob, E. (2002). Identification of Tah11/Sid2 as the Ortholog of the Replication Licensing Factor Cdt1 in Saccharomyces cerevisiae. Curr Biol *12*, 689-694.

Dirick L., Bohm, T. and Nasmyth, K. (1995). Roles and regulation of Cln-Cdc28p kinases at the start of the cell cycle of *Saccharomyces cerevisiae*. EMBO J. 14, 4803-4813.

Drury, L. S., Perkins, G. and Diffley, J. F. (1997). The Cdc4/34/53 pathway targets Cdc6p for proteolysis in budding yeast. EMBO J. *16*, 5966-5976.

Duan, D. R., Pause, A., Burgess, W. H., Aso, T., Chen, D. Y. T., Garrett, K. P., Conaway, R. C., Conaway, J. W., Linehan, W. M., and Klausner, R. D. (1995). Inhibition of transcription elongation by the VHL tumor suppressor protein. Science *269*, 1402-1406.

Edgar, B. A., and Orr-Weaver, T. L. (2001). Endoreplication cell cycles: more for less. Cell *105*, 297-306.

Edgar, L. G., and McGhee, J. D. (1988). DNA synthesis and the control of embryonic gene expression in *C. elegans*. Cell *53*, 589-599.

Elsasser, S., Chi, Y., Yang, P. and Campbell, J. L. (1999). Phosphorylation controls timing of Cdc6p destruction: A biochemical analysis.*10*, 3263-3277.

Evans, T., Rosenthal, E. T., Youngblom, J., Distel, D. and Hunt, T. (1983). Cyclin: a protein specified by maternal mRNA in sea urchin eggs that is destroyed at each cleavage division. Cell. *33*, 389-396.

Feng, H., Zhong, W., Punkosdy, G., Gu, S., Zhou, L., Seabolt, E. K., and Kipreos, E. T. (1999). CUL-2 is required for the G1-to-S phase transition and mitotic chromosome condensation. Nat Cell Biol *1*, 486-492.

Feldman, R. M. R., Correll, C. C., Kaplan, K. B., and Deshaies, R. J. (1997). A complex of Cdc4p, Skp1p, and Cdc53p/Cullin catalyzes ubiquitination of the phosphorylated CDK inhibitor Sic1p. Cell *91*, 221-230.

Findeisen, M., El-Denary, M., Kapitza, T., Graf, R. and Strausfeld, U. (1999). Cyclin A-dependent kinase activity affects chromatin binding of ORC, Cdc6, and MCM in egg extracts of *Xenopus laevis*. Eur J Biochem. *264*, 415-426.

Fire, A., Xu, S., Montgomery, M. K., Kostas, S. A., Driver, S. E., and Mello, C. C. (1998). Potent and specific genetic interference by double-stranded RNA in *Caenorhabditis elegans*. Nature *391*, 806-811.

Francis, R., and Waterston, R. H. (1991). Muscle cell attachment in *Caenorhabditis elegans*. J. Cell Biol. *114*, 465-479.

Gardner, R. D. and Burke, D. J. (2000). The spindle checkpoint: two transitions, two pathways. Trends Cell Biol. *10*, 154-158.

Gautier, J., Norbury, C., Lohka, M., Nurse, P. and Maller, J. (1988). Purified maturation-promoting factor contains the product of a *Xenopus* homolog of the fission yeast cell cycle control gene cdc2+. Cell. *54*, 433-439.

Gerhart, J., Wu, M. and Kirschner, M. (1984). Cell cycle dynamics of an M-phase-specific cytoplasmic factor in *Xenopus laevis* oocytes and eggs. J. Cell Biol. *98*, 1247-1255.

Gillespie, P. J., Li, A. and Blow, J. J. (2001). Reconstitution of licensed replication origins on *Xenopus* sperm nuclei using purified proteins. BMC Biochem. *2*, 15.

Goebl, M. G., Yochem, J., Jentsch, S., McGrath, J. P., Varshavsky, A., and Byers, B. (1988). The yeast cell cycle gene CDC34 encodes a ubiquitin-conjugating enzyme. Science *241*, 1331-1335.

Guo, X. W., Th'ng, J. P., Swank, R. A., Anderson, H. J., Tudan, C., Bradbury, E. M. and Roberge, M. (1995). Chromosome condensation induced by fostriecin does not require p34cdc2 kinase activity and histone H1 hyperphosphorylation, but is associated with enhanced histone H2A and H3 phosphorylation. EMBO J. *14*, 976-985.

Hara, K., Tydeman, P. and Kirschner, M. (1980). A cytoplasmic clock with the same period as the division cycle in Xenopus eggs. Proc Natl Acad Sci U S A *77*, 462-466.

Harbour, J. W. and Dean, D. C. (2000). Chromatin remodeling and Rb activity. Curr Opin Cell Biol. *12*, 685-689.

Harlow, E., and Lane, D. (1988). Antibodies (A Laboratory Manual) (Cold Spring Harbor, N.Y.: Cold Spring Harbor Laboratories).

Hartwell, L. H., Culotti, J., Pringle, J. R. and Reid, B. J. (1974). Genetic control of the cell division cycle in yeast. Science. *183*, 46-51.

Hartwell, L. H., Cullotti, J. and Reid, B. (1970) Genetic control of the cell-division cycle in yeast. I. Detection of mutants. Proc Natl Acad Sci U S A. *66*, 352-359.

Hayes, S., Shiyanov, P., Chen, X. and Raychaudhuri, P. (1998). DDB, a putative DNA repair protein, can function as a transcriptional partner of E2F1. Mol Cell Biol *18*, 240-249.

Heck, M. M. S. (1997). Condensins, cohesins, and chromosome architecture: How to make and break a mitotic chromosome. Cell *91*, 5-8.

Hedgecock, E. M., Culotti, J. G., and Hall, D. H. (1990). The *unc-5*, *unc-6*, and *unc-40* Genes Guide Circumferential Migrations of Pioneer Axons and Mesodermal Cells on the Epidermis in C. elegans. Neuron *2*, 61-85.

Hedgecock, E. M., and White, J. G. (1985). Polyploid tissues in the nematode *Caenorhabditis elegans*. Dev. Biol. *107*, 128-133

Henchoz, S., Chi, Y., Catarin, B., Herskowitz, I., Deshaies, R. J., and Peter, M. (1997). Phosphorylation- and ubiquitin-dependent degradation of the cyclin-dependent kinase inhibitor Far1p in budding yeast. Genes and Dev. *11*, 3046-3060.

Hendzel, M. J., Wei, Y., Mancini, M. A., Van Hooser, A., Ranalli, T., Brinkley, B. R., Bazett-Jones, D. P., and Allis, C. D. (1997). Mitosis-specific phosphorylation of histone H3 initiates primarily within pericentromeric heterochromatin during G2 and spreads in an ordered fashion coincident with mitotic chromosome condensation. Chromosoma *106*, 348-360.

Hershko, A., and Ciechanover, A. (1998). The ubiquitin system. Annu Rev Biochem *67*, 425-479.

Hindley, J. and Phear, G. A. (1984). Sequence of the cell division gene CDC2 from *Schizosaccharomyces pombe*; patterns of splicing and homology to protein kinases. Gene. *31*, 129-134.

Hirano, T. (2000). Chromosome cohesion, condensation, and separation. Annu Rev Biochem. *69*, 115-144.

Hirano, T., Kobayashi, R. and Hirano, M.. (1997). Condensins, chromosome condensation protein complexes containing XCAP-C, XCAP-E and a *Xenopus* homolog of the *Drosophila* Barren protein. Cell. *89*, 511-521.

Hirano, T. and Mitchison, T.J. (1993). Topoisomerase II does not play a scaffolding role in the organization of mitotic chromosomes assembled in Xenopus egg extracts. J Cell Biol. 120, 601-612.

Hirano, T. and Mitchison, T.J. (1994). A heterodimeric coiled-coil protein required for mitotic chromosome condensation in vitro. Cell. *79*, 449-458.

Hochstrasser, M. (1998). There's the rub: a novel ubiquitin-like modification linked to cell cycle regulation. Genes Dev. *12*, 901-907.

Hong, G., Roy, R., and Ambros, V. (1998). Developmental regulation of a cyclin-dependent kinase inhibitor controls postembryonic cell cycle progression in *C. elegans*. Development *125*, 3585-3597.

Hsieh, T. and Brutlag, D. (1980). ATP-dependent DNA topoisonmerase from *D. melanogaster* reversibly catenates duplex DNA rings. Cell. *21*, 115-125.

Hua, X. H. and Newport, J. (1998). Identification of a preinitiation step in DNA replication that is independent of origin ecognition complex and cdc6, but dependent on cdk2. J Cell Biol. *140*, 271-281.

Huang, J. N., Park, I., Ellingson, E., Littlepage, L. E. and Pellman, D. (2001). Activity of the APC(Cdh1) form of the anaphase-promoting complex persists until S phase and prevents the premature expression of Cdc20p. J Cell Biol. *154*, 85-94.

Ishimi, Y. (1997). A DNA helicase activity is associated with an MCM4, -6, and -7 protein complex. J Biol Chem. 272, 24508-24513.

Jaquenoud, M., Gulli, M. P., Peter, K. and Peter, M. (1998). The Cdc42p effector Gic2p is targeted for ubiquitin-dependent degradation by the SCFGrr1 complex. EMBO J. *17*, 5360-5373.

Johnson, R. T. and Mullinger, A. M. (1975). The induction of DNA synthesis in the chick red cell nucleus in heterokaryons during the first cell cycle after fusion with HeLa cells. J Cell Sci. *18*, 455-490.

Kaelin, W. G., and Maher, E. R. (1998). The VHL tumour-suppressor gene paradigm. Trends Genet. *14*, 423-426.

Kaiser, P., Sia, R. A. L., Bardes, E. G. S., Lew, D. J., and Reed, S. I. (1998). Cdc34 and the F-box protein Met30 are required for degradation of the cdk-inhibitory kinase Swe1. Genes and Dev. *12*, 2587-2597.

Kamizono, S., Hanada, T., Yasukawa, H., Minoguchi, S., Kato, R., Minoguchi, M., Hattori, K., Hatakeyama, S., Yada, M., Morita, S., Kitamura, T., Kato, H., Nakayama, Ki.and Yoshimura, A. (2001). The SOCS box of SOCS-1 accelerates ubiquitin-dependent proteolysis of TEL-JAK2. J Biol Chem. *276*, 12530-12538.

Kamura, T., Conrad, M. N., Yan, Q., Conaway, R.C. and Conaway, J. W. (1999). The Rbx1 subunit of SCF and VHL E3 ubiquitin ligase activates Rub1 modification of cullins Cdc53 and Cul2. Genes Dev. *13*, 2928-2933.

Kamura, T., Sato, S., Haque, D., Liu, L., Kaelin, W. G. Jr, Conaway, R. C., Conaway, J. W. (1998). The Elongin BC complex interacts with the conserved SOCS-box motif present in members of the SOCS, ras, WD-40 repeat, and ankyrin repeat families. Genes Dev. *12*, 3872-3881 .

Keeney, S., Eker, A. P., Brody, T., Vermeulen, W., Bootsma, D., Hoeijmakers, J. H. and Linn, S. (1994). Correction of the DNA repair defect in xeroderma pigmentosum group E by injection of a DNA damage-binding protein. Proc Natl Acad Sci U S A *91*, 4053-4056.

Kibel, A., Iliopoulos, O., DeCaprio, J. A., and Kaelin, W. G. (1995). Binding of the von Hippel-Lindau tumor suppressor protein to Elongin B and C. Science *269*, 1444-1446.

Kim, M., Katayose, Y., Li, Q., Rakkar, A. N., Li, Z., Hwang, S. G., Katayose, D., Trepel, J., Cowan, K. H. and Seth, P. (1998). Recombinant adenovirus expressing Von Hippel-Lindau-mediated cell cycle arrest is associated with the induction of cyclin-dependent kinase inhibitor $p27^{KIP1}$. Biochem. Biophys. Res. Comm. *253*, 672-677.

Kimble, J., and Hirsh, D. (1979). The postembryonic cell lineages of the hermaphrodite and male gonads in *Caenorhabditis elegans*. Dev. Biol. *70*, 396-417.

Kimelman, D., Kirschner, M. and Scherson, T. (1987). The events of the midblastula transition in Xenopus are regulated by changes in the cell cycle. Cell *48*, 399-407.

Kimura, K. and Hirano, T. (1997). ATP-dependent positive supercoiling of DNA by 13S condensin: a biochemical implication for chromosome condensation. Cell. *90*, 625-634.

Kimura, K., Hirano, M., Kobayashi, R., and Hirano, T. (1998). Phosphorylation and activation of 13S condensin by cdc2 *in vitro*. Science *282*, 487-490.

King, R.W., Deshaies, R.J., Peters, J.-M. and Kirschner, M.W. (1996). How Proteolysis Drives the Cell Cycle. Science *274*, 1652-1659 .

Kipreos, E.T., Lander, L.E., Wing, J.P., He, W.W. and Hedgecock, E.M. (1996). *cul-1* is Required for Cell Cycle Exit in *C. elegans* and Identifies a Novel Gene Family. Cell *85*, 829-839.

Kipreos, E. T. and Pagano, M. (2000). The F-box protein family. Genome Biol. *1*, REVIEWS3002.

Kirby, C., Kusch, M., and Kemphues, K. (1990). Mutation in the par genes of *Caenorhabditis elegans* affect cytoplasmic reorganization during the first cell cycle. Dev. Biol. *142*, 203-215.

Koch, C. and Nasmyth, K. (1994). Cell cycle regulated transcription in yeast. Curr. Opin Cell Biol. *6*, 451-459.

Koegl, M., Hoppe, T., Schlenker, S., Ulrich, H. D., Mayer, T. U., and Jentsch, S. (1999). A novel ubiquitination factor, E4, is involved in multiubiquitin chain assembly. Cell *96*, 635-644.

Kominami, K., Ochotorena, I. and Toda, T. (1998). Two F-box/WD-repeat proteins Pop1 and Pop2 form hetero- and homo-complexes together with cullin-1 in the fission yeast SCF (Skp1-Cullin-1-F-box) ubiquitin ligase. Genes Cells. *3*, 721-735.

Kominami, K. and Toda, T. (1997). Fission yeast WD-repeat protein pop1 regulates genome ploidy through ubiquitin-proteasome-mediated degradation of the CDK inhibitor Rum1 and the S-phase initiator Cdc18. Genes Dev. 11:1548-1560.

Kornitzer, D., Raboy, B., Kulka, R. G. and Fink, G. R. (1994). Regulated degradation of the transcription factor Gcn4. EMBO J. *13*, 6021-6030.

Koshland, D., and Strunnikov, A. (1996). Mitotic chromosome condensation. Annu. Rev. Cell Dev. Biol. *12*, 305-333.

Kreitz, S., Ritzi, M., Baack, M. and Knippers, R. (2001). The human origin recognition complex protein 1 dissociates from chromatin during S phase in HeLa cells. J Biol Chem. *276*, 6337-6342.

Kreuzer, K. N. and Cozzarelli, N. R. (1980). Formation and resolution of DNA catenanes by DNA gyrase. Cell. *20*, 245-254.

Kurz, T., Pintard, L., Willis, J. H., Hamill, D. R., Gonczy, P., Peter, M. and Bowerman, B. (2002). Cytoskeletal regulation by the Nedd8 ubiquitin-like protein modification pathway. Science. *295*, 1294-1298.

Labbe, J. C., Capony, J. P., Caput, D., Cavadore, J. C., Derancourt, J., Kaghad, M., Lelias, J. M., Picard, A. and Doree, M. (1989). MPF from starfish oocytes at first meiotic metaphase is a heterodimer containing one molecule of cdc2 and one molecule of cyclin B. EMBO J. *8*, 3053-3058.

Labib, K., Tercero, J. A. and Diffley, J. F. (2000). Uninterrupted MCM2-7 function required for DNA replication fork progression. Science. *288*, 1643-1647.

Lammer, D., Mathias, N., Laplaza, J. M., Jiang, W., Liu, Y., Callis, J., Goebl, M. and Estelle, M. (1998). Modification of yeast Cdc53p by the ubiquitin-related protein Rub1p affects function of the SCFcdc4 complex. Genes Dev. *12*, 914-926.

Lanker, S., Valdivieso, M. H. and Wittenberg, C. (1996). Rapid degradation of the G1 cyclin Cln2 induced by CDK-dependent phosphorylation. Science. *271*, 1597-1601.

Latres, E., Chiaur, D.S. and Pagano, M. (1999). the human F-box protein b-Trcp associates with the Cul1/Skp1 complex and regulates the stability of b-catenin. Oncogene *18*, 849-854.

Lee, J. K. and Hurwitz, J. (2001) Processive DNA helicase activity of the minichromosome maintenance proteins 4, 6, and 7 complex requires forked DNA structures. Proc Natl Acad Sci U S A. *98*, 54-59.

Li, C. J. and DePamphilis, M. L. (2002). Mammalian Orc1 protein is selectively released from chromatin and ubiquitinated during the S-to-M transition in the cell division cycle. Mol Cell Biol. *22*, 105-116.

Lisztwan, J., marti, A., Sutterluty, H., Gstaiger, M., Wirbelauer, C., and Krek, W. (1998). Association of human CUL-1 and ubiquitin-conjugating enzyme CDC34 with the F-box

protein p45^{SKP2}: evidence for evolutionary conservation in the subunit composition of the CDC34-SCF pathway. EMBO J. *17*, 368-383.

Lonergan, K. M., Iliopoulos, O., Ohh, M., Kamura, T., Conaway, R. C., Conaway, J. W., and Kaelin, W. G. (1998). Regulation of hypoxia-inducible mRNAs by the von Hippel-Lindau tumor suppressor protein requires binding to complexes containing Elongins B/C and Cul2. Mol. Cell. Biol. *18*, 732-741.

Lorincz, A. T. and Reed, S. I. (1984). Primary structure homology between the product of yeast cell division control gene CDC28 and vertebrate oncogenes. Nature. *307*, 183-185.

Lorson, M. A., Horvitz, H. R., and van den Heuvel, S. (2000). LIN-5 is a novel component of the spindle apparatus required for chromosome segregation and cleavage plane specification in Caenorhabditis elegans. J Cell Biol *148*, 73-86.

Lyapina, S. A., Correll, C. C., Kipreos, E. T., and Deshaies, R. J. (1998). Human CUL1 forms an evolutionarily conserved ubiquitin ligase complex (SCF) with SKP1 and an F-box protein. Proc. Natl. Acad. Sci. *95*, 7451-7456.

Maine, G. T., Sinha, P. and Tye, B. K. (1984). Mutants of *S. cerevisiae* defective in the maintenance of minichromosomes. Genetics. *106*, 365-385.

Mains, P. E., Kemphues, K. J., Sprunger, S. A., Sulston, I. A., and Wood, W. B. (1990). Mutations affecting the meiotic and mitotic divisions of the early *Caenorhabditis elegans* embryo. Genetics *126*, 593-605.

Maiorano, D., Moreau, J., and Mechali, M. (2000). XCDT1 is required for the assembly of pre-replicative complexes in Xenopus laevis. Nature *404*, 622-625.

Marti, A., Wirbelauer, C., Scheffner, M. and Krek, W. (1999). Interaction between ubiquitin-protein ligase SCFSKP2 and E2F-1 underlies the regulation of E2F-1 degradation. *Nat Cell Biol.* **1**, 14-19.

Mastrandrea, L.D., You, J., Niles, E. G., and Pickart, C. M. (1999). E2/E3-mediated assembly of lysine 29-linked polyubiquitin chains. J Biol Chem *274*, 27299-27306.

Masumoto, H., Muramatsu, S., Kamimura, Y., Araki, H. (2002). S-Cdk-dependent phosphorylation of Sld2 essential for chromosomal DNA replication in budding yeast. Nature *415*, 651-655.

Masui, Y. and Markert, C. (1971). Cytoplasmic control of nuclear behavior during meiotic maturation of frog oocytes. J. Exp. Zoology. *177*, 129-145.

Mathias, N., Johnson, S. L., Winey, M., Adams, A. E. M., Goetsch, L., Pringle, J. R., Byers, B., and Goebl, M. G. (1996). Cdc53p acts in concert with Cdc4p to control the

G1-to-S-phase transition and identifies a conserved family of proteins. Mol. Cell. Biol. *16*, 6634-6643.

Maxwell, P. H., Wiesener, M. S., Chang, G. W., Clifford, S. C., Vaux, E. C., Cockman, M. E., Wykoff, C. C., Pugh, C. W., Maher, E. R. and Ratcliffe, P. J. (1999). The tumour suppressor protein VHL targets hypoxia-inducible factors for oxygen-dependent proteolysis. Nature *399*, 271-275.

McCarter, J., Bartlett, B., Dang, T. and Schedl, T. (1997). Soma-germ cell interactions in Caenorhabditis elegans: multiple events of hermaphrodite germline development require the somatic sheath and spermathecal lineages. Developmental Biology *181*, 121-143.

Mendez, J. and Stillman, B. (2000). Chromatin association of human origin recognition complex, cdc6, and minichromosome maintenance proteins during the cell cycle: assembly of prereplication complexes in late mitosis. Mol Cell Biol. *20*, 8602-8612.

Michael, W. M. and Newport, J. (1998). Coupling of mitosis to the completion of S phase through Cdc34-mediated degradation of Wee1. Science *282*, 1886-1889 .

Michel, J. J., and Xiong, Y. (1998). Human CUL-1, but not other Cullin family members, selectively interacts with SKP1 to form a complex with SKP2 and Cyclin A. Cell Growth Diff. *9*, 435-449.

Miller, D. M., and Shakes, D. C. (1995). Immunofluorescence microscopy. In Caenorhabditis elegans: Modern Biological Analysis of an Organism, H. F. Epstein and D. C. Shakes, eds. (San Diego: Academic Press), pp. 365-394.

Min, J. H., Yang, H., Ivan, M., Gertler, F., Kaelin, W. G. Jr and Pavletich, N. P. (2002). Structure of an HIF-1alpha -pVHL complex: hydroxyproline recognition in signaling. Science. *296*, 1886-1889.

Morgan DO. (1997). Cyclin-dependent kinases: engines, clocks, and microprocessors. Annu Rev Cell Dev Biol. *13*, 261-291.

Murray, A. W., Solomon, M. J. and Kirshner, M. W. (1989). The role of cyclin synthesis and degradation in the control of MPF activity. Nature *339*, 280-285.

Nag, A., Bondar, T., Shiv, S. and Raychaudhuri, P. (2001). The xeroderma pigmentosum group E gene product DDB2 is a specific target of cullin 4A in mammalian cells. Mol Cell Biol. *21*, 6738-6747.

Nakayama, K., Nagahama, H., Minamishima, Y. A., Matsumoto, M., Nakamichi, I., Kitagawa, K., Shirane, M., Tsunematsu, R., Tsukiyama, T., Ishida, N., Kitagawa, M., Nakayama, K. and Hatakeyama, S. (2000). Targeted disruption of Skp2 results in accumulation of cyclin E and p27(Kip1), polyploidy and centrosome overduplication. EMBO J *19*, 2069-2081 .

Nasmyth, K. (1996). At the heart of the budding yeast cell cycle. Trends Genet. *12*, 405-412.

Nasmyth, K. and Nurse, P. (1981). Cell division cycle mutants altered in DNA replication and mitosis in the fission yeast *Schizosaccharomyces pombe*. Mol Gen Genet. *182*, 119-124.

Natale, D. A., Li, C. J., Sun, W. H. and DePamphilis, M. L. (2000). Selective instability of Orc1 protein accounts for the absence of functional origin recognition complexes during the M-G(1) transition in mammals. EMBO J. *19*, 2728-2738.

Nayak, S., Santiago, F. E., Jin, H., Lin, D., Schedl, T. and Kipreos, E. T. (2002). The *Caenorhabditis elegans* Skp1-Related Gene Family. Diverse Functions in Cell Proliferation, Morphogenesis, and Meiosis. Curr Biol. *12*, 277-287.

Newport, J. W. and Kirschner, M. W. (1984). Regulation of the cell cycle during early *Xenopus* development. Cell. *37*, 731-742.

Nguyen, V. Q., Co, C. and Li, J. J. (2001). Cyclin-dependent kinases prevent DNA re-replication through multiple mechanisms. Nature. *411*, 1068-1073.

Nishitani, H., Lygerou, Z., Nishimoto, T., and Nurse, P. (2000). The Cdt1 protein is required to license DNA for replication in fission yeast. Nature *404*, 625-628.

Nishitani, H. and Nurse, P. (1995). p65cdc18 plays a major role controlling the initiation of DNA replication in fission yeast. Cell. *83*, 397-405.

Nishitani, H., Taraviras, S., Lygerou, Z., and Nishimoto, T. (2001). The human licensing factor for DNA replication Cdt1 accumulates in G1 and is destabilized after initiation of S-phase. J Biol Chem *276*, 44905-44911.

Ogawa, Y., Takahashi, T. and Masukata, H. (1999). Association of fission yeast Orp1 and Mcm6 proteins with chromosomal replication origins. Mol Cell Biol. *19*, 7228-7236.

Ohta, T., Michel, J.J., Schottelius, A.J. and Xiong, Y. (1999). ROC1, a homolog of APC11, represents a family of cullin partners with an associated ubiquitin ligase activity. Mol. Cell *3*, 535-541.

Okuda, H., Saitoh, K., Hirai, S., Iwai, K., Takaki, Y., Baba, M., Minato, N., Ohno, S. and Shuin, T. (2001). The von Hippel-Lindau tumor suppressor protein mediates ubiquitination of activated atypical protein kinase C. J Biol Chem. *276*, 43611-43617.

Okuno, Y., McNairn, A. J., den Elzen, N., Pines, J. and Gilbert, D. M. (2001). Stability, chromatin association and functional activity of mammalian pre-replication complex proteins during the cell cycle. EMBO J. *20*, 4263-4277.

Ortega, S., Malumbres, M.. and Barbacid, M. (2002). Cyclin D-dependent kinases, INK4 inhibitors and cancer. Biochim Biophys Acta. *1602*, 73-87.

Pak, D. T., Pflumm, M., Chesnokov, I., Huang, D. W., Kellum, R., Marr, J., Romanowski, P. and Botchan, M. R. (1997). Association of the origin recognition complex with heterochromatin and HP1 in higher eukaryotes. Cell. *91*, 311-323.

Patton, E. E., Peyraud, C., Rouillon, A., Surdin-Kerjan, Y., Tyers, M. and Thomas, D. (2000). SCF(Met30)-mediated control of the transcriptional activator Met4 is required for the G(1)-S transition. EMBO J. *19*, 1613-1624.

Patton, E. E., Willems, A. R., and Tyers, M. (1998). Combinatorial control in ubiquitin-dependent proteolysis: don't Skp the F-box hypothesis. Trends Genet. *14*, 236-243.

Pause, A., Lee, S., Lonergan, K. M., and Klausner, R. D. (1998). The von Hippel-Lindau tumor suppressor gene is required for cell cycle exit upon serum withdrawl. Proc. Natl. Acad. Sci. *95*, 993-998.

Pause, A., Lee, S., Worrell, R. A., Chen, D. Y., Burgess, W. H., Linehan, W. M., and Klausner, R. D. (1997). The von Hippel-Lindau tumor-suppressor gene product forms a stable complex with human CUL-2, a member of the Cdc53 family of proteins. Proc. Natl. Acad. Sci. *94*, 2155-2161.

Peters, J. M. (2002). The anaphase-promoting complex: proteolysis in mitosis and beyond. Mol Cell. *9*, 931-943.

Petersen, B. O., Lukas, J., Sorensen, C. S., Bartek, J. and Helin, K. (2000). Phosphorylation of mammalian CDC6 by cyclin A/CDK2 regulates its subcellular localization. EMBO J. *18*, 396-410.

Petersen, B. O., Wagener, C., Marinoni, F., Kramer, E. R., Melixetian, M., Denchi, E.L., Gieffers, C., Matteucci, C., Peters, J. M. and Helin, K. (2000). Cell cycle- and cell growth-regulated proteolysis of mammalian CDC6 is dependent on APC-CDH1. Genes Dev. *14*, 2330-2343.

Pfleger, C. M., Kirschner., M. W. (2000). The KEN box: an APC recognition signal distinct from the D box targeted by Cdh1. Genes Dev *14*, 655-665.

Pflumm, M. F. and Botchan, M. R. (2001). Orc mutants arrest in metaphase with abnormally condensed chromosomes. Development. *128*, 1697-1707.

Pines, J. (1995). Cyclins and cyclin-dependent kinases: a biochemical view. Biochem. J. *308*, 697-711.

Pinto, S., Quintana, D. G., Smith, P., Mihalek, R. M., Hou, Z. H., Boynton, S., Jones, C. J., Hendricks, M., Velinzon, K., Wohlschlegel, J. A., Austin, R. J., Lane, W. S., Tully, T. and Dutta, A. (1999). latheo encodes a subunit of the origin recognition complex and

disrupts neuronal proliferation and adult olfactory memory when mutant. Neuron. *23*, 45-54.

Plasterk, R. H. A. (1995). Reverse genetics: from gene sequence to mutant worm. In Caenorhabditis elegans: Modern Biological Analysis of an Organism, H. F. Epstein and D. C. Shakes, eds. (San Diego: Academic Press), pp. 59-80.

Quinn, L. M., Herr, A., McGarry, T. J., and Richardson, H. (2001). The Drosophila Geminin homolog: roles for Geminin in limiting DNA replication, in anaphase and in neurogenesis. Genes Dev *15*, 2741-2754.

Reimann, J. D., Freed, E., Hsu, J. Y., Kramer, E. R., Peters, J. M. and Jackson, P. K. (2001). Emi1 is a mitotic regulator that interacts with Cdc20 and inhibits the anaphase promoting complex. Cell. *105*, 645-655.

Romanowski, P., Madine, M. A., Rowles, A., Blow, J. J. and Laskey, R. A. (1996). The *Xenopus* origin recognition complex is essential for DNA replication and MCM binding to chromatin. Curr Biol. *6*, 1416-1425.

Rowles, A., Tada, S. and Blow, J. J. (1999). Changes in association of the *Xenopus* origin recognition complex with chromatin on licensing of replication origins. J Cell Sci. *112*, 2011-2018.

Saha, P., Chen, J., Thome, K. C., Lawlis, S. J., Hou, Z. H., Hendricks, M., Parvin, J. D. and Dutta, A. (1998). Human CDC6/Cdc18 associates with Orc1 and cyclin-cdk and is selectively eliminated from the nucleus at the onset of S phase. Mol Cell Biol. *18*, 2758-2767.

Saka, Y., Sutani, T., Yamashita, Y., Saitoh, S., Takeuchi, M., Nakaseko, Y. and Yanagida, M. (1994). Fission yeast cut3 and cut14, members of a ubiquitous protein family, are required for chromosome condensation and segregation in mitosis. EMBO J. *13*, 4938-4952.

Schumacher, J. M., Ashcroft, N., Donovan, P. J., and Golden, A. (1998). A highly conserved centrosomal kinase, AIR-1, is required for accurate cell cycle progression and segregation of developmental factors in *Caenorhabditis elegans* embryos. Dev. *125*, 4391-4402.

Schwob, E., Bohm, T., Mendenhall, M.D. and Nasmyth, K. (1994). The B-type cyclin kinase inhibitor $p40^{SIC1}$ controls the G1 to S transition in *S. cerevisiae*. Cell *79*, 233-244 .

Schwob, E. and Nasmyth, K. (1993). CLB5 and CLB6, a new pair of B cyclins involved in DNA replication in *Saccharomyces cerevisiae*. Genes Dev. *7*, 1160-1175.

Seydoux, G., and Schedl, T. (2001). The germline in *C. elegans*: origins, proliferation, and silencing. Int Rev Cytol *203*, 139-185.

Sherr, C. J. (1996). Cancer cell cycles. Science 274, 1672-1677.

Shiyanov, P., Nag, A. and Raychaudhuri, P. (1999). Cullin 4A associates with the UV-damaged DNA-binding protein DDB. J Biol Chem *274*, 35309-35312 .

Singer, J.D., Gurian-West, M., Clurman, B. and Roberts, J.M. (1999). Cullin-3 targets cyclin E for ubiquitination and controls S phase in mammalian cells. Genes Dev *13*, 2375-2387 .

Skowyra, D., Craig, K. L., Tyers, M., Elledge, S. J., and Harper, J. W. (1997). F-Box proteins are receptors that recruit phosphorylated substrates to the SCF ubiquitin-ligase complex. Cell *91*, 209-219.

Speliotes, E. K., Uren, A., Vaux, D. and Horvitz, H. R. (2000). The survivin-like *C. elegans* BIR-1 protein acts with the Aurora-like kinase AIR-2 to affect chromosomes and the spindle midzone. Mol Cell. *6*, 211-223.

Stebbins, C.E., Kaelin, W.G. and Pavletich, N. P. (1999) Structure of the VHL-ElonginC-ElonginB complex: implications for VHL tumor suppressor function. Science *284*, 455-461

Steffensen, S., Coelho, P. A., Cobbe, N., Vass, S., Costa, M., Hassan, B., Prokopenko, S. N., Bellen, H., Heck, M. M. and Sunkel, C. E. (2001). A role for Drosophila SMC4 in the resolution of sister chromatids in mitosis. Curr Biol. *11*, 295-307.

Strunnikov, A.V., Hogan, E., Koshland, D. (1995). SMC2, a *Saccharomyces cerevisiae* gene essential for chromosome segregation and condensation, defines a subgroup within the SMC family. Genes Dev. *9*, 587-599.

Strunnikov, A.V., Larionov, V.L. and Koshland, D. (1993). SMC1: an essential yeast gene encoding a putative head-rod-tail protein is required for nuclear division and defines a new ubiquitous protein family. J Cell Biol. *123*, 1635-1648.

Sulston, J. and Hodgkin, J. (1988). Methods. In The Nematode *Caenorhabditis elegans*, W. B. Wood, ed. (Cold Spring Harbor, New York: Cold Spring Harbor Laboratory), pp. 587-606.

Sulston, J. E., and Horvitz, H. R. (1977). Post-embryonic Cell Lineages of the Nematode, *Caenorhabditis elegans*. Dev. Biol. *56*, 110-156.

Sundin, O. and Varshavsky, A. (1981). Arrest of segregation leads to accumulation of highly intertwined catenated dimers: dissection of the final stages of SV40 DNA replication. Cell. *25*, 659-669.

Sutani, T., Yuasa, T., Tomonaga, T., Dohmae, N., Takio, K. and Yanagida, M. (1999). Fission yeast condensin complex: essential roles of non-SMC subunits for condensation and Cdc2 phosphorylation of Cut3/SMC4. Genes Dev. *13*, 2271-2283.

Suzuki, H., Chiba, T., Kobayashi, M., Takeuchi, M., Suzuki, T., Ichiyama, A., Ikenoue, T., Omata, M., Furuichi, K., and Tanaka, K. (1999). IKBa ubiquitination is catalyzed by an SCF-like complex containing Skp1, cullin-1, and two F-box/WD40-repeat proteins, bTrCP1 and bTrCP2. Biochem. Biophys. Res. Commun. *256*, 127-132.

Tabara, H., Grishok, A., and Mello, C. C. (1998). RNAi in *C. elegans*: soaking in the genome sequence. Science *282*, 430-431.

Tada, S., Li, A., Maiorano, D., Mechali, M., and Blow, J. J. (2001). Repression of origin assembly in metaphase depends on inhibition of RLF-B/Cdt1 by geminin. Nat. Cell Biol. *3*, 107-113.

Tanaka, T., Knapp, D. and Nasmyth, K. (1997). Loading of an Mcm protein onto DNA replication origins is regulated by Cdc6p and DKs. Cell. *90*, 649-660.

Timmons, L., and Fire, A. (1998). Specific interference by ingested dsRNA. Nature *395*, 854.

Tyers, M., and Jorgensen, P. (2000). Proteolysis and the cell cycle: with this RING I do thee destroy. Curr Opin Genet Dev *10*, 54-64.

Uemura, T., Ohkura, H., Adachi, Y., Morino, K., Shiozaki, K. and Yanagida, M. (1987). DNA topoisomerase II is required for condensation and separation of mitotic chromosomes in *S. pombe*. Cell. *50*, 917-925.

Uhlmann, F. (2001). Chromosome condensation: packaging the genome. Curr Biol. *11*, R384-387.

Vas, A., Mok, W. and Leatherwood, J. (2001). Control of DNA rereplication via Cdc2 phosphorylation sites in the origin recognition complex. Mol Cell Biol. *21*, 5767-5777.

Weaver, D. T., Fields-Berry, S. C. and DePamphilis, M. L. (1985) The termination region for SV40 DNA replication directs the mode of separation for the two sibling molecules. Cell. *41*, 565-575.

Wei, Y., Yu, L., Bowen, J., Gorovsky, M. A. and Allis, C. D. (1999). Phosphorylation of histone H3 is required for proper chromosome condensation and segregation. Cell. *97*, 99-109.

Whittaker, A. J., Royzman, I. and Orr-Weaver, T.L. (2000). Drosophila double parked: a conserved, essential replication protein that colocalizes with the origin recognition complex and links DNA replication with mitosis and the down-regulation of S phase transcripts. Genes Dev. *14*, 1765-1776.

Wilkinson, K. (2000). Ubiquitination and deubiquitination: targeting of proteins for degradation by the proteasome. Semin Cell Dev Biol. *11*, 141-148.

Wilson, R., Ainscough, R., Anderson, K., Baynes, C., Berks et al. (1994). 2.2 Mb of contiguous nucleotide sequence from chromosome III of *C. elegans*. Nature *368*, 32-38.

Winston, J. T., Strack, P., Beer-Romero, P., Chu, C.Y., Elledge, S. J. and Harper, J. W. (1999). The $SCF^{b\text{-}TRCP}$-ubiquitin ligase complex associates specifically with phosphorylated destruction box motifs in IKBa and b-catenin and stimulates IKBa ubiquitination *in vitro*. Genes and Dev. *13*, 270-283.

Wohlschlegel, J. A., Dwyer, B. T., Dhar, S. K., Cvetic, C., Walter, J. C., and Dutta, A. (2000). Inhibition of eukaryotic DNA replication by geminin binding to cdt1 [In Process Citation]. Science *290*, 2309-12.

Wood, W. B. (1988). Embryology. In The Nematode *Caenorhabditis elegans*, W. B. Wood, ed. (Cold Spring Harbor, New York: Cold Spring Harbor Laboratory), pp. 215-241.

Yanow, S.K., Lygerou, Z., Nurse, P. (2001) Expression of Cdc18/Cdc6 and Cdt1 during G2 phase induces initiation of DNA replication. EMBO 20(17):4648-4656.

Yu, H., Peters, J. M., King, R. W., Page, A. M., Hieter, P., Kirschner, M. W. (1998a). Identification of a cullin homology region in a subunit of the anaphase-promoting complex. Science. *279*, 1219-1222.

Yu, Z.-K., Gervais, J.L.M. and Zhang, H. (1998b). Human CUL-1 associates with the SKP1/SKP2 complex and regulates $p21^{CIP1/WAF1}$ and cyclin D proteins. *Proc. Natl. Acad. Sci.* **95**, 11324-11329.

Zachariae, W., Shin, T. H., Galova, M., Obermaier, B. and Nasmyth, K. (1996). Identification of subunits of the anaphase-promoting complex of *Saccharomyces cerevisiae*. Science. *274*, 1201-1204.

Zhang, J. G., Farley, A., Nicholson, S. E., Willson, T. A., Zugaro, L. M., Simpson, R. J., Moritz, R. L., Cary, D., Richardson, R., Hausmann, G., Kile, B. J., Kent, S. B., Alexander, W. S., Metcalf, D., Hilton, D. J., Nicola, N. A. and Baca, M. (1999). The conserved SOCS box motif in suppressors of cytokine signaling binds to elongins B and C and may couple bound proteins to proteasomal degradation. Proc. Natl Acad. Sci. USA *96*, 2071-2076.

Zhang, P., Wong, C., DePinho, R. A., Harper, J. W., and Elledge, S. J. (1998). Cooperation between the *Cdk* inhibitors $p27^{KIP1}$ and $p57^{KIP2}$ in the control of tissue growth and development. Genes and Dev. *12*, 3162-3167.

Zheng, N., Schulman, B. A., Song, L., Miller, J. J., Jeffrey, P. D., Wang, P., Chu, C., Koepp, D. M., Elledge, S. J., Pagano, M., Conaway, R. C., Conaway, J. W., Harper, J. W. and Pavletich, N. P. (2002). Structure of the Cul1-Rbx1-Skp1-F box Skp2 SCF ubiquitin ligase complex. Nature. *416*, 703-709.